

## Appendix II-J2

### Sediment Dispersion Modeling Report

March 2024

**Note:** Atlantic Shores has updated the Project Design Envelope to include the following landfall sites: Monmouth Landfall Site, Asbury Landfall Site, Kingsley Landfall Site, Lemon Creek Landfall Site, Wolfe's Pond Landfall Site, and Fort Hamilton Landfall Site. The information included in this report demonstrates the completeness of Atlantic Shores' multi-year development efforts and should be considered representative for the Project. For additional information regarding the layout of the Project, please refer to COP Volume I Project Information, Sections 1.0 Introduction and 4.7 Landfall Sites, as well as Figure 1.1-2 Project Overview.

# SEDIMENT DISPERSION MODELING TECHNICAL REPORT

## Atlantic Shores Offshore Project Area

Prepared by:

**RPS**

Melissa Gloekler, Matt Doelp, Olivia Amante, Tayebah  
Tajalli Bakhsh, Jenna Ducharme, Matthew Frediani,  
Shlomit Chelst, and Jill Rowe

55 Village Square Drive  
South Kingstown RI 02879

T +1 401 789 6224

E [Missy.Gloekler@rpsgroup.com](mailto:Missy.Gloekler@rpsgroup.com)

Prepared for:

**Environmental Design & Research (EDR),  
Landscape Architecture, Engineering &  
Environmental Services, D.P.C.**

RPS Project: P-22-2  
Report Version: 3  
Submitted: May 5, 2023  
Revised: July 15, 2023

# Contents

**EXECUTIVE SUMMARY .....iv**

**1 INTRODUCTION .....1**

    1.1 Study Scope and Objectives .....4

**2 HYDRODYNAMIC MODELING .....6**

    2.1 Environmental Data.....6

        2.1.1 Bathymetry and Shoreline .....8

        2.1.2 Meteorological Observations .....9

        2.1.3 Sea Surface Height (Tides) .....10

        2.1.4 River Data .....10

        2.1.5 Ocean Current Observations .....11

    2.2 Delft3D Hydrodynamic Model Application.....11

        2.2.1 Delft3D Model Description .....11

        2.2.2 Model Grid .....12

        2.2.3 Boundary and Initial Conditions .....15

        2.2.4 Model Calibration .....15

        2.2.5 Model Validation .....18

        2.2.6 Model Results for Use in Sediment Transport Modeling Scenarios .....22

**3 SEDIMENT MODELING .....25**

    3.1 SSFATE Modeling Approach .....25

        3.1.1 SSFATE Model Description .....25

        3.1.2 Model Theory .....25

    3.2 SSFATE Data Needs .....27

        3.2.1 Sediment Characteristics .....27

        3.2.2 Hydrodynamic Forcing .....32

        3.2.3 Route Definition .....32

        3.2.4 Source & Sediment Load Characterization .....44

    3.3 Sediment Modeling Results .....46

        3.3.1 Results Summary Tables.....47

        3.3.2 Seabed Preparation: Sandwave Clearance .....52

        3.3.3 Seabed Preparation: Large OSS & WTG Foundations .....67

        3.3.4 Lease Area: Cable Installation.....87

        3.3.5 Northern ECC and Monmouth ECC: Cable Installation.....92

        3.3.6 Landfall Approaches: HDD Pit Construction.....102

        3.3.7 Results Discussion .....111

**4 REFERENCES .....113**

## Figures

Figure 1-1: Map of Atlantic Shores Offshore Project Region with Offshore Components. ....3

Figure 2-1: Location of project components, bathymetry data coverages, and environmental data observation stations.....7

Figure 2-2: Comparison between wind measurement at NDBC buoy 44065 and interpolated data over the same time frame (July 1, 2019 through September 1, 2019) and location from the ERA5 dataset.....10

Figure 2-3: Schematic of the D-Flow FM vertical sigma (left) and vertical Z-coordinate (right) systems (Deltares, 2022). ....11

Figure 2-4: D-Flow FM model grid coverage of the Atlantic Shores North AOI, and location of open boundaries. ....13

Figure 2-5: Illustration of the bathymetry of the domain interpolated to the D-Flow FM. ....14

Figure 2-6: Bottom layer current velocity components from NOAA station observation at a depth of 9.5 m (blue) and hydrodynamic model predictions at a depth of 8.1 m (orange dashed) at NYH1901 for the calibration period. ....17

Figure 2-7: Bottom layer current velocity components from NOAA station observation at a depth of 8.5 m (blue) and hydrodynamic model predictions at a depth of 8.1 m (orange dashed) at NYH1903 for the calibration period. ....17

Figure 2-8: Bottom layer current velocity components from NOAA station observation at a depth of 12.1 m (blue) and hydrodynamic model predictions at a depth of 11.9 m (orange dashed) at NYH1904 for the calibration period. ....18

Figure 2-9: SSH (in meters) of NOAA station (blue) and Delft3D (orange dashed) at each of the three tidal stations (Table 2-1) during the validation period.....20

Figure 2-10: Bottom-layer current velocity components of NOAA station at a depth of 9.5 m (blue) and hydrodynamic model predictions at a depth of 8.1 m (orange dashed) at NYH1901 station for the validation period.....21

Figure 2-11: Bottom-layer current velocity components of NOAA station at a depth of 8.5 m (blue) and hydrodynamic model predictions at a depth of 8.1 m (orange dashed) at NYH1903 station for the validation period.....21

Figure 2-12: Bottom-layer current velocity components of NOAA station at a depth of 12.2 m (blue) and hydrodynamic model predictions at a depth of 11.9 m (orange dashed) at NYH1904 station for the validation period.....22

Figure 2-13: Color contour map showing bottom current velocity magnitude, overlaid with vectors (red) for a flood timestep (18-May-2019 22:00).....23

Figure 2-14: Color contour map showing bottom current velocity magnitude, overlaid with vectors (red) for an ebb timestep (19-May-2019 04:00). ....24

Figure 3-1: Sediment Grain Size Distributions for the Upper 2 m of the Seabed in the Lease Area. ....29

Figure 3-2: Sediment Grain Size Distributions for the Upper 2 m of the Seabed along the Monmouth ECC. ....30

Figure 3-3: Sediment Grain Size Distributions for the Upper 1.8 m of the Seabed along the Northern ECC and inset showing the 3 m depth weighted near landfall. ....31

Figure 3-4: Modeled Northern ECC Representative Sandwave Clearance Route. ....34

Figure 3-5: Modeled Monmouth ECC Representative Sandwave Clearance Route. ....35

Figure 3-6: Modeled Representative Lease Area Sandwave Clearance Route.....36

Figure 3-7: Modeled Seabed Preparation Locations at a Representative WTG Foundation Site and Three Large OSS Foundation Sites. ....37

Figure 3-8: Modeled Representative Inter-Array Cable Route. ....39

Figure 3-9: Modeled Northern ECC Representative Landfall Approach. ....40

Figure 3-10: Modeled Northern ECC Approach. ....41

Figure 3-11: Modeled Monmouth Export Cable, Branch 1 and Branch 2. ....42

Figure 3-12: Modeled Monmouth ECC Representative Landfall Approach. ....43

Figure 3-13: Snapshot of instantaneous TSS concentrations for a time step during the Representative Northern ECC Sandwave Clearance – TSHD simulation.....53

Figure 3-14: Map of time-integrated maximum concentrations associated with the Representative Northern ECC Sandwave Clearance – TSHD simulation.....54

Figure 3-15: Map of duration of TSS ≥ 10 mg/L associated with the Representative Northern ECC Sandwave Clearance – TSHD simulation. ....55

Figure 3-16: Map of deposition thickness associated with the Representative Northern ECC Sandwave Clearance – TSHD simulation. ....56

Figure 3-17: Snapshot of Instantaneous TSS Concentrations Associated with Sandwave Clearance along the Monmouth ECC. ....58

Figure 3-18: Map of Time-Integrated Maximum TSS Concentrations Associated with Sandwave Clearance along the Monmouth ECC. ....59

Figure 3-19: Map of Duration of TSS ≥10 mg/L Associated with Sandwave Clearance along the Monmouth ECC. ....60

Figure 3-20: Map of Deposition Thickness Associated with Sandwave Clearance along the Monmouth ECC. ....61

Figure 3-21: Snapshot of instantaneous TSS concentrations for a time step during the Representative Inter-array Cable Sandwave Clearance – TSHD simulation. ....63

Figure 3-22: Map of time-integrated maximum concentrations associated with the Representative Inter-array Cable Sandwave Clearance – TSHD simulation. ....64

Figure 3-23: Map of duration of TSS ≥ 10 mg/L associated with the Representative Inter-array Cable Sandwave Clearance – TSHD simulation. ....65

Figure 3-24: Map of deposition thickness associated with the Representative Inter-array Cable ECC Sandwave Clearance – TSHD simulation. ....66

Figure 3-25: Snapshot of instantaneous TSS concentrations for a time step during the Large OSS Seabed Foundation Preparation simulation using TSHD at Site 1. ....68

Figure 3-26: Map of time-integrated maximum concentrations associated with the Large OSS Seabed Foundation Preparation simulation using TSHD at Site 1. Note that the cross-section spans north to south along the plume. ....69

Figure 3-27: Map of duration of TSS ≥ 10 mg/L associated with the Large OSS Seabed Foundation Preparation simulation using TSHD at Site 1. ....70

Figure 3-28: Map of deposition thickness associated with the Large OSS Seabed Foundation Preparation simulation using TSHD at Site 1. ....71

Figure 3-29: Snapshot of instantaneous TSS concentrations for a time step during the Large OSS Seabed Foundation Preparation simulation using TSHD at Site 2. ....73

Figure 3-30: Map of time-integrated maximum concentrations associated with the Large OSS Seabed Foundation Preparation simulation using TSHD at Site 2. Note that the cross-section spans north to south along the plume. ....74

Figure 3-31: Map of duration of TSS ≥ 10 mg/L associated with the Large OSS Seabed Foundation Preparation simulation using TSHD at Site 2. ....75

Figure 3-32: Map of deposition thickness associated with the Large OSS Seabed Foundation Preparation simulation using TSHD at Site 2. ....76

Figure 3-33: Snapshot of instantaneous TSS concentrations for a time step during the Large OSS Seabed Foundation Preparation simulation using TSHD at Site 3. ....78

Figure 3-34: Map of time-integrated maximum concentrations associated with the Large OSS Seabed Foundation Preparation simulation using TSHD at Site 3. Note that the cross-section spans north to south along the plume. ....79

Figure 3-35: Map of duration of TSS ≥ 10 mg/L associated with the Large OSS Seabed Foundation Preparation simulation using TSHD at Site 3. ....80

Figure 3-36: Map of deposition thickness associated with the Large OSS Seabed Foundation Preparation simulation using TSHD at Site 3. ....81

Figure 3-37: Snapshot of instantaneous TSS concentrations for a time step during the Representative WTG Seabed Foundation Preparation simulation using TSHD. ....83

Figure 3-38: Map of time-integrated maximum concentrations associated with the Representative WTG Seabed Foundation Preparation simulation using TSHD. ....84

Figure 3-39: Map of duration of TSS ≥ 10 mg/L associated with the Representative WTG Seabed Foundation Preparation simulation using TSHD. ....85

Figure 3-40: Map of deposition thickness associated with the Representative WTG Seabed Foundation Preparation simulation using TSHD. ....86

Figure 3-41: Snapshot of instantaneous TSS concentrations for a time step during the Representative IAC Installation simulations using Jet Trenching (top) and Mechanical Trenching (bottom). ....88

Figure 3-42: Map of time-integrated maximum concentrations associated with the Representative IAC Installation simulations using Jet Trenching (top) and Mechanical Trenching (bottom). ....89

Figure 3-43: Map of duration of TSS ≥ 10 mg/L associated with the Representative IAC Installation simulations using Jet Trenching (top) and Mechanical Trenching (bottom). ....90

Figure 3-44: Map of deposition thickness associated with the Representative IAC Installation simulations using Jet Trenching (top) and Mechanical Trenching (bottom). ....91

Figure 3-45: Snapshot of instantaneous TSS concentrations for a time step during simulation for the Representative Northern ECC Cable Installation— Jet Trencher simulation. ....93

Figure 3-46: Map of time-integrated maximum concentrations associated with the Representative Northern ECC Cable Installation — Jet Trencher simulation. ....94

Figure 3-47: Map of duration of TSS ≥ 10 mg/L associated with the Representative Northern ECC Cable Installation — Jet Trencher simulation. ....95

Figure 3-48: Map of deposition thickness associated with Representative Northern ECC Cable Installation — Jet Trencher simulation. ....96

Figure 3-49: Snapshot of Instantaneous TSS Concentrations Associated with Cable Burial along the Monmouth ECC – Branch 1. ....98

Figure 3-50: Map of Time-Integrated Maximum TSS Concentrations Associated with Cable Burial along the Monmouth ECC for Branch 1 and Branch 2. ....99

Figure 3-51: Map of Duration of TSS ≥10 mg/L Associated with Cable Burial along the Monmouth ECC for Branch 1 and Branch 2. ....100

Figure 3-52: Map of Deposition Thickness Associated with Cable Burial along the Monmouth ECC for Branch 1 and Branch 2. ....101

Figure 3-53: Snapshot of instantaneous TSS concentrations for a time step during the Representative HDD Pit - Northern ECC Landfall Approach. ....103

Figure 3-54: Map of time-integrated maximum concentrations associated with the Representative HDD Pit - Northern ECC Landfall Approach. ....104

Figure 3-55: Map of duration of TSS  $\geq$  10 mg/L associated with the Representative HDD Pit - Northern ECC Landfall Approach. ....105

Figure 3-56: Map of deposition thickness associated with the Representative HDD Pit - Northern ECC Landfall Approach. ....106

Figure 3-57: Map of Time-Integrated TSS Concentrations Associated with Monmouth ECC Representative HDD Pit Excavation. ....108

Figure 3-58: Map of Duration of TSS  $\geq$ 10 mg/L Associated with Monmouth ECC Representative HDD Pit Excavation. ....109

Figure 3-59: Map of Deposition Thickness Associated with Monmouth ECC Representative HDD Pit Excavation. ....110

**Tables**

Table 2-1: Summary of model and observation data in 2019, used in the modeling study. ....8

Table 2-2: Specifics of bathymetry datasets used for modeling. ....9

Table 2-3: Statistical evaluation of bottom current velocity components (m/s) of the Delft3D application compared with observations at NYH1901, NYH1903, and NYH1904. ....16

Table 2-4: Statistical evaluation of SSH ( m) of the Delft3D application compared with observations at three NOAA Stations. ....19

Table 2-5: Statistical evaluation of bottom current velocity components (m/s) of the Delft3D application compared with observations at three NYH Stations. ....19

Table 3-1: Sediment Size Classes used in SSFATE. ....26

Table 3-2: Construction Activities Modeled. ....33

Table 3-3: Construction Activity Modeling Parameters .....45

Table 3-4: Areas over Above-Ambient TSS Threshold Concentrations for Longer than 2 Hours for Each Scenario. ....47

Table 3-5: Areas over Above-Ambient TSS Threshold Concentrations for Longer than 4 Hours for Each Scenario. ....48

Table 3-6: Areas over Above-ambient TSS Threshold Concentrations for Longer than 6 Hours for Each Scenario. ....49

Table 3-7: Areas over Above-ambient TSS Threshold Concentrations for Longer than 12 Hours for Each Scenario. ....50

Table 3-8: Maximum Extent to the 10 mg/L and 100 mg/L TSS Contours from the Route Centerline and Maximum Duration of Exposure to TSS >10 mg/L and >100 mg/L for Each Scenario. ....51

Table 3-9: Deposition over Thresholds for Each Scenario. ....52

## List of Acronyms

AOI	Area of Interest
BOEM	Bureau of Ocean Energy Management
COP	Construction and Operations Plan
ECC	Export Cable Corridor
ECMWF	European Centre for Medium-Range Weather Forecasts
ENC	Electronic Navigational Charts
ERA5	ECMWF ReAnalysis 5th generation Wind
FM	Flexible Mesh
GEBCO	General Bathymetric Chart of the Oceans
GIS	Geographic Information System
HDD	Horizontal Directional Drilling
Hr	Hour
HVAC	High Voltage Alternating Current
IAC	Inter-Array Cable
km	kilometer
km <sup>2</sup>	kilometers squared
MAE	Mean Absolute Error
m	meter
m <sup>2</sup>	meters squared
m/s	meters per second
mi	mile
mm	millimeter
mg/L	milligrams per liter
MSL	Mean Sea Level
NDBC	National Data Buoy Center
NJWEA	New Jersey Wind Energy Area
NOAA	National Oceanic and Atmospheric Administration
OCS	Outer Continental Shelf
OSS	Offshore Substation
OTPS	Oregon State University Tidal Prediction Software
OTIS	Oregon State University Tidal Inversion Software
PDE	Project Design Envelope
RMSE	Root Mean Square Error
SSFATE	Suspended Sediment FATE
SSH	Sea Surface Height
3D	Three-dimensional



TPXO	TOPEX/Poseidon Global Inverse Solution tidal model
TSHD	Trailing Suction Hopper Dredge
TSS	Total Suspended Sediment
USACE	United States Army Corp of Engineers
USGS	United States Geological Survey
NJWEA	New Jersey Wind Energy Area
WTG	Wind Turbine Generator

## EXECUTIVE SUMMARY

### **Project Background:**

Atlantic Shores Offshore Wind, LLC (Atlantic Shores) is a 50/50 joint venture between EDF-RE Offshore Development, LLC (an indirect, wholly owned subsidiary of EDF Renewables, Inc. [EDF Renewables]) and Shell New Energies US LLC (Shell). Atlantic Shores is submitting this Construction and Operations Plan (COP) supplement to the Bureau of Ocean Energy Management (BOEM) for the development of offshore wind energy generation known as the Atlantic Shores North Project (the Project) within the Lease Area OCS-A 0549 (Lease Area).

Atlantic Shores' Lease Area is located on the Outer Continental Shelf (OCS) within the New Jersey Wind Energy Area (NJWEA), which was identified by BOEM as suitable for offshore renewable energy development through a multi-year, public environmental review process. Atlantic Shores' proposed offshore wind energy generation facilities will be located in Lease Area OCS-A 0549, which is 81,129 acres (328.3 square kilometers [km<sup>2</sup>]) in area. Lease Area OCS-A 0549 is located north of and is adjacent to Atlantic Shores' Lease Area OCS-A 0499. At its closest point, the Lease Area is approximately 8.4 miles (mi) (13.5 kilometers [km]) from the New Jersey coast and approximately 60 mi (96.6 km) from the New York coast. The facilities to be installed within the Lease Area will include: a maximum of up to 157 wind turbine generators (WTGs); up to 8 small, 4 medium, or 3 large offshore substations (OSSs); inter-array and/or inter-link cables connecting the WTGs and OSSs; and up to one permanent meteorological (met) tower. The WTGs and OSSs will be connected by a system of 66-kilovolt (kV) to 150 kV high voltage alternating current (HVAC) inter-array cables (IAC). OSSs within the Lease Area may be connected to each other via 66 kV to 275 kV HVAC inter-link cables.

Energy from the OSSs will be delivered to landfall sites on the New Jersey and/or New York coastlines via buried export cables. These cables will be located within designated Export Cable Corridors (ECCs), which extend from the Lease Area through New Jersey and/or New York State waters as well as Federal waters. Atlantic Shores has identified potential landfall sites in the following locations: southern Monmouth County, New Jersey (the Monmouth Landfall Site); northern Monmouth County (near Asbury), New Jersey (the Asbury Landfall Sites); southwest Staten Island, New York (The Raritan Bay Landfall Sites); and northeast Staten Island as well as Brooklyn, New York (The Narrows Landfall Sites).

The Monmouth ECC extends from south to north along the eastern side of the Lease Area. The Monmouth ECC then continues north prior to turning west to a terminus at the Monmouth Landfall Site. The total length of the Monmouth ECC associated with the Project from the Lease Area to the furthest potential landfall location is approximately 66.7 mi (97.5 km). This ECC will also be used to convey export cables associated with the Atlantic Shores South Project (Lease Area OCS-A 0499).

The Northern ECC extends north from the Lease Area to the New York State waters boundary, where it splits into branches to reach the Raritan Bay Landfall Sites on southwest Staten Island in Richmond County, New York and The Narrows Landfall Sites on northeast Staten Island, New York and Brooklyn in Kings County, New York. The total length of the Northern ECC associated with the Project from the Lease Area to the furthest potential landfall location is approximately 97.9 mi (146.3 km). The Asbury Branch of the Northern ECC extends westward from the Northern ECC approximately 8.6 mi (13.9 km) to the potential Asbury Landfall Sites in northern Monmouth County, New Jersey. Atlantic Shores will use horizontal directional drilling (HDD) technology to install the export cables from the end of the ECCs to the Landfall Sites to minimize impacts to the intertidal and nearshore habitats and ensure stable burial of the cables.

The COP has been developed in accordance with 30 CFR Part 585, applicable BOEM and other regulatory guidance, and the stipulations in Atlantic Shores' Lease Agreement OCS-A 0549. Atlantic Shores is requesting BOEM review and authorization of the Project in accordance with their Project Design Envelope (PDE) guidance (BOEM, 2018). Atlantic Shores has sited the Project facilities and developed the PDE to maximize renewable energy production, minimize environmental effects, minimize cost to ratepayers, and address stakeholder concerns. The PDE articulates the maximum design scenario for key project components, such as the type and number of WTGs, foundation types, OSS types, cable types, and installation techniques. The PDE provides Atlantic Shores with the necessary flexibility to respond to anticipated advancements in industry

technologies and techniques that, even under a maximum scenario, will not exceed an unreasonable level of environmental effects.

**Study Scope and Objectives:**

This appendix to the COP documents the sediment dispersion modeling assessment of the sediment-disturbing offshore cable installation activities associated with the development of the Project. The cable installation methods may vary along the route depending on subsurface conditions. The installation methods are described in detail in the COP and the details of the assumed modeling parameters are documented within this report.

Consistent with the PDE, this study simulated multiple scenarios to capture a conservative design and range of effects associated with seabed preparation in the Lease Area and the ECCs, the installation of IACs in the Lease Area, offshore export cables in the two ECCs, and landfall approaches. While it is proposed that multiple cables will be installed within each ECC, each cable will be installed in a separate trench at different timeframes. To assess potential effects of cable installation, one representative cable installation simulation was performed along each of the ECCs. Installation of each cable will take place during separate time periods such that potential effects from installation of one cable will have long since dissipated prior to the start of subsequent cable installations. Based on environmental surveys conducted for the Project, sand bedforms were identified within the ECCs and Lease Area. Therefore, dredging is anticipated and was modeled within a representative section of the Northern and Monmouth ECCs and within the Lease Area, to simulate sandwave clearance prior to cable installation using a Trailing Suction Hopper Dredge (TSHD). Seabed preparation of the foundations at the three Large OSS sites and one representative WTG site was simulated using a TSHD. The WTG seabed foundation preparation simulation provides a conservative, representation of the other 156 WTG sites and one possible Permanent Met Tower and the Large OSS simulation is representative of the small and medium OSS sites.

The representative scenarios include:

- Northern ECC sandwave clearance using TSHD;
- Monmouth ECC sandwave clearance using TSHD;
- Lease Area sandwave clearance using TSHD;
- Large OSS Seabed Foundation Preparation – Site 1 using TSHD;
- Large OSS Seabed Foundation Preparation – Site 2 using TSHD;
- Large OSS Seabed Foundation Preparation – Site 3 using TSHD;
- Representative WTG Seabed Foundation preparation using TSHD;
- IAC installation with jet trenching installation parameters;
- IAC installation with mechanical trenching installation parameters;
- Monmouth ECC cable installation (Branch 1) with jet trenching installation parameters;
- Monmouth ECC cable installation (Branch 2) with jet trenching installation parameters;
- Northern ECC cable installation with jet trenching installation parameters;
- Monmouth ECC landfall approach with HDD pit construction activities; and
- Northern ECC landfall approach with HDD pit construction activities.

**Modeling Approach:**

RPS applied customized hydrodynamic and sediment dispersion models to assess potential effects from sediment suspension during construction activities. Specifically, this analysis includes two interconnected modeling tasks:

- Developing a three-dimensional (3D) hydrodynamic modeling application of a domain encompassing Atlantic Shores' activities using the Deflt3D Flexible Mesh (FM) modeling suite; and

- Simulating the suspended sediment's fate and transport, including evaluation of seabed deposition and suspended sediment plumes, were performed using an RPS in-house model, Suspended Sediment FATE (SSFATE), to simulate installation activities. Velocity fields developed using the Delft3D FM modeling suite were used as the primary forcing for SSFATE.

This study was carried out to characterize the effects associated with the seabed preparation, offshore cable installation activities, and HDD pit excavation and backfill. These effects were quantified using two parameters: 1) water column concentrations of total suspended sediment (TSS) above-ambient conditions, and 2) sediment thickness on the seabed resulting from the deposition of the suspended sediments over time. These thresholds were selected either because they are thresholds of biological significance or because they provide an effective means of demonstrating the physical effects. The results are presented with respect to the following thresholds:

- Water column concentrations thresholds: 10, 25, 50, 100, 200, and 650 milligrams per liter (mg/L);
- Water column exposure durations: 2, 4, 6, and 12 hours (hrs); and
- Seabed deposition: 1, 5, 10, 20, and 100 millimeters (mm).

### **Results and Discussion:**

All seabed preparation simulations were modeled using TSHD and conservative equipment parameters (i.e., 100% of mass released at or near the water surface). For sandwave clearance simulations and due to the periodic disposal of sediment, the resulting footprint exhibited higher concentrations especially when currents were parallel with the route, because this resulted in compounding plumes.

The discrete locations of deposition along the route were a product of the periodic disposal of sediments during dump and overflow and can be attributed to the relatively large volume of sediment released at or near the water surface, as compared to the continual release of sediment near the seabed for the cable installation simulations. Above-ambient TSS concentrations stemming from sandwave clearance activities extended farther from the route centerline compared with the cable installation or HDD simulations due to the introduction of sediments at the water surface and the orientation of the route to the currents. When comparing the sandwave clearance results to the seabed foundation preparation simulations, the time for water column concentrations to dissipate to less than 10 mg/L were of similar magnitude for the Large OSS foundation simulations. The representative IAC sandwave clearance simulation was predicted to take the longest time to dissipate and the representative Northern ECC sandwave clearance simulation was predicted to have the largest maximum extent to the 10 mg/L contour compared to all other construction activities. For all sandwave scenarios, above-ambient TSS concentrations substantially dissipated within 4 to 6 hours and fully dissipated in less than 14.3 hours.

Alternatively, the Large OSS seabed foundation preparation simulations were predicted to have the largest maximum extent of deposition  $\geq 1$  mm and  $\geq 10$  mm compared with all other scenarios. All seabed preparation activities were estimated to have depositional thicknesses exceeding 100 mm, while none of the cable installation or HDD pit scenarios were predicted to have areas greater than 0.01 km<sup>2</sup> associated with deposition  $>100$  mm. The extent and persistence of the plumes and the extent and thickness of deposition were largely influenced by sediment grain size distribution, the volume of sediment suspended, and the location of the sediment's introduction within the water column; however, other factors of influence include the route orientation relative to currents, timing of the currents, and installation parameters.

Simulations of several possible IAC or offshore export cable installation methods using either jet trenching installation parameters (for IAC and export cable installation) or mechanical trenching installation parameters (for IAC installation only) predicted TSS  $\geq 100$  mg/L and deposition  $\geq 10$  mm stayed relatively close to the route centerline and remained within the bottom few meters of the water column. TSS concentrations  $\geq 10$  mg/L extended a maximum distance of approximately 2.71 km, 2.60 km, and 2.42 km for the Representative IAC (Mechanical Trencher scenario), Monmouth ECC, and Northern ECC cable installations, respectively. For the landfall approach scenarios, it was assumed that no cofferdam was deployed during construction activities, an excavator was used, and sediment was introduced at the surface to simulate side casting directly into the water. This resulted in a maximum distance for the predicted above-ambient TSS concentrations  $\geq 10$  mg/L of approximately 3.30 km and 1.85 km for the Monmouth and Northern representative HDD pits, respectively.

Model scenarios indicate that higher TSS concentrations (i.e.,  $\geq 100$  mg/L) associated with the installation of the IAC, Monmouth ECC, and Northern ECC cable installation model scenarios were constrained to the bottom of the water column and were short-lived. For the IAC model scenarios, above-ambient TSS concentrations substantially dissipated within 4 to 6 hours and fully dissipated in 8.7 hours. For the Northern ECC and Monmouth ECC model scenarios, above-ambient TSS concentrations substantially dissipated within 2 to 6 hours but require approximately 17.7 hours to fully dissipate. This increased time compared to the IAC modeled scenarios is likely due to the relatively longer routes (i.e., larger volume of suspended sediment), the routes' orientations in relation to currents, and the more frequent occurrence of fine sediment along these routes.

For the landfall approach scenarios, the tails of the plumes oscillated with the currents, and higher concentrations (e.g.,  $>650$  mg/L) remained centered around the source. After the excavation subsided, the concentrations dissipated due to the strong hydrodynamic forcing conditions. Above-ambient TSS concentrations around the HDD pits dissipated within 12.3 hours for the Monmouth HDD pit and 10.3 hours for the Northern ECC HDD pit. The Monmouth HDD pit model's larger areas of TSS concentrations above thresholds and the longer time for the plume to diminish to ambient conditions may be attributed to the release in deeper water, the higher fraction of fine sediments taking longer to settle, and the slightly stronger currents transporting the sediments parallel with the shore. For the HDD modeling, a conservative approach was used by assuming no mitigation techniques would be deployed during construction activities (e.g., cofferdam, silt screen) and sediment would be side cast rather than being stored on a barge. Use of a cofferdam would likely reduce the extent of the plume and minimize transport of the plume by currents, thus resulting in more localized settling of sediment around the release location.

For the Lease Area IAC installation simulations, deposition  $\geq 1$  mm was not predicted to result from mechanical trenching and was predicted to be de minimis (i.e.,  $<0.01$  km<sup>2</sup> with a max extent of 0.05 km) as a result of jet trenching. This is likely due to the orientation of the route with respect to the currents and the high fraction of fine material within that location. Variations in plume extent and duration for IAC installation can be attributed to differences in advance rates, which impacted the timing of the currents, and because the same volume of sediment was released over a longer period. Deposition  $\geq 1$  mm was limited to 0.20 km from the Monmouth ECC centerline and to 0.09 km of the Northern ECC centerline for the cable installation scenarios. For the jet-trenching cable installation scenarios, the maximum deposition associated with the IAC, Northern ECC, and Monmouth ECC was less than 1 mm, between 1-5 mm, and between 10-20 mm, respectively.

For the Monmouth and Northern representative HDD pit excavations, deposition  $\geq 1$  mm was predicted to extend a maximum distance of 0.48 km and 0.15 km, respectively. The representative Monmouth HDD pit excavation scenario was predicted to be the HDD pit with higher areas of deposition for the 1 mm, 5 mm, and 20 mm thresholds due to a higher fraction of fine sediment and the strong currents in that region. However, the representative Northern HDD pit excavation was predicted to have small areas ( $<0.01$  km<sup>2</sup>) exceeding the deposition threshold of 100 mm because the pit area primarily consisted of coarse sediment and therefore settled quickly within the vicinity of the source.

While the plume patterns for the respective representative IAC scenarios, offshore export cable scenarios, and HDD pit construction simulations were generally similar, differences in the extent and persistence of the plumes and the extent and thickness of deposition may be attributed to a variety of factors, including the following: the respective route orientation relative to currents, the timing of the currents, the depth at which the sediment is introduced to the water column, the relevant installation parameters, the volume of suspended sediment, and sediment grain size distribution.

This study summarizes a comprehensive analysis of the potential sediment disturbing activities associated with the construction activities anticipated within the Lease Area and ECCs. Several conservative assumptions were applied to the various scenarios and are outlined throughout this report. Based on the assumptions and model inputs used in this evaluation, results from this assessment provide an upper bound of the potential environmental impacts induced during seabed preparation, cable installation, and HDD pit excavation and backfill.

# 1 INTRODUCTION

Atlantic Shores Offshore Wind, LLC (Atlantic Shores) is a 50/50 joint venture between EDF-RE Offshore Development, LLC (an indirect, wholly owned subsidiary of EDF Renewables, Inc. [EDF Renewables]) and Shell New Energies US LLC (Shell). Atlantic Shores is submitting this Construction and Operations Plan (COP) supplement to the Bureau of Ocean Energy Management (BOEM) for the development of offshore wind energy generation known as the Atlantic Shores North Project (the Project) within the Lease Area OCS-A 0549 (Lease Area; Figure 1-1).

Atlantic Shores' Lease Area is located on the Outer Continental Shelf (OCS) within the New Jersey Wind Energy Area (NJWEA), which was identified by BOEM as suitable for offshore renewable energy development through a multi-year, public environmental review process. Atlantic Shores' proposed offshore wind energy generation facilities will be located in Lease Area OCS-A 0549, which is 81,129 acres (328.3 square kilometers [km<sup>2</sup>]) in area. Lease Area OCS-A 0549 is located north of and is adjacent to Atlantic Shores' Lease Area OCS-A 0499. At its closest point, the Lease Area is approximately 8.4 miles (mi) (13.5 kilometers [km]) from the New Jersey coast and approximately 60 mi (96.6 km) from the New York State coast. The facilities to be installed within the Lease Area will include: a maximum of up to 157 wind turbine generators (WTGs); up to 8 small, 4 medium, or 3 large offshore substations (OSSs); inter-array and/or inter-link cables connecting the WTGs and OSSs; and up to one permanent meteorological (met) tower. The WTGs and OSSs will be connected by a system of 66-kilovolt (kV) to 150 kV high voltage alternating current (HVAC) inter-array cables (IAC). OSSs within the Lease Area may be connected to each other via 66 kV to 275 kV HVAC inter-link cables.

Energy from the OSSs will be delivered to landfall sites on the New Jersey and/or New York coastlines via buried export cables. These cables will be located within designated Export Cable Corridors (ECCs), which extend from the Lease Area through New Jersey and/or New York State waters as well as Federal waters. Atlantic Shores has identified potential landfall sites in the following locations: southern Monmouth County, New Jersey (the Monmouth Landfall Site); northern Monmouth County (near Asbury), New Jersey (the Asbury Landfall Sites); southwest Staten Island, New York (The Raritan Bay Landfall Sites); and northeast Staten Island as well as Brooklyn, New York (The Narrows Landfall Sites).

The Monmouth ECC extends from south to north along the eastern side of the Lease Area (Figure 1-1). The Monmouth ECC then continues north prior to turning west to a terminus at the Monmouth Landfall Site. The total length of the Monmouth ECC associated with the Project from the Lease Area to the furthest potential landfall location is approximately 66.7 mi (97.5 km). This ECC will also be used to convey export cables associated with the Atlantic Shores South Project (Lease Area OCS-A 0499).

The Northern ECC extends from south to north along the eastern side of the Lease Area (Figure 1-1). It then continues north from the Lease Area to the New York State waters boundary, where it splits into branches to reach the Raritan Bay Landfall Sites on southwest Staten Island in Richmond County, New York and The Narrows Landfall Sites on northeast Staten Island and Brooklyn in Kings County, New York. The total length of the Northern ECC associated with the Project from the Lease Area to the furthest potential landfall location is approximately 97.9 mi (146.3 km). The Asbury Branch of the Northern ECC extends westward from the Northern ECC approximately 8.6 mi (13.9 km) to the potential Asbury Landfall Sites in northern Monmouth County, New Jersey. Atlantic Shores will use horizontal directional drilling (HDD) technology to install the export cables from an offshore point near the end of the ECCs to the Landfall Sites to minimize impacts to the intertidal and nearshore habitats and ensure stable burial of the cables.

The COP has been developed in accordance with 30 CFR Part 585, applicable BOEM and other regulatory guidance, and the stipulations in Atlantic Shores' Lease Agreement OCS-A 0549. Atlantic Shores is requesting BOEM review and authorization of the Project in accordance with their Project Design Envelope (PDE) guidance (BOEM, 2018). Atlantic Shores has sited the Project facilities and developed the PDE to maximize renewable energy production, minimize environmental effects, minimize cost to ratepayers, and address stakeholder concerns. The PDE articulates the maximum design scenario for key project components, such as the type and number of WTGs, foundation types, OSS types, cable types, and installation techniques. The

PDE provides Atlantic Shores with the necessary flexibility to respond to anticipated advancements in industry technologies and techniques, that even under a maximum scenario will not exceed an unreasonable level of environmental effects.

This appendix to the COP documents the sediment dispersion modeling assessment of the sediment-disturbing activities induced by offshore cable installation and seabed preparation operations associated with the development of the Project. While the cable installation methods may vary along the route depending on subsurface conditions, the installation methods are described in detail in the COP and the details of the assumed modeling parameters are documented within this report. Based on environmental surveys conducted for the Project, sand bedforms were identified within the ECCs and Lease Area. Therefore, dredging is anticipated and was modeled within a representative section of the Northern and Monmouth ECCs and within the Lease Area; this modeling simulated the impacts of sandwave clearance activities prior to cable installation using a Trailing Suction Hopper Dredge (TSHD).

Prior to installing the OSS and WTG foundations, the seabed will likely need to be cleared so that foundations are installed in a stable seabed. Therefore, four seabed foundation preparation simulations were evaluated: three at the Large OSS locations and the fourth at a single, representative WTG location. All seabed foundation preparation analyses assumed the use of a TSHD. Consistent with the PDE, this study simulated multiple scenarios to capture a conservative design and range of effects associated with seabed preparation activities, the installation of IACs in the Lease Area, offshore export cables in the two ECCs, and landfall approaches.

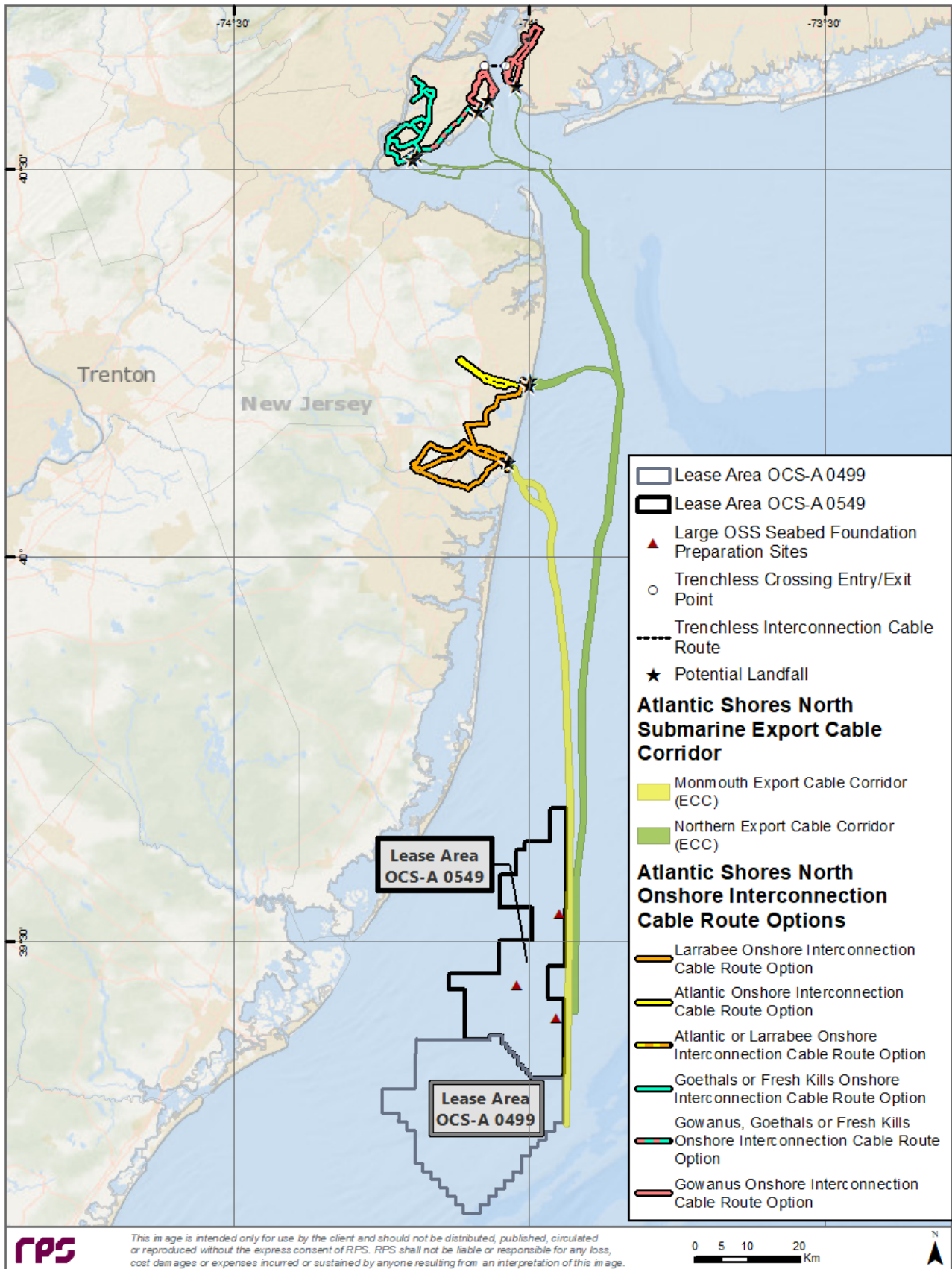


Figure 1-1: Map of Atlantic Shores Offshore Project Region with Offshore Components.



## 1.1 Study Scope and Objectives

RPS applied customized hydrodynamic and sediment dispersion models to assess potential effects from sediment suspension during construction activities. Specifically, this analysis includes two interconnected modeling tasks:

- Development of a three-dimensional (3D) hydrodynamic modeling application of a domain encompassing Atlantic Shores' activities using the Delft3D Flexible Mesh (FM) modeling suite; and
- Simulations of the suspended sediment fate and transport, including evaluation of seabed deposition and suspended sediment plumes, were performed using an RPS in-house model Suspended Sediment FATE (SSFATE) to simulate installation activities. Velocity fields developed using the Delft3D FM modeling suite were used as the primary forcing for SSFATE.

This study simulated multiple scenarios to capture a conservative design and an encompassing range of effects associated with seabed preparation prior to cable installation in the Lease Areas and ECCs, seabed preparation prior to foundation installation at three Large OSS locations and a representative WTG site, the installation of IACs in the Lease Area, offshore export cables in the two ECCs, and landfall approaches. Sand bedforms are mobile features. Removing the upper portions of the sand bedforms will facilitate cable installation within the stable seabed beneath, thereby ensuring that sand bedform migration will not lead to the exposure of a cable on the seafloor. The amount of required sand bedform dredging will vary based on the size of the sand bedforms and the achievable burial depth of the cable installation equipment employed. Once any needed sand bedform removal occurs, the installation and burial of the cable can occur.

Prior to cable installation, seabed preparation (in the form of dredging) may be required to clear sand bedforms within the Monmouth and Northern ECC. Use of a TSHD is assumed for this modeling assessment. A TSHD removes sediment by suction dredging through a drag arm near the seabed. The sediment-water slurry is stored in a hopper, with the majority of coarse material (e.g., sands) settling to the bottom and most of the fine material overflowing with the sediment-laden waters. Overflow occurs once the hopper reaches its maximum capacity, and then the TSHD releases the remaining sediment below the water surface within the ECC. For this modeling assessment, the dump sites are considered representative and are based on an estimated dredge capacity; more or fewer may be used during the actual construction activities. To bound the potential impacts for the dredging assessment, modeling was performed along a continuous portion (approximately 20% of ECC) of the Monmouth ECC and Northern ECC, and within the Lease Area, assuming approximately 10% of the anticipated total distance of the inter-array cables.

It is expected that there will be sufficient time between sandwave clearance and cable installation such that the effects from sandwave clearance do not compound or influence effects from cable installation activities. While several corridors may be cleared of sandwaves, each corridor would be cleared at different timeframes. Therefore, the simulation modeled for a single corridor in this study can be considered representative of other sandwave clearance activities in proximity to the Monmouth ECC and Northern ECC.

Prior to installing the OSS and WTG foundations, dredging around the actual foundation locations may be required to clear sandwaves and ensure foundations are installed in a stable seabed. It was assumed that a TSHD would be used for the foundation preparation operations at the three Large OSS sites and at one representative WTG site. It is anticipated that suspended sediment induced by seabed preparation activities for the WTG foundations will be separated in time and space such that the subsurface plumes will not interact. The representative WTG site was modeled at a sediment sampling location that contained a mixture of fine and coarse sediment because the Lease Area primarily consists of coarse sediment, with small regions in the southern portion comprised of clay and fine silt. This additional conservatism was included because these results are considered representative of the other 156 WTGs and one possible Permanent Met Tower which are distributed throughout the Lease Area. Modeling the seabed foundation preparation in a region with high fractions of clay and silt is considered representative because fine material takes longer to settle due to it being lighter than sand. Therefore, the sediment plume contains elevated water column concentrations for longer and is transported further from the release location. The same approach and grain size distribution was applied when modeling seabed foundation preparation at the three Large OSS sites.

The PDE describes multiple foundation types, some of which require dredging prior to the actual foundation installation (e.g., gravity-based structures). The actual approach is unknown at the time and may change depending on available technology and *in-situ* conditions at the time of construction. Therefore, additional conservatism was built into the study by selecting the largest potential disturbance area which was dictated by the Suction Bucket Jacket approach for both the WTG and OSS simulations. The largest area and in turn the largest volume of sediment released to the environment poses the highest potential environmental impact. The Large OSS locations were selected as representative, worst-case scenarios because they are anticipated to have the largest foundations which corresponds to the largest potential area that requires dredging. Thus, the seabed foundation preparation simulations at the Large OSS sites can be considered representative of the small and medium OSS sites because disturbance volumes and environmental impact, would be of lesser extent.

While it is proposed that multiple cables will be installed within each ECC, each cable will be installed in a separate trench at different timeframes. Therefore, the modeled scenarios can be considered as a single representative cable per ECC. The Monmouth export cable route diverges nearshore, resulting in two “branches”, the two branches were modeled separately for the Monmouth ECC to account for the environmental forcing conditions. The Northern ECC also has multiple landfall approaches, so one of the longest routes (Gowanus – South Beach Approach), within the most complex hydrodynamic conditions was selected and modeled in this assessment. Being one of the longer routes corresponds to the largest potential volume of resuspended sediment, and because it resides in an area of complex hydrodynamics the potential suspended sediment plume is subject to higher current velocities transporting it further from the source. Herein, this simulation will be referred to as the representative Northern ECC route as it provides a conservative approach and results can be considered representative of the other approach options in its proximity. While multiple landfall approaches are proposed, one landfall approach per ECC was simulated and can be considered representative of other landfall approaches in proximity to the ECC landfall locations.

This study was carried out to characterize the effects associated with the seabed preparation operations, offshore cable installation activities, and HDD pit excavation and backfill. These effects were quantified using two parameters: 1) water column concentrations of total suspended sediment (TSS), and 2) sediment thickness on the seabed resulting from the deposition of the suspended sediments over time. These thresholds were selected either because they are thresholds of biological significance or because they provide an effective means of demonstrating the physical effects. The results are presented with respect to the following thresholds:

- Water column concentrations thresholds: 10, 25, 50, 100, 200, and 650 milligrams per liter (mg/L);
- Water column exposure durations: 2, 4, 6, and 12 hours (hrs); and
- Seabed deposition: 1, 5, 10, 20, and 100 millimeters (mm).

These analyses provide conservative predictions of suspended sediment concentrations above ambient conditions that could result from the HDD pit excavations and cable installation activities associated with this Project. The selected thresholds are of biological significance (Anderson and Mackas, 1986; Berry et al., 2011; Cake, 1983; Essink, 1999; Fabricius, 2005; Gilmour, 1999; Hendrick et al., 2016; Murphy, 1985; Rayment, 2002; Read et al., 1982, 1983; Rogers, 1990; Turner and Miller, 1991; Wilber and Clarke, 2001) or because they provide an effective means of demonstrating the physical effects. Thresholds associated with biological significance are documented in Sections 4.5 and 4.6 of the COP, which are the benthic resources and finfish, invertebrates and essential fish habitat sections, respectively.

This report describes the models used, modeling approach, and results of the study. The hydrodynamic modeling approach is provided in Section 2 and the sediment dispersion modeling approach and results are summarized in Section 3. The references are provided in Section 0.

## 2 HYDRODYNAMIC MODELING

To capture near seabed sediment disturbance during construction activities, accurate representation of the hydrodynamic circulation in the bottom layer, just above the seabed, was necessary. A 3D model application in the area of interest (AOI) was developed using the Delft3D FM Flow model. The AOI spans from the entrance to Delaware Bay through New York Harbor and major adjoining rivers (e.g., Hudson, Raritan). These extents are significantly larger than the Atlantic Shores North project area, to accurately define the boundary condition, and capture the characteristic circulation close to sediment dispersion modeling sites.

The hydrodynamic model was used to simulate the current fields throughout the water column in this region during a representative time frame of construction activities for input to the sediment dispersion modeling. The following sections describe the environmental data used in the modeling, Delft3D FM framework, and the details of model development and application, including model setup and discussion of results.

### 2.1 Environmental Data

As inputs to the hydrodynamic model, environmental data were collected to reproduce the AOI's predominant conditions. Environmental data, including shoreline, bathymetry, winds, river discharge tidal elevations, and currents, were acquired to develop model boundary conditions and forcing, and calibrate and validate the model predictions. The locations of various data in relation to the project components are shown in Figure 2-1 and summarized in Table 2-1. Analysis and presentation of the data used for the study are detailed in subsequent sections.

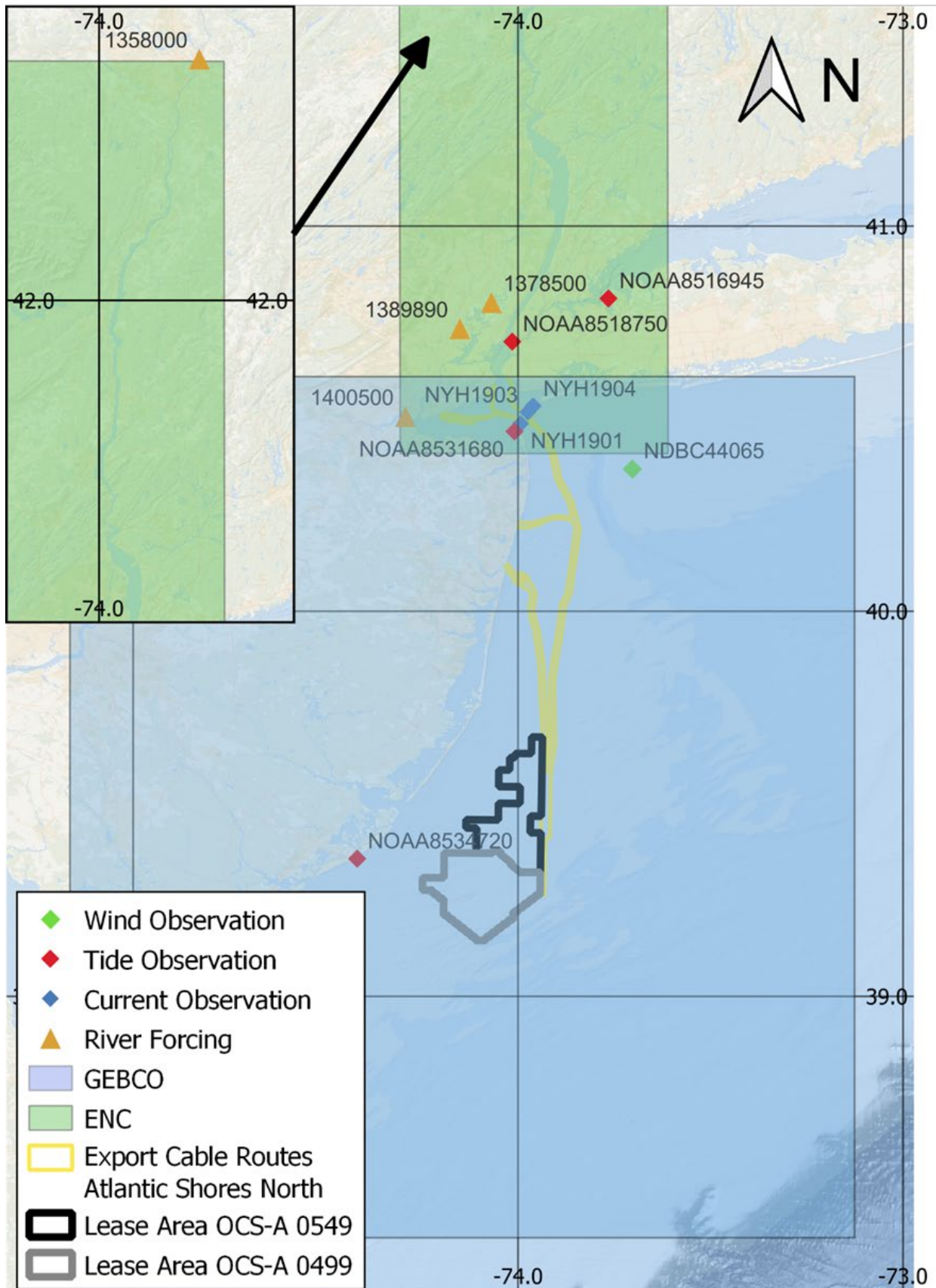


Figure 2-1: Location of project components, bathymetry data coverages, and environmental data observation stations

**Table 2-1: Summary of model and observation data in 2019, used in the modeling study.**

Data Source	Name	Location	Time Step	Longitude (°W)	Latitude (°N)
Wind Model Data (Forcing)	ERA5	10 m height, Global Model	1-hourly	75.2 – 73.0	38.2 – 42.8
Wind Observation (Validation)	NDBC 44065	4.1 m height, New York Bight	1-hourly	73.703	40.369
Tidal Elevation (Forcing)	TPX08 model	Offshore; Delaware Bay Entrance	-	-	-
	NOAA 8516945	Kings Point	6-Minute	73.765	40.811
Tidal Elevation (Validation)	NOAA 8534720	Atlantic City, NJ	6-Minute	74.418	39.357
	NOAA 8531680	Sandy Hook	6-Minute	74.009	40.467
	NOAA 8518750	The Battery	6-minute	74.015	40.700
River Discharge (Forcing)	USGS 1378500	Hackensack River	15-minute	74.027	40.948
	USGS 1358000	Hudson River	15-minute	73.688	42.752
	USGS 1389890	Passaic River	15-minute	74.128	40.885
	USGS 1400500	Raritan River	15-minute	74.583	40.555
Current Observation (Calibration and Validation)	NYH1901	New York Harbor (Depth of Measurement: -9.5 m MSL)	6-minute	73.993	40.487
	NYH1903	New York Harbor (Depth of Measurement: -8.5 m MSL)	6-minute	73.975	40.517
	NYH1904	New York Harbor (Depth of Measurement: -12.1 m MSL)	6-minute	73.961	40.533

### 2.1.1 Bathymetry and Shoreline

Publicly available bathymetry data were gathered from the National Oceanic and Atmospheric Administration (NOAA) Electronic Navigational Charts (ENC) datasets for coastal, offshore, and riverine locations. Data from the 2021 General Bathymetric Chart of the Oceans (GEBCO) were also downloaded for coastal and offshore waters of NJ and NY. The irregular spaced soundings referenced to mean sea level (MSL) from both datasets were interpolated to the hydrodynamic grid to provide complete coverage of water depths within the AOI. Table 2-2 provides a summary of the bathymetric datasets that were utilized, with the coverages shown in Table 2-1. The dataset was smoothed at the transition areas, to remove sharp gradients when moving from one source to another. The smoothing helps to create a featureless transition among different bathymetric datasets, and to increase the stability of the hydrodynamic model.

The shoreline for the modeling domain was developed using a 2017 Global Self-consistent, Hierarchical, High-resolution Geography Database (Wessel and Smith, 1996) to define the land and water boundary. The shoreline along the Hudson River was developed using the Hudson River Estuary project shapefile (New York State Department of Environmental Conservation, 2016).

**Table 2-2: Specifics of bathymetry datasets used for modeling.**

Name of Dataset	Owner/Provider	Minimum Horizontal Grid Size
GEBCO (2021)	British Oceanographic Data Centre	~320 m
ENC	NOAA	~10 m

### 2.1.2 Meteorological Observations

To force the surface boundary of the hydrodynamic model, atmosphere variables were obtained from the European Centre for Medium-Range Weather Forecasts (ECMWF) ReAnalysis 5th generation Wind (ERA5) product (Hersbach et al., 2020). ERA5 global wind data are available on an atmospheric model grid with 0.25° horizontal resolution (Copernicus Climate Change Service, 2018; Hersbach et al., 2020). Gridded U and V components of wind data at 10 m elevation over the modeling domain, with 1-hour timestep, was collected and used in this study (Table 2-1).

To validate the wind forcing dataset, ERA5 model output was interpolated from the four neighboring grid points to the location of the National Data Buoy Center (NDBC) buoy 44065 (Figure 2-1 and Table 2-1) for the modeling period of July 1<sup>st</sup>, through September 1<sup>st</sup>, 2019. The observed wind speed was adjusted from 4.1 m height to 10 m height, to be compared with 10 m wind from ERA5, using Bratton and Womeldorf (2011) equation:

$$V_2 = V_1 \left( \frac{H_2}{H_1} \right)^\alpha$$

where the wind velocity  $V_2$  at height  $H_2$  can be estimated using the wind speed velocity  $V_1$  recorded for a different elevation  $H_1$ , at the same site location. As the NDBC stations are in open water, the value of wind shear exponent ( $\alpha$ ) was set as 0.1 (Bratton and Womeldorf 2011). The comparison between the NDBC wind measurement and ERA5 output shows that ERA5 captures the directionality and speed of the wind in the study area quite well (Figure 2-2), and it was an appropriate wind source for forcing the hydrodynamic model.

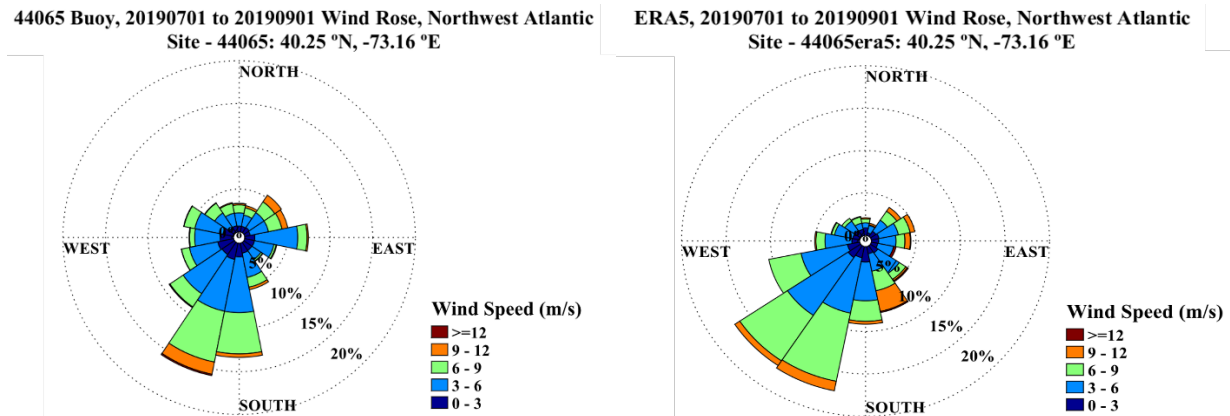


Figure 2-2: Comparison between wind measurement at NDBC buoy 44065 and interpolated data over the same time frame (July 1, 2019 through September 1, 2019) and location from the ERA5 dataset.

### 2.1.3 Sea Surface Height (Tides)

To force the open boundaries of the hydrodynamic model, surface tidal elevation at the open boundaries should be defined to appropriately model the ingoing and outgoing tidal flow into the domain. The specification of the sea surface height (SSH) can be introduced to the model in one of two methods: (1) defining tidal harmonic constituents (e.g., M2, K1, O1, S2, etc.) amplitude and phase, or (2) application of a tidal time series; both of which were used in this model.

Using the first method, nine harmonic constituents (phase and amplitude of M2, S2, N2, K1, K2, O1, P1, Q1, and M4), were derived from the Oregon State University Tidal Prediction Software (OTPS) at the offshore open boundary, at each vertex along the boundary. OTPS allows extracting harmonic constants from the TOPEX/Poseidon Global Inverse Solution tidal model (TPXO) at given locations (Egbert and Erofeeva, 2002). The TPXO is a series of fully-global models of ocean tides. The model output contains tidal harmonic constituent data across the globe. The model is based on data from the TOPEX/Poseidon and Jason satellites. TPXO was developed by assimilating altimetry and coastal tide gauge data into shallow water Laplace tidal equations on a  $1/30^\circ$  (~3 km) bathymetric grid, based on the Oregon State University Tidal Inversion Software (OTIS; Egbert et al., 1994; Egbert and Erofeeva, 2002). The depth grid for TPXO was made from GEBCO bathymetry model and from regional bathymetry data (Seifi et al., 2019). The implementation of the TPXO data, as the boundary forcing of the hydrodynamic model, is further discussed in Section 2.2.3.

Using the second method, SSH timeseries were downloaded from available NOAA Tidal Stations (Figure 2-1; Table 2-1) to develop model forcing at the tidal open boundaries closer to coastlines, where TPXO data were not available. Astronomical tidal elevation time series from NOAA Stations 8516945 (King’s Point) available at a 6-minute timestep, were obtained for the entirety of 2019 (Table 2-1). Tide elevation time series were also obtained for the entirety of 2019 for calibration and validation of the model at three station locations inside the modeling domain (Figure 2-1; Table 2-1).

### 2.1.4 River Data

River flux data were collected from four US Geological Survey (USGS) monitoring stations at the Hackensack, Hudson, Passaic, and Raritan rivers (Figure 2-1; Table 2-1). Discharges from these four rivers impact the flow and circulation of the estuarine environment along the coast and in the Harbor near the locations of the cable route. The 15-minute flow rate data from these stations were specified in the model as discharge open boundary conditions as a function of time (see Section 2.2.3).

## 2.1.5 Ocean Current Observations

Observations of ocean currents were obtained at three stations within New York Harbor (Figure 2-1; Table 2-1). The current observations were used to calibrate and validate model predictions through comparisons of timeseries at similar model and observation depths.

## 2.2 Delft3D Hydrodynamic Model Application

The Delft3D FM modeling suite (Deltares, 2022) was used to develop a 3D hydrodynamic model application for the AOI offshore northeastern U.S., to capture the circulation patterns, and to provide the hydrodynamic input for the sediment dispersion modeling. This modeling suite is widely used for hydrodynamics studies, is very well accepted by scientific communities, and has been validated in comparison with lab experiments. List of publication that have used and validated Delft3D model can be accessed on Delft3D Google Scholar (2022).

### 2.2.1 Delft3D Model Description

The hydrodynamic module of Delft3D FM modeling suite, D-Flow FM, simulates tidal and/or meteorological forced unsteady flow and transport phenomena (Deltares, 2022). D-Flow FM solves the one-, two- and three-dimensional shallow-water equations (Kernkamp et al., 2011; Lesser et al., 2004). D-Flow FM is a multi-dimensional, boundary-fitted hydrodynamic model that operates with either cartesian or spherical coordinates, in either two or three dimensions (Deltares, 2022). The boundary-fitting technique matches the grid coordinates with shoreline and bathymetric feature boundaries for highly accurate representations of areas with complex coastal or riverine geometries. This allows for easy development of model grids that conform well to complex shorelines and sinuous channels and can include high resolution only in desired areas.

Two vertical grid co-ordinate systems are available, the sigma-grid system (a more common application initially designed for atmospheric models) and the Z-grid system (for simulations of weakly forced stratified water systems). The sigma-grid has several layers bounded by two sigma-planes, which follow the bottom topography and the free surface (Figure 2-3) to obtain a smooth representation of the topography. The Z-grid has horizontal coordinate lines that are (nearly) parallel with density interfaces (isopycnals) in regions with steep bottom slopes, for modeling stratified systems with horizontal density gradient (Deltares, 2022).

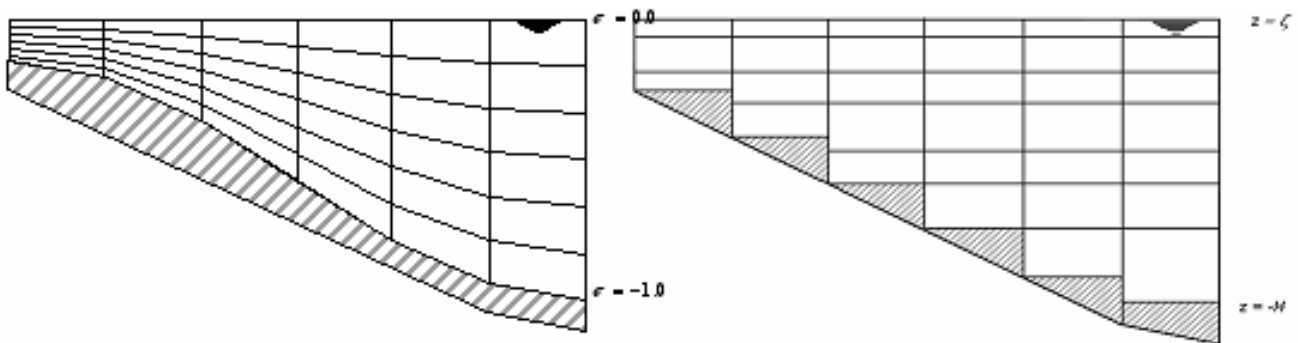


**Figure 2-3: Schematic of the D-Flow FM vertical sigma (left) and vertical Z-coordinate (right) systems (Deltares, 2022).**

The model was run using sigma and spherical coordinates, and a variable time step that is determined based on the metrics of model stability as a function of velocity, water depth, and grid cell size (also known as Courant Number). The maximum model time step was set at 30 seconds. The model was calibrated for currents for a two month-long period (Section 2.2.4) and validated for a two-month period (Section 2.2.5). The validation period overlapped with the period used to generate currents for sediment dispersion modeling. The hydrodynamic modeling was initiated one week prior to the calibration and validation, serving as a warm-up period to allow the boundary condition, and forcing to propagate throughout the domain and reach an optimal



state. The flow was forced by tide or river discharges at the open boundaries and wind stress at the free surface.

## **2.2.2 Model Grid**

To appropriately capture the current circulation patterns in the AOI, a FM grid was developed to cover the study area using the Delft RGFRID tool. The full extent of the hydrodynamic model grid is represented in Figure 2-4. The model is forced by tidal elevation and river discharge at the open boundaries, and also by wind at the surface boundary. The domain starts inside the continental shelf and extends west and north towards the New Jersey and Long Island shorelines, and into New York Harbor.

The minimum grid cell's edge length was about 40 m in New York Harbor, with larger grid cell dimensions ranging from approximately 4 km at the offshore boundary. The grid was developed using an iterative process to ensure there was sufficient grid resolution throughout the model domain to capture the physics accurately, especially close to the cable routes, while optimizing computational modeling time. The final computational grid for the entire domain consists of 33,679 cells and 19,017 nodes.

The Delft model gridding tool, QUICKIN, was then used to grid the bathymetry data and assign a unique depth value to each cell, either through averaging of multiple values in a designated cell or interpolating for the occasional cell where no depth data are available (see Section 2.1.1). The resulting grid and associated depths relative to MSL were then manually checked for outliers. The maximum depth in the model bathymetry was 73 m close to the offshore open boundary (Figure 2-5).

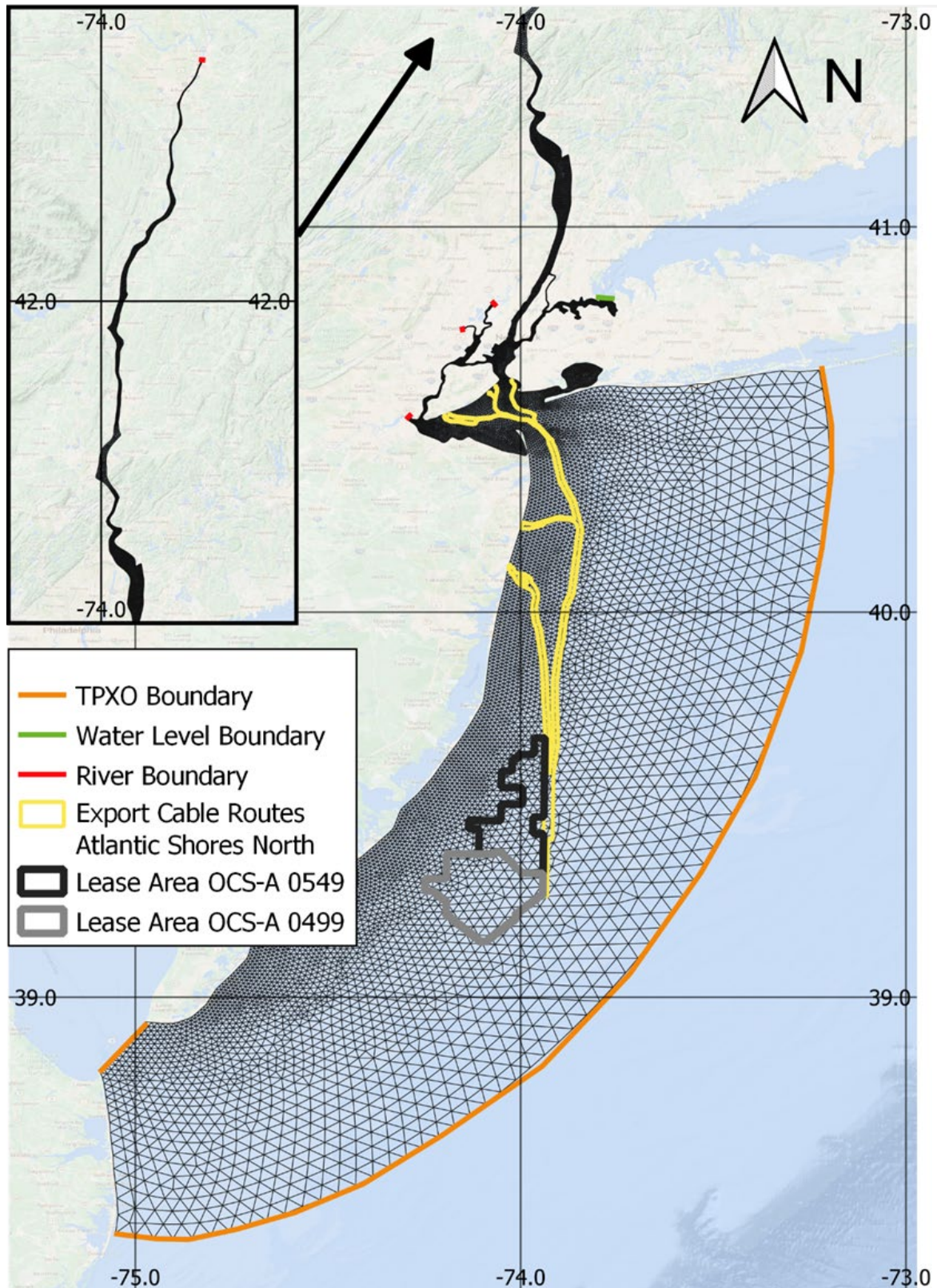


Figure 2-4: D-Flow FM model grid coverage of the Atlantic Shores North AOI, and location of open boundaries.

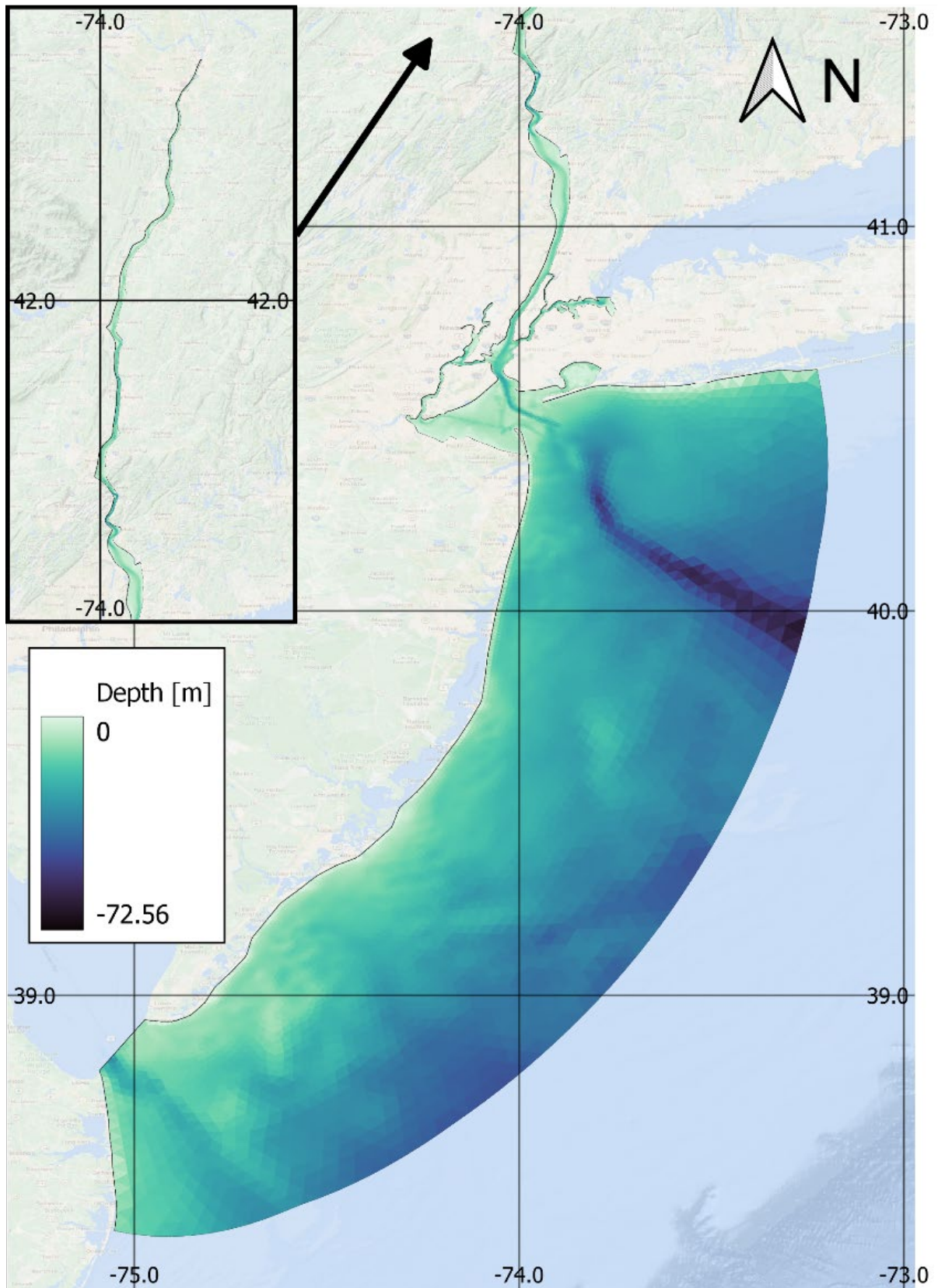


Figure 2-5: Illustration of the bathymetry of the domain interpolated to the D-Flow FM.

### 2.2.3 Boundary and Initial Conditions

Model boundary conditions for this application include specification of wind speed 10 m above the free surface applied over the modeling domain, in addition to tidal characteristics at open boundaries. Boundary conditions as mapped in Figure 2-4 are:

- **Meteorological Boundary Conditions (See Section 2.1.2):** The wind forcing as the surface boundary covers the entire gridded area. Meteorological data were obtained from the ERA5 model dataset and was applied to the entire grid surface as U (Eastward) and V (Northward) velocities.
- **Tidal Boundary Conditions (See Section 2.1.3):** The D-Flow FM model requires water levels, or tidal phase and amplitude prescribed along open boundaries. These tidal boundaries allow the transfer of external tidal flow into the domain. For this modeling study, the offshore open boundary of the model domain was located in the Atlantic Ocean (Figure 2-4). Spatially varying tidal amplitude and phases of harmonic constituent were extracted from the TPXO dataset at each offshore boundary node. TPXO data were also prescribed at the southern boundary along Delaware Bay. Water levels were also prescribed along the Long Island Sound boundary in the model domain. This water level boundary condition was prescribed with timeseries data from a NOAA station at Kings Point (Figure 2-1; Table 2-1).
- **River Boundary Conditions (See Section 2.1.4):** River discharges were included from four rivers (i.e., Hackensack, Hudson, Passaic, and Raritan Rivers) with significant flows into the model domain (Figure 2-1; Table 2-1). The boundary conditions were specified by a time series extracted from the corresponding USGS gauge and applied to the Delft3D model at 15-minute intervals.

### 2.2.4 Model Calibration

Parameters in the Delft3D setup were analyzed for month-long periods at three current observation locations (Figure 2-1) to calibrate the model before validating and applying the model for hindcast simulation. These calibration months were selected based on the availability of observation data near the export cable route. Parameters that were considered in the calibration process included horizontal resolution of the grid and bottom roughness as a Manning's n coefficient. Comparisons of U and V components of velocity are shown in Figure 2-10 to Figure 2-12. The figures show that the model was able to recreate the semidiurnal nature of the tides and the spring/neap cycle of changing tidal amplitude. To reach a better agreement between modeled and measured values, the Manning's n coefficient was adjusted to calibrate the modeled currents to the observations at the observation station. Table 2-3 summarizes the statistics of model performance in comparison with the observation for currents.

Table 2-3: Statistical evaluation of bottom current velocity components (m/s) of the Delft3D application compared with observations at NYH1901, NYH1903, and NYH1904.

NYH1901				
Velocity Component	Statistical measure	n = 0.02	n = 0.025	n = 0.03
U	Root mean square error (RMSE; m/s)	0.28	0.23	0.19
	Mean absolute error (MAE; m/s)	0.23	0.19	0.16
V	RMSE (m/s)	0.13	0.14	0.15
	MAE (m/s)	0.11	0.12	0.12

NYH1903				
Velocity Component	Statistical measure	n = 0.02	n = 0.025	n = 0.03
U	RMSE (m/s)	0.13	0.12	0.11
	MAE (m/s)	0.10	0.10	0.09
V	RMSE (m/s)	0.09	0.09	0.09
	MAE (m/s)	0.08	0.07	0.07

NYH1904				
Velocity Component	Statistical measure	n = 0.02	n = 0.025	n = 0.03
U	RMSE (m/s)	0.11	0.10	0.09
	MAE (m/s)	0.09	0.07	0.07
V	RMSE (m/s)	0.10	0.09	0.08
	MAE (m/s)	0.09	0.07	0.07

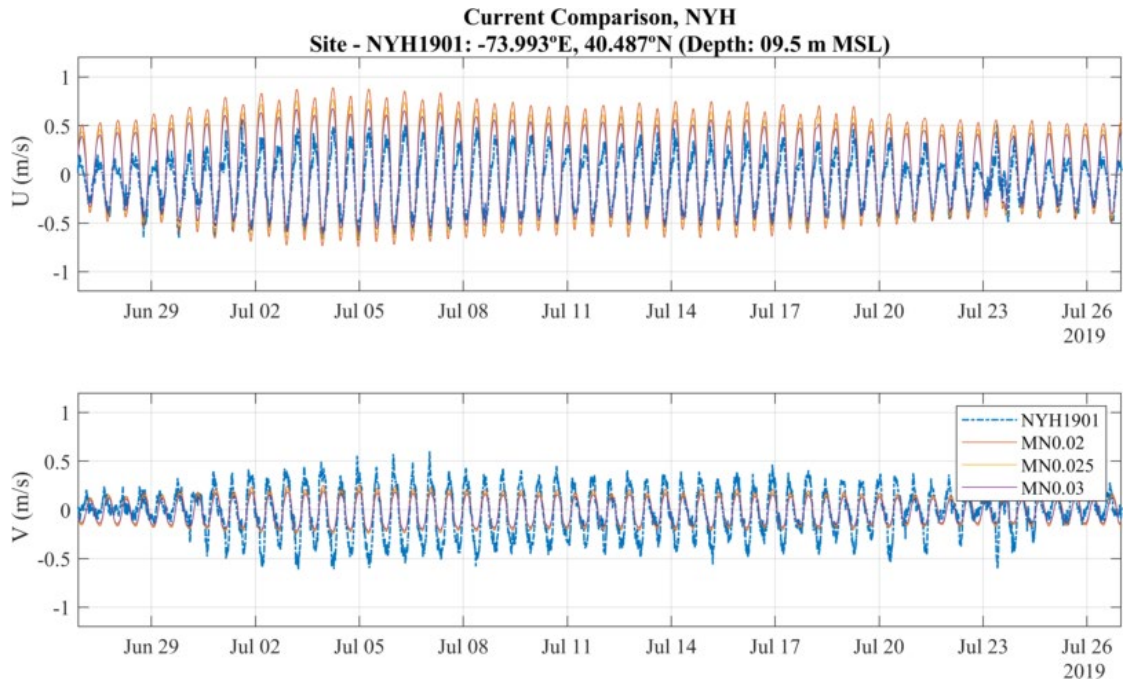


Figure 2-6: Bottom layer current velocity components from NOAA station observation at a depth of 9.5 m (blue) and hydrodynamic model predictions at a depth of 8.1 m (orange dashed) at NYH1901 for the calibration period.

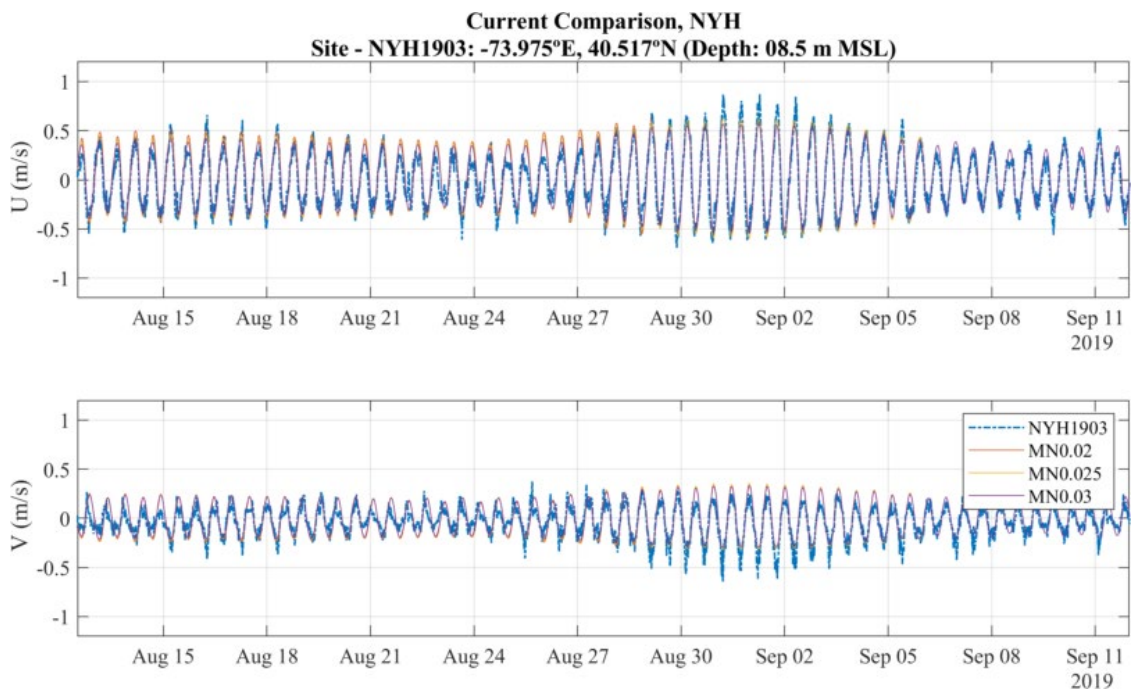
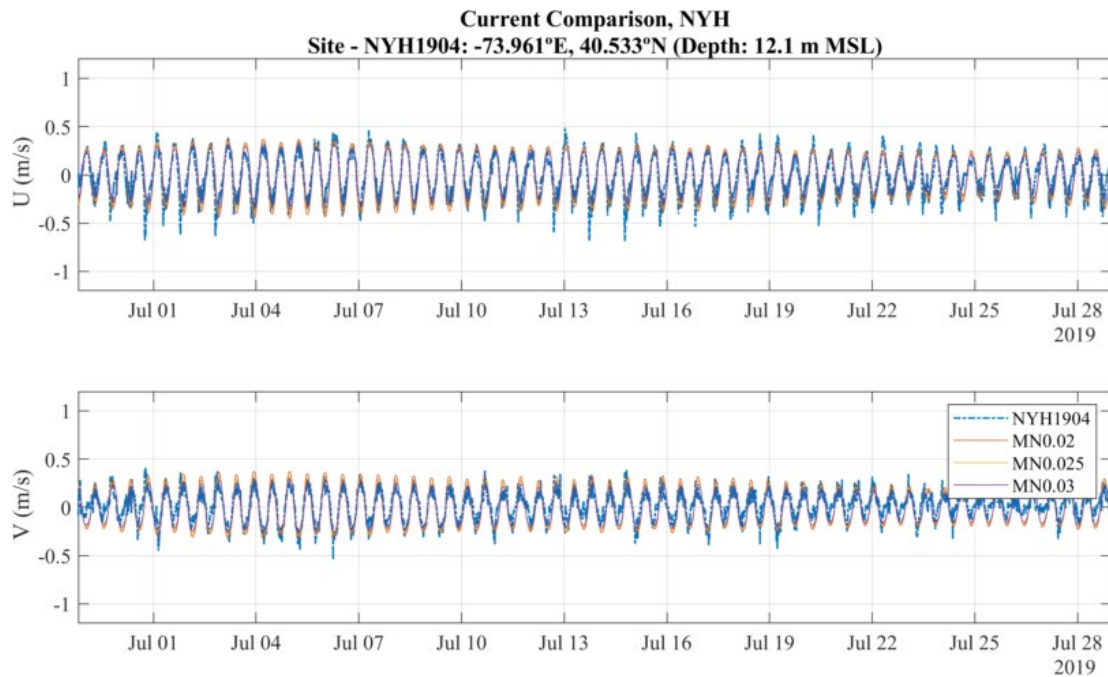


Figure 2-7: Bottom layer current velocity components from NOAA station observation at a depth of 8.5 m (blue) and hydrodynamic model predictions at a depth of 8.1 m (orange dashed) at NYH1903 for the calibration period.



**Figure 2-8: Bottom layer current velocity components from NOAA station observation at a depth of 12.1 m (blue) and hydrodynamic model predictions at a depth of 11.9 m (orange dashed) at NYH1904 for the calibration period.**

### 2.2.5 Model Validation

The Delft3D model was validated for a two-month period from April 15, 2019, through June 15, 2019, which overlapped with the sediment dispersion modeling time frame. Table 2-4 shows the statistics of model performance for tidal elevation predictions in comparisons with the NOAA stations (Figure 2-9). Table 2-5 shows the statistics of model performance for current comparison (Figure 2-10 - Figure 2-12). The model was able to predict the water level at different locations in the domain accurately (Figure 2-9). The model recreated the semidiurnal nature of the tides and further was able to reproduce the spring/neap cycle of changing tidal amplitude. The model did have trouble with capturing the portion of the water level related to non-cyclical forcing.

Statistics of model performance for eastward (U component) and northward (V component) velocities (Table 2-5) show that, in general, the model was able to recreate the trends of speed and direction well. The model captured the current speed well for stations NYH1903 and NYH1904 but did not perform as well with recreating currents at station NYH1901. As any changes in Manning coefficient and other parameters will impact the current magnitude at the other two stations, which already showed good agreement with the observation, the model was accepted as is, and the hydrodynamic modeling for forcing sediment dispersion model was run using this final validated model.

**Table 2-4: Statistical evaluation of SSH ( m) of the Delft3D application compared with observations at three NOAA Stations.**

Velocity Component	Statistical measure	The Battery	Sandy Hook	Atlantic City
SSH	RMSE (m)	0.21	0.17	0.14
	MAE (m)	0.17	0.13	0.11

**Table 2-5: Statistical evaluation of bottom current velocity components (m/s) of the Delft3D application compared with observations at three NYH Stations.**

Velocity Component	Statistical measure	NYH1901	NYH1903	NYH1904
U	RMSE (m/s)	0.19	0.08	0.07
	MAE (m/s)	0.16	0.06	0.06
V	RMSE (m/s)	0.12	0.07	0.06
	MAE (m/s)	0.09	0.05	0.05



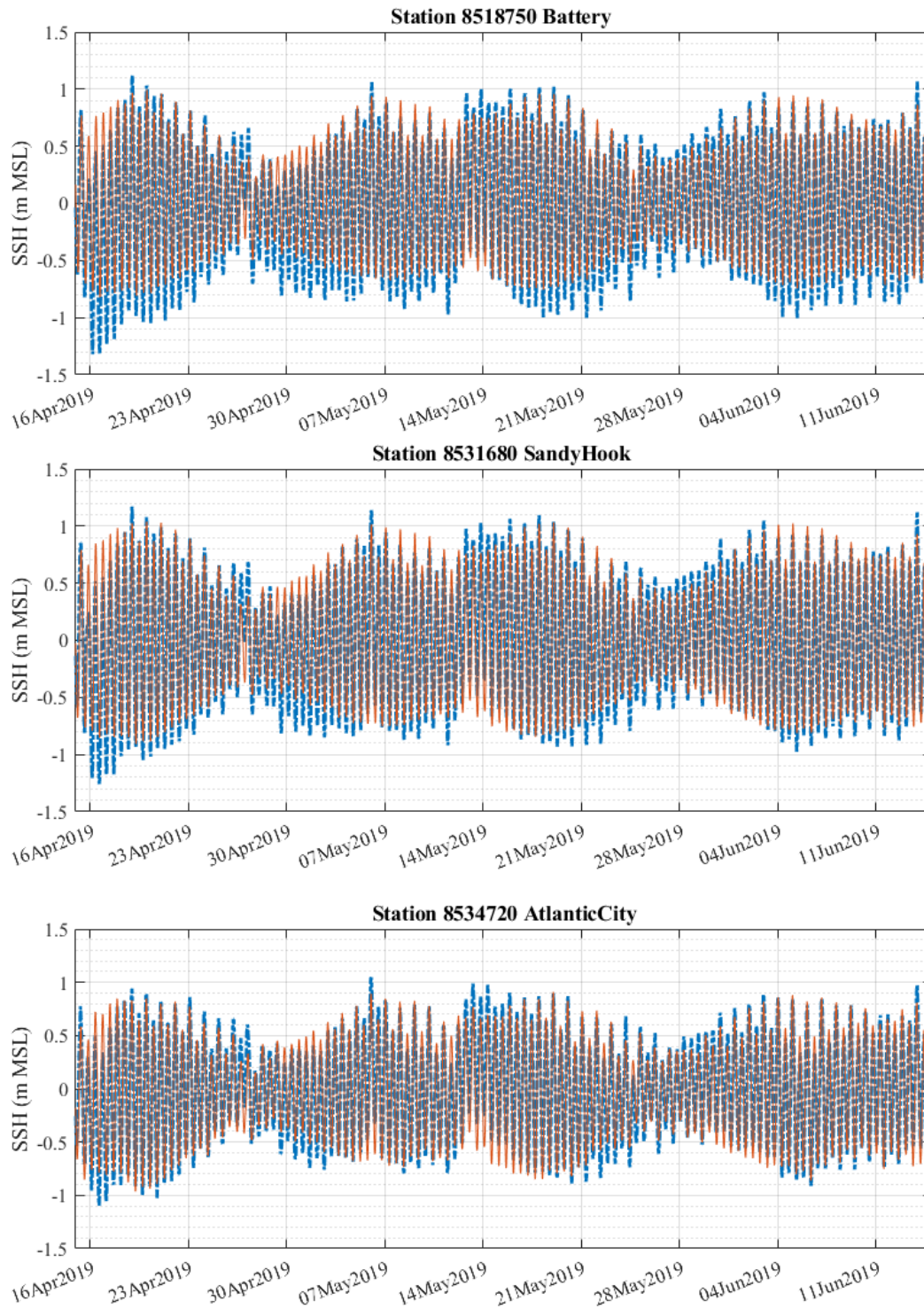
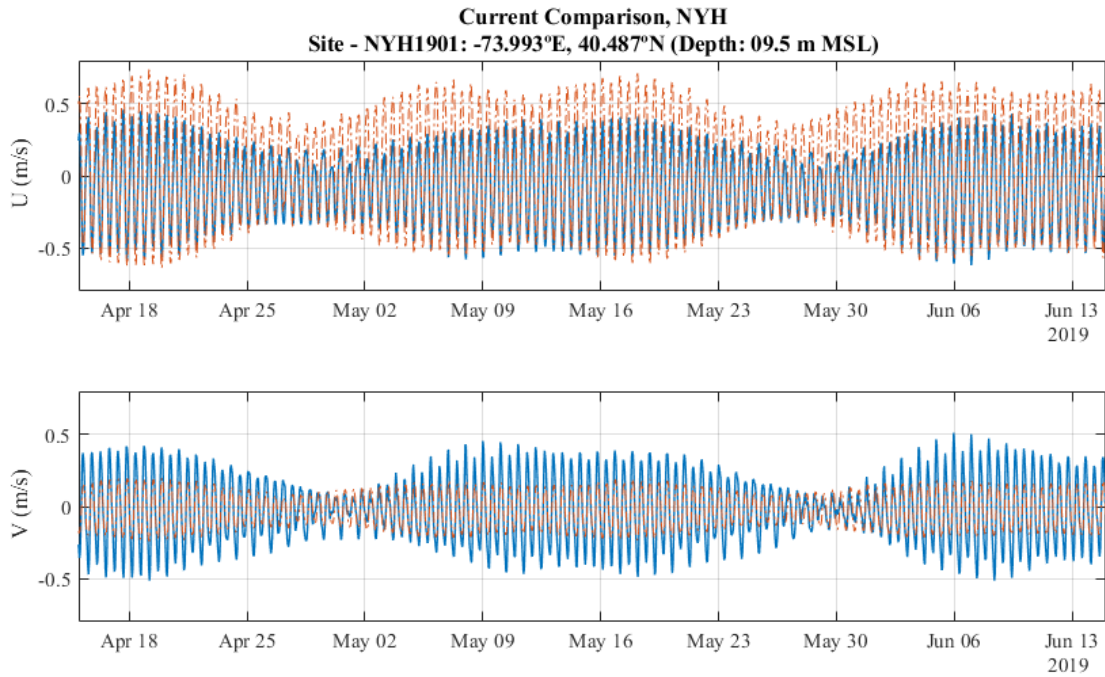
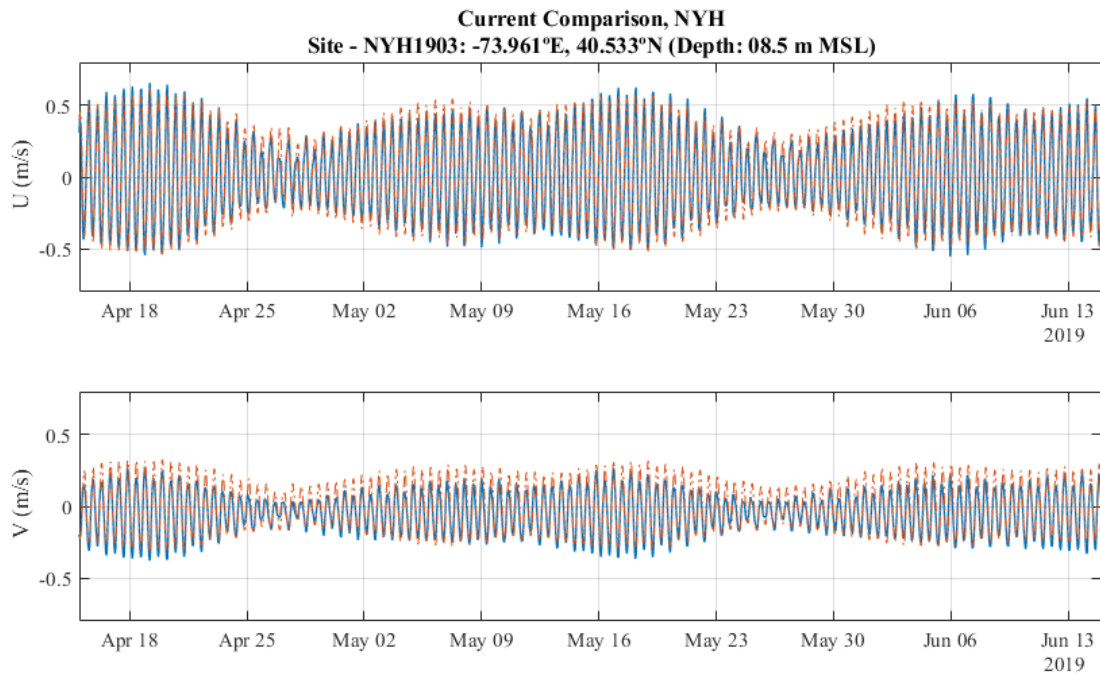


Figure 2-9: SSH (in meters) of NOAA station (blue) and Delft3D (orange dashed) at each of the three tidal stations (Table 2-1) during the validation period.



**Figure 2-10: Bottom-layer current velocity components of NOAA station at a depth of 9.5 m (blue) and hydrodynamic model predictions at a depth of 8.1 m (orange dashed) at NYH1901 station for the validation period.**



**Figure 2-11: Bottom-layer current velocity components of NOAA station at a depth of 8.5 m (blue) and hydrodynamic model predictions at a depth of 8.1 m (orange dashed) at NYH1903 station for the validation period.**

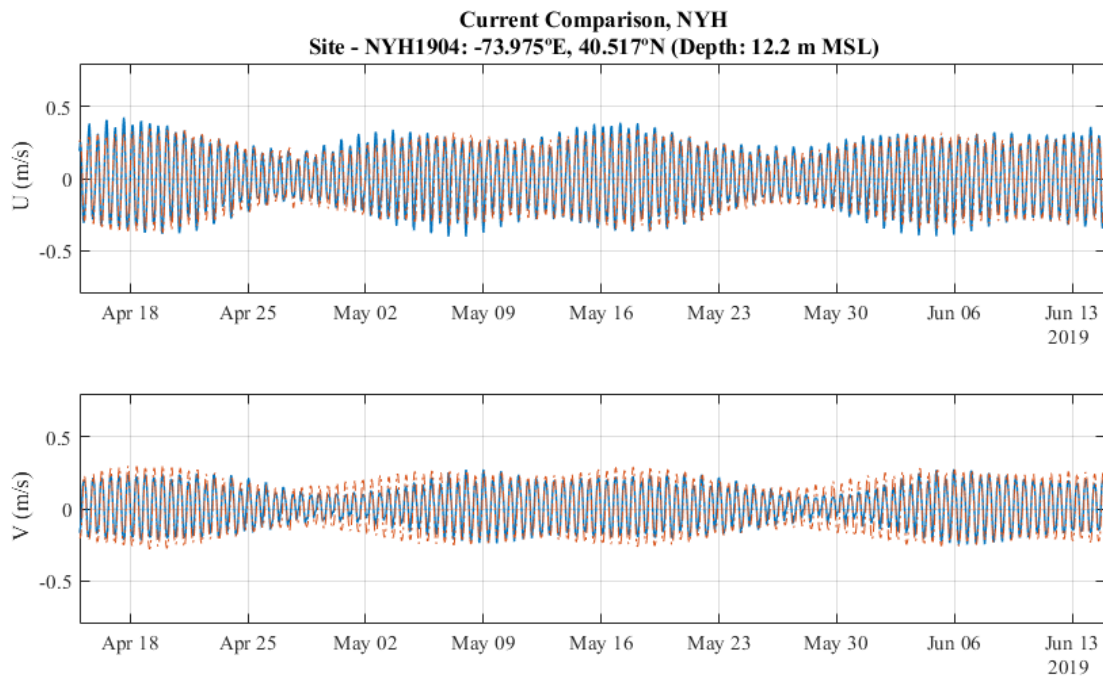


**Figure 2-12: Bottom-layer current velocity components of NOAA station at a depth of 12.2 m (blue) and hydrodynamic model predictions at a depth of 11.9 m (orange dashed) at NYH1904 station for the validation period.**

### 2.2.6 Model Results for Use in Sediment Transport Modeling Scenarios

Following the model validation, a scenario time period was selected based on the anticipated construction schedule of Spring, as provided by the client. The time period starting in May of 2019 was established as a period that represented normal conditions, based on long-term analysis of the wind forcing. The bottom current magnitude at each grid cell location during a flood time step (18-May-2019 22:00) is shown in Figure 2-13. Similarly, bottom current magnitude at each grid cell location during a flood time step (19-May-2019 18:30) is shown in Figure 2-14.

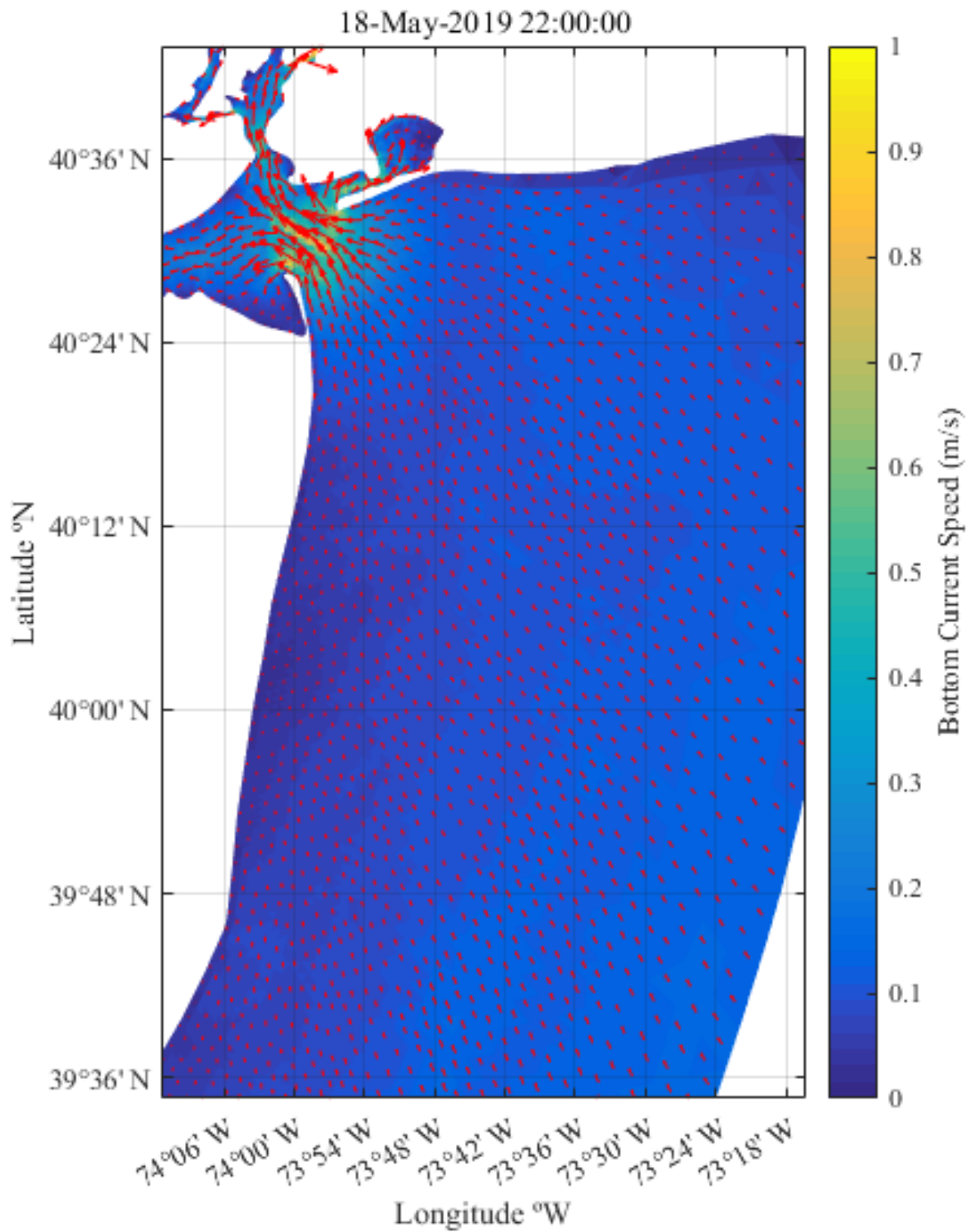


Figure 2-13: Color contour map showing bottom current velocity magnitude, overlaid with vectors (red) for a flood timestep (18-May-2019 22:00).

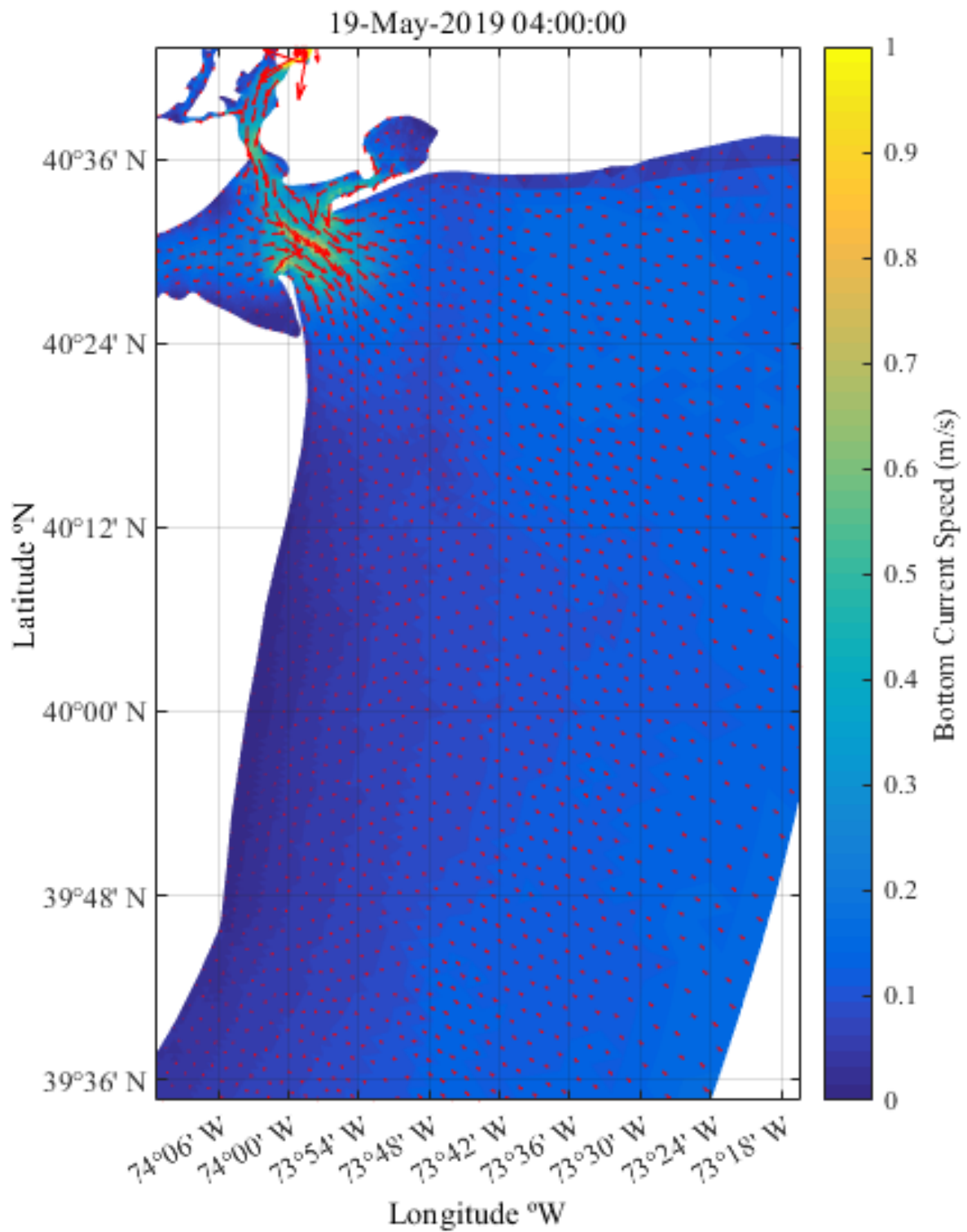


Figure 2-14: Color contour map showing bottom current velocity magnitude, overlaid with vectors (red) for an ebb timestep (19-May-2019 04:00).

## 3 SEDIMENT MODELING

### 3.1 SSFATE Modeling Approach

Sediment transport associated with the construction activities was simulated using RPS's SSFATE model. The model requires inputs defining the environment (e.g., water depths, currents) and the construction activity loading (e.g., sediment grain size, resuspended volume) to predict the associated sediment plume and seabed deposition. Details of the model and theory are provided in the following sections.

#### 3.1.1 SSFATE Model Description

SSFATE is a 3D Lagrangian (particle) model developed jointly by the United States Army Corp of Engineers' (USACE) Environmental Research and Development Center and Applied Science Associates (now RPS) to simulate sediment resuspension and deposition originally from marine dredging operations. Model development was documented in a series of USACE' Dredging Operations and Environmental Research Program technical notes (Johnson et al., 2000; Swanson et al., 2000), at previous World Dredging Conferences (Anderson et al. 2001), and at a series of Western Dredging Association Conferences (Swanson et al., 2004; Swanson & Isaji, 2006). Following dozens of technical studies, which demonstrated successful application to dredging, SSFATE was further developed to include simulation of cable and pipeline burial operations using water jet trenchers (Swanson & Isaji, 2006) and mechanical ploughs, as well as sediment dumping and dewatering operations. The current modeling system includes a Geographic Information System (GIS)-based interface for visualization and analysis of model output.

SSFATE computes TSS concentrations in the water column and sedimentation patterns on the seabed resulting from sediment-disturbing activities. The model requires a spatial and time-varying circulation field (typically from hydrodynamic model output), definition of the water body bathymetry, and parameterization of the sediment disturbance (source), which includes sediment grain size data and sediment flux description. The model predicts the transport, dispersion, and settling of suspended sediment released to the water column. The focus of the model is on the far-field processes (i.e., beyond the initial disturbance) affecting the dispersion of suspended sediment. The model uses specifications for the suspended sediment source strengths (i.e., mass flux), vertical distributions of sediments, and sediment grain-size distributions to represent loads to the water column from different types of mechanical or hydraulic dredges, sediment dumping practices, or other sediment-disturbing activities, such as jetting or ploughing for cable or pipeline burial. Multiple sediment types or fractions can be simulated simultaneously, as can discharges from moving sources.

SSFATE has been successfully applied to a number of recent modeling studies with these studies receiving acceptance from federal and state regulatory agencies.


#### 3.1.2 Model Theory

SSFATE addresses the short-term movement of sediments that are disturbed during mechanical ploughing, hydraulic jetting, dredging, and other processes where sediment is suspended into the water column. The model predicts the 3D path and fate of sediment particles based on sediment properties, sediment loading characteristics, and environmental conditions (e.g., bathymetry and currents). The computational model uses a Lagrangian or particle-based scheme to represent the total mass of sediments suspended over time, which provides a method to track suspended sediment without any loss of mass as compared to Eulerian (continuous) models due to the nature of the numerical approximation used for the conservation equations. Thus, the method is not subject to artificial diffusion near sharp concentration gradients and can easily simulate all types of sediment sources.

Sediment particles in SSFATE are divided into five size classes, each having unique behaviors for transport, dispersion, and settling (Table 3-1). For any given location (segment of the route), the sediment characterization is defined by this set of five classes, with each class representing a portion of the distribution and all five classes summing to 100%. The model determines the number of particles used per time step

depending on the model time step and overall duration thereby ensuring an equal number of particles is used to define the source throughout the simulation. While a minimum of one particle per sediment size class per time step is enforced, typically multiple particles are used. The mass per particle varies depending on the total number of particles released, the grain size distribution, and the mass flux per time step.

**Table 3-1: Sediment Size Classes used in SSFATE.**

Description	Class	Type	Size Range (microns)
Fine  Coarse	1	Clay	0-7
	2	Fine silt	8-35
	3	Coarse silt	36-74
	4	Fine sand	75-130
	5	Coarse sand	>130

Horizontal transport, settling, and turbulence-induced suspension of each particle are computed independently by the model for each time step. Particle advection is based on the relationship that a particle moves linearly, in three-dimensions, with a local velocity obtained from the hydrodynamic field, for a specified model time step. Diffusion is assumed to follow a simple random walk process, with the diffusion distance defined as the square root of the product of an input diffusion coefficient, and at each time step is decomposed into X and Y displacements via a random direction function. The vertical Z diffusion distance is scaled by a random positive or negative direction.

Particle settling rates are calculated using Stokes equations and are based on the size and density of each particle class. Settling of mixtures of particles is a complex process due to interaction of the different size classes, some of which tend to be cohesive and thus clump together to form larger particles that have different settling rates than would be expected based on their individual sizes. Enhanced settlement rates due to flocculation and scavenging are particularly important for clay and fine-silt sized particles (Swanson et al., 2004; Teeter 1998), and these processes have been implemented in SSFATE. These processes are bound by upper and lower concentration limits, defined through empirical studies, which contribute to flocculation for each size class of particles. Above and below these limits, particle collisions are either too infrequent to promote aggregation or so numerous that the interactions hinder settling.

Deposition is calculated as a probability function of the prevailing bottom stress and local sediment concentration and size class. The bottom shear stress is based on the combined velocity due to waves (if used) and currents using the parametric approximation by Soulsby (1998). Sediment particles that are deposited may be subsequently resuspended into the lower water column if critical levels of bottom stress are exceeded, and the model employs two different resuspension algorithms. The first applies to material deposited in the last tidal cycle (Lin et al., 2003). This accounts for the fact that newly-deposited material will not have had time to consolidate and will be resuspended with less effort (lower shear force) than consolidated bottom material. The second algorithm is the established Van Rijn (1989) method and applies to all other material that has been deposited prior to the start of the last tidal cycle. Swanson et al. (2007) summarize the justifications and tests for each of these resuspension schemes. Particles initially released by operations are continuously tracked for the length of the simulation, whether in suspension or deposited.

For each model time step, the suspended concentration of each sediment class as well as the total concentration is computed on a concentration grid. The concentration grid is a uniform rectangular grid in the horizontal dimension with user-specified cell size and a uniform thickness in the vertical dimension (z-grid). The concentration grid is independent of the resolution of the hydrodynamic data used to calculate transport, thus supporting finer spatial differentiation of plume concentrations and avoiding underestimation of concentrations caused by spatial averaging over larger volumes/areas. Model outputs include but are not limited to: water-column concentrations in both horizontal and vertical dimensions; time-series plots of suspended sediment concentrations at points of interest; and thickness contours of sediment deposited on the

seafloor. Deposition is calculated as the mass of sediment particles that accumulate over a unit area and is calculated on the same grid as concentration. Because the amount of water in the deposited sediment is unknown, by default, SSFATE converts deposition mass to thickness by assuming no water content.

For a detailed description of the SSFATE model equations governing sediment transport, settling, deposition, and resuspension, the interested reader is directed to Swanson et al. (2007).

## **3.2 SSFATE Data Needs**

The sediment modeling was carried out using RPS in-house model SSFATE. Setup of an SSFATE model scenario consists of defining how each sediment disturbance activity will be parameterized, establishing the sediment source terms, and defining environmental and numerical calculation parameters. For each scenario, the source definition includes:

- Sediment characteristics (e.g., grain size distribution, moisture content) along the route;
- The geographic extent of the activity (point release versus line source [route]);
- Timing and duration of the activity;
- Volumes, cross-sectional areas, and depths of the trench or excavation pit;
- The production rate for each sediment disturbance method;
- Loss (mobilization) rates for each sediment disturbance method; and
- The vertical distribution of sediments as they are initially released to the water column.

The sediment source for HDD pit excavation and backfill, seabed preparation, and cable installation simulations are defined through a load source file, which defines the location of the sources, mass flux of sediment disturbed through operations, loss rate of the disturbed flux resuspended into the water column, vertical position of the mass introduced to the water column, and grain size distribution of the mass introduced to the water column along the route of installation. A component of the sediment grain size distribution is a definition of the percent solids, which is used in the mass flux calculation. Bed sediments contain some water within interstitial pore spaces, and therefore the trench volume consists of both sediment and interstitial water. Consequently, the percent solid of the sediment sample, as based on laboratory measure of moisture content, is used in the calculation of total mass flux. The sediment source can vary spatially, and therefore the line source file is broken into multiple discrete entries, each representing a segment of the route with uniform characteristics. These segments are defined as such in order to capture curved route geometry and provide a continuous route aligned with the installation plan.

A model scenario also requires characterization of the environment, including a definition of the study area's spatially and time-varying currents (Delft3D output) and water body bathymetry. Model setup also involves specification of the concentration and deposition grid, which is the grid at which concentration and deposition calculations are made. The concentration and deposition grid in SSFATE is independent of the resolution of the bathymetric data (Section 2.1.1) or hydrodynamic model grid (Section 2.2.2); this allows finer resolution which better captures water column concentrations without being biased by numerical diffusion. The concentration and deposition gridding are based on a prescribed square grid resolution in the horizontal plan view and a constant thickness in the vertical. The extent of the concentration is determined dynamically, fit to the extent the sediments travel.

The following sections describe the sediment characteristics used in modeling (Section 3.2.1), model timeframe (Section 3.2.2), and the relevant input parameters used in this assessment (Section 3.2.3 and Section 3.2.4).

### **3.2.1 Sediment Characteristics**

The sediment characteristics are a key factor of the sediment load definition input to the SSFATE model. The spatially varying sediment characteristics were developed based on analysis of the vibracore samples. The details of the sediment sampling and laboratory analysis for the sediment sampling are documented in Volume II, Appendix II-A3 of the COP. A description of the data manipulation process, as it pertains to modeling, is



described below. The objective of the RPS analysis of the sediment data was to develop the sediment characteristics that represent the depth of disturbance into the seabed for each construction activity to represent the depth of sediments that may get resuspended during the simulated activities. Specifically, the objective was to determine the distribution within the five delineated classes used in SSFATE (Table 3-1) and the percentage of the upper seabed that is solid based on the measure of sediment water content. Sediment water content (i.e., moisture content) is a measure of the interstitial pore waters in the sediments.

The samples were taken from a vibracore and depth weighted to produce a sediment distribution at each sample location. All vibracore samples contained measurements of the water, which was factored into the sediment depth weighting process. Depending on the installation technique, the target trench depth varied from 1 to 3 m. Therefore, the depth weighted sediment characteristics used in modeling reflected the target burial depth.

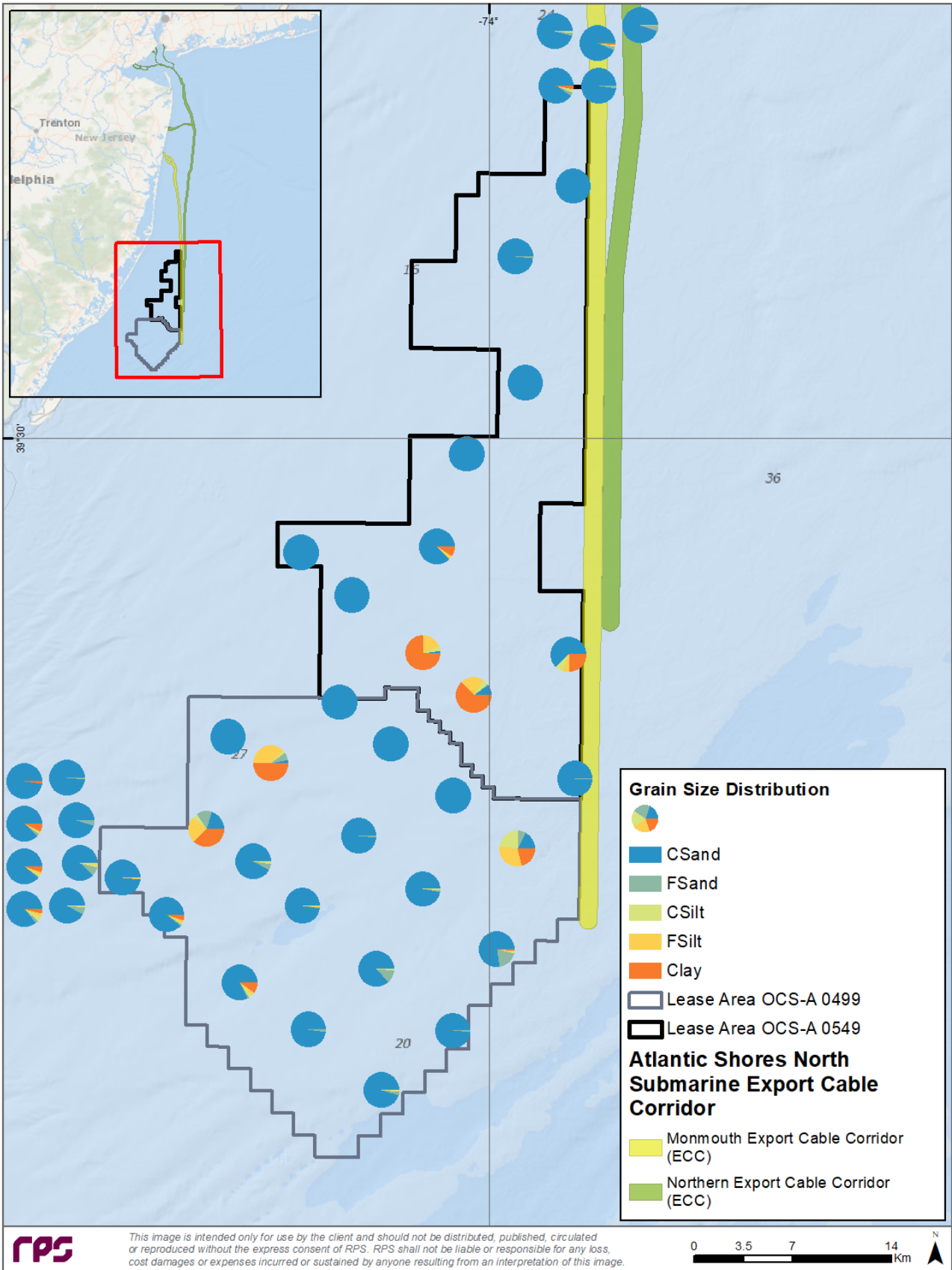
The sampling included vibracores, which provide a vertical profile of sediments that are then analyzed at multiple depths from the profile. All samples were analyzed by a sieve. Sieve analyses are performed to determine a percent finer curve for the coarse sediment sizes (i.e., the fraction of coarse and fine sand as it pertains to the classes in SSFATE). To resolve the fine grain sediment classes, samples undergo a hydrometer analysis. For all stations without hydrometer data, the remaining fraction (percent finer than fine sand) was split evenly between the three classes of coarse silt, fine silt, and clay.

Within the Lease Area (Figure 3-1), along the Monmouth ECC (Figure 3-2), and Northern ECC (Figure 3-3) most of the sediment samples consist of primarily fine and coarse sand. However, there are samples with noticeable fractions of fine materials (i.e., clay, fine silt, and coarse silt) with intermittent sections of fine sediments. The Monmouth ECC contained more samples with higher percentages of fine material than the Northern ECC. The lease area had more coarse sediment samples, with fine sediment samples scattered throughout.

For the Monmouth ECC, Northern ECC, and Lease Area cable installation simulations, grain size data were depth weighted to the target burial depth (whereas the grain size data used in the landfall pit excavation and backfill assumed deeper penetration and samples were depth weighted to 3 meters). As the actual disturbance depth is unknown for the seabed preparation activities, the vibracores used in the cable installation simulations were applied to the seabed preparation scenarios. For all scenarios, the grain size distribution and moisture content data at the closest sampling location to the sediment disturbing activity was applied (subset of Figure 3-3).

Samples along the ECC reflected similar compositions and were made of almost exclusively coarse sand. The sample closest to the representative landfall site showcased a similar composition. It contained higher fractions of coarse sand with a small percentage of fine sand and clays. The location of the representative cable installation simulations within the Lease Area was selected because the sampled contained extremely high fractions of fine material (e.g., clay, silts) and minimal coarse material. As the actual layout of the Lease Area's inter-array cables has not been finalized, by modeling the installation within an area containing mostly fine material, the simulation is conservative with respect to water column concentrations because fine material is less dense than sands and takes longer to settle. Because of the material properties, fine material lingers longer in the water column and tends to be transported farther from the source by subsurface currents and takes longer for water column concentrations to return to ambient.

For the sandwave clearance activities along the Monmouth ECC, a representative sample with a higher fraction of silt was selected and applied to the route. For the Northern ECC sandwave clearance simulation, the spatially varying grain size distributions were used because most of the segment contained coarse sand, with only a few samples containing coarse silt as the route approached the coastline. As described in Section 1.1, the representative WTG site was modeled at a sediment sampling location that contained a mixture of fine and coarse sediment because the Lease Area primarily consists of coarse sediment, with small regions in the southern portion include clay and fine silt. This was done to build in additional conservatism because these results are considered representative of the other 156 WTGs and one possible Permanent Met Tower which are distributed throughout the Lease Area. The same conservative approach with respect to grain size distribution was assumed for the three Large OSS sites because those locations span across the Lease Area.



This image is intended only for use by the client and should not be distributed, published, circulated or reproduced without the express consent of RPS. RPS shall not be liable or responsible for any loss, cost damages or expenses incurred or sustained by anyone resulting from an interpretation of this image.

Figure 3-1: Sediment Grain Size Distributions for the Upper 2 m of the Seabed in the Lease Area.

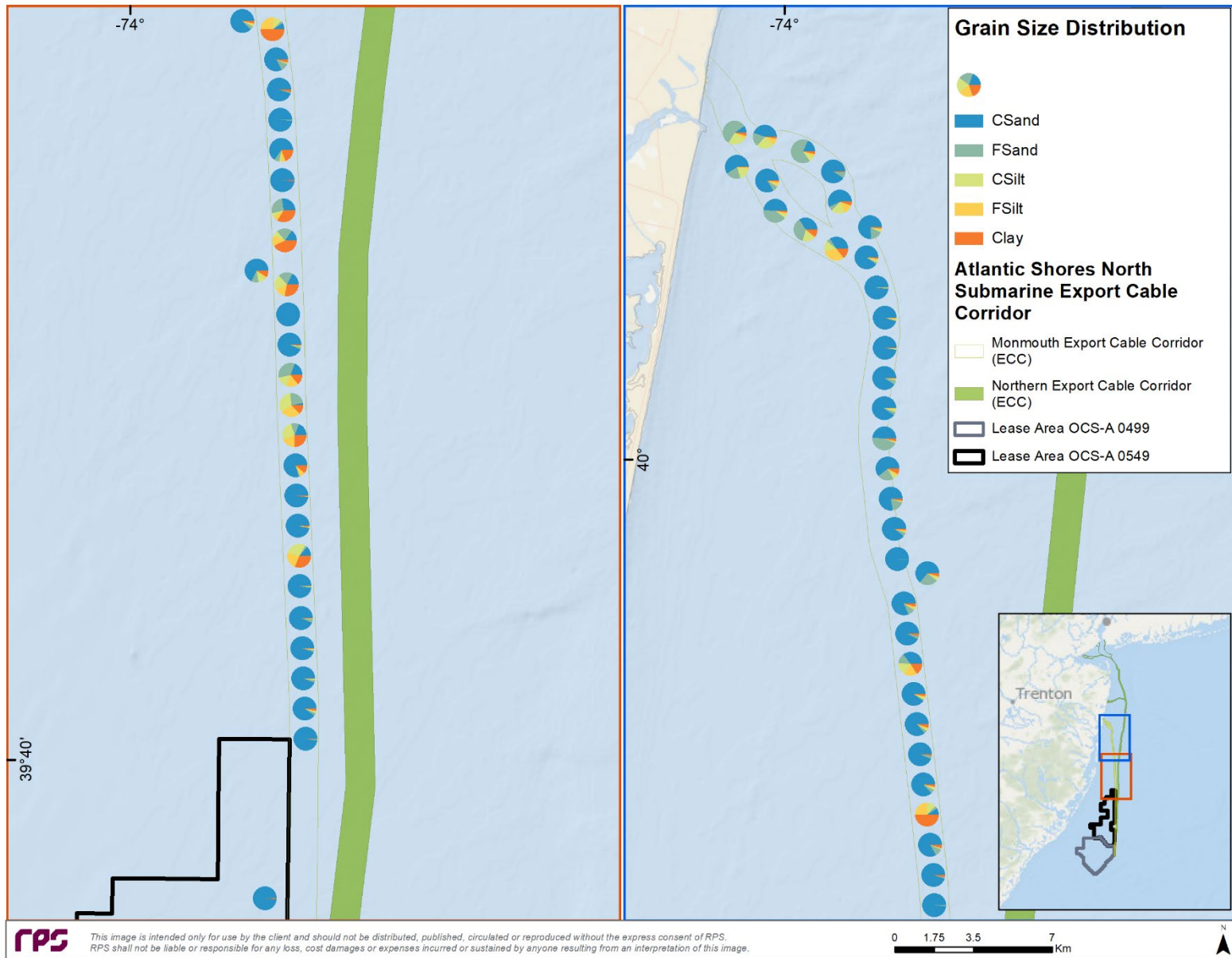


Figure 3-2: Sediment Grain Size Distributions for the Upper 2 m of the Seabed along the Monmouth ECC.

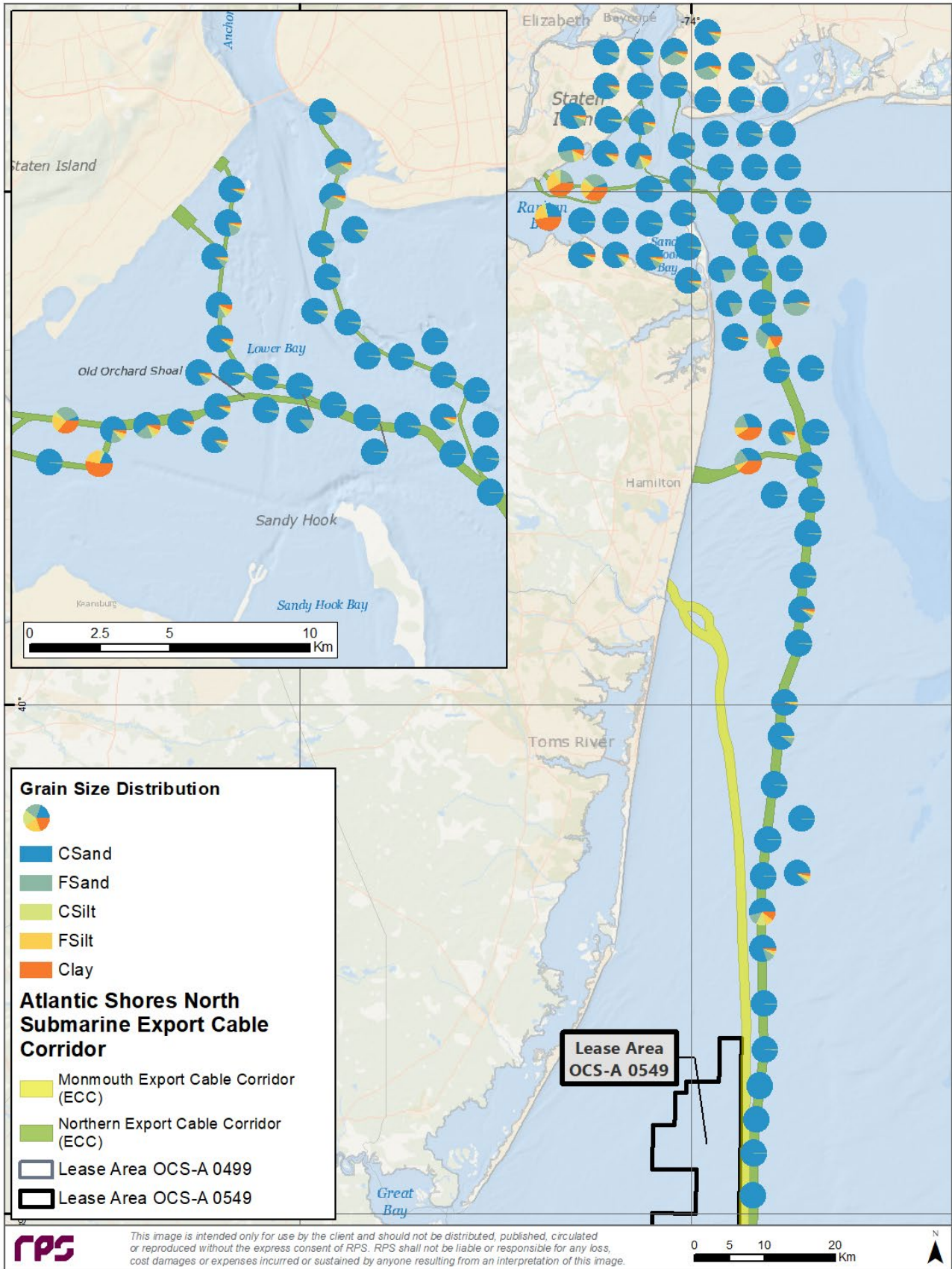


Figure 3-3: Sediment Grain Size Distributions for the Upper 1.8 m of the Seabed along the Northern ECC and inset showing the 3 m depth weighted near landfall.

### 3.2.2 Hydrodynamic Forcing

A scenario time period of May 2019 was established as a window of time that could be used as forcing for the sediment dispersion modeling as it was representative of normal environmental conditions (Section 2.2). Based on that validated time period and the length required for each simulation, modeling was performed within the period of May 1<sup>st</sup> to May 25<sup>th</sup>, 2019.

The specific start time for the modeling depended on the duration of the sediment disturbing activity. Activities that extended for longer than 12 hours experienced a minimum of one full tidal cycle (i.e., one ebb tide and one flood tide) which allowed sediment plumes to oscillate with the tides. In those instances, preliminary simulations were performed during different tidal cycles (i.e., flood and ebb) and the timing that produced the worst-case results were presented. The worst-cases were defined as those with the highest water column concentrations lasting the longest, plumes that extended further for the thresholds of interest, and those that contained the highest areas with the thickest sediment deposits.

For scenarios when sediment disturbing activities were shorter than 12 hours (i.e., HDD pit construction), preliminary studies were performed to determine which tidal stage (i.e., ebb vs. flood) caused the worst impacts. For both the representative Northern ECC Landfall Approach simulating HDD Exit Pit excavation and backfill operations, sediment was systematically released over 10 hours to simulate excavation and side-cast. This timing did not coincide with a full tidal cycle thus making them more susceptible to tidal influences (i.e., ebb vs. flood). The simulations that coincided with the start of a flood tide, resulted in longer exposures to water column concentrations and larger areas of depositional thickness  $\geq 1$  mm. Therefore, results for the Northern ECC Landfall Approach coinciding with a flood tide were presented below.

### 3.2.3 Route Definition

Fourteen sediment dispersion simulations were performed to encompass the landfall site HDD pit construction, WTG and OSS seabed foundation preparation, sandwave clearance, and cable installation activities included in the PDE. The model scenarios have been separated into three components: (1) seabed preparation, (2) the representative IAC located within the Lease Area, (3) the representative landfall approaches for each ECC, and (4) the representative offshore export cables located within the Monmouth and Northern ECCs. A key component of the modeling is the delineated geographical extent of the source. Therefore, seabed preparation equipment, the cable routes modeled, and corresponding burial equipment types are presented in Table 3-2.

#### **Seabed Preparation: Sandwave Clearance**

Based on offshore survey data, the modeled sandwave clearance simulations corresponded to locations within the ECC or Lease Area with regions of sandwaves. The representative Northern ECC sandwave clearance scenario was simulated from the Gowanans – Beltway landfall approach approximately 28.5 km south to accurately reflect the PDE (i.e., 20% of sandwaves may be present along the route; Figure 3-4). This portion was selected and used for the representative sandwave clearance simulation, because it contained one of the highest areas with contiguous sandwaves predicted to be in the Northern ECC. Additionally, it falls within a region of extremely complex hydrodynamics which will result in suspended sediment being transported farther from the source which may result in larger areas with elevated TSS concentrations. Therefore, this Northern ECC simulation can be considered a conservative estimate of impacts associated sandwave clearance and is representative of other potential sandwave clearance operations within proximity of the modeled route. It was assumed that a TSHD would be used to perform sandwave clearance operations within the Northern ECC.

Because a greater number of sandwaves are predicted to be present along the northern end of the Monmouth ECC, and the PDE indicates 20% of the ECC may require sandwave clearance, a representative sandwave clearance route was selected (Figure 3-5). The route begins at the northern end of the Monmouth ECC, near the shoreline, and extends 20 km south along the modeled Monmouth ECC – Branch 2 cable route. Sandwave clearance along this route was modeled using a TSHD and a sediment sample representative of typical sandwave composition. As a conservative approach, a representative sample with a higher fraction of fine sediment was selected and applied to the route. Fine sediments (e.g., clays, silts) tend to last longer in the water column, whereas coarse sediment (e.g., fine sand, coarse sand) will settle at a faster rate. The sandwave

clearance simulation within the Lease Area coincides with an area anticipated to have the longest section of continuous sandwaves and satisfies the PDE’s indication that approximately 10% of the inter-array cable routes may require sandwave clearance (Figure 3 6). Additionally, the route falls within areas containing both coarse and fine material so provides a realistic representation of potential impacts.

**Table 3-2: Construction Activities Modeled.**

Component	Equipment Type	Total Route Length (km)
Northern ECC Sandwave Clearance	TSHD	28.5
Monmouth ECC Sandwave Clearance	TSHD	20
Representative IAC Sandwave Clearance	TSHD	11.2
Large OSS Seabed Foundation Preparation – 1	TSHD	N/A
Large OSS Seabed Foundation Preparation – 2	TSHD	N/A
Large OSS Seabed Foundation Preparation – 3	TSHD	N/A
Representative WTG Seabed Foundation Preparation	TSHD	N/A
Representative IAC	Mechanical Trencher	4.7
Representative IAC	Jet Trencher	4.7
Northern ECC Landfall Approach, Representative HDD Pit	Excavator	N/A
Northern ECC	Jet Trencher	183
Monmouth ECC Landfall Approach, Representative HDD Pit	Excavator	N/A
Monmouth ECC – Branch 1	Jet Trencher	96.9
Monmouth ECC – Branch 2	Jet Trencher	97.5

**Seabed Preparation: Large OSS & WTG Foundations**

The PDE describes multiple foundation types, some of which require dredging prior to the actual foundation installation (e.g., gravity-based structures). To build in additional conservatism the largest potential disturbance area, as dictated by the Suction Bucket Jacket approach, was selected for modeling. The largest area and in turn the largest volume of sediment released to the environment poses the highest potential environmental impact. This approach was applied to both the Large OSS and representative WTG seabed foundation preparation simulations. The location of the representative WTG site was selected because it corresponds to a sediment sample that contains a mixture of fine and coarse sediment along the southeastern boarder of the Lease Area (Figure 3-7). The locations of the three Large OSS sites span across the Lease Area from north to south and will therefore be exposed to different environmental conditions. The Large OSS Site 2 is the northern most site near the eastern boarder of the Lease Area, Large OSS Site 1 falls in the middle of the Lease Area and other two Large OSS locations, and Large OSS Site 3 is the southernmost location, near the representative WTG location (Figure 3-7).

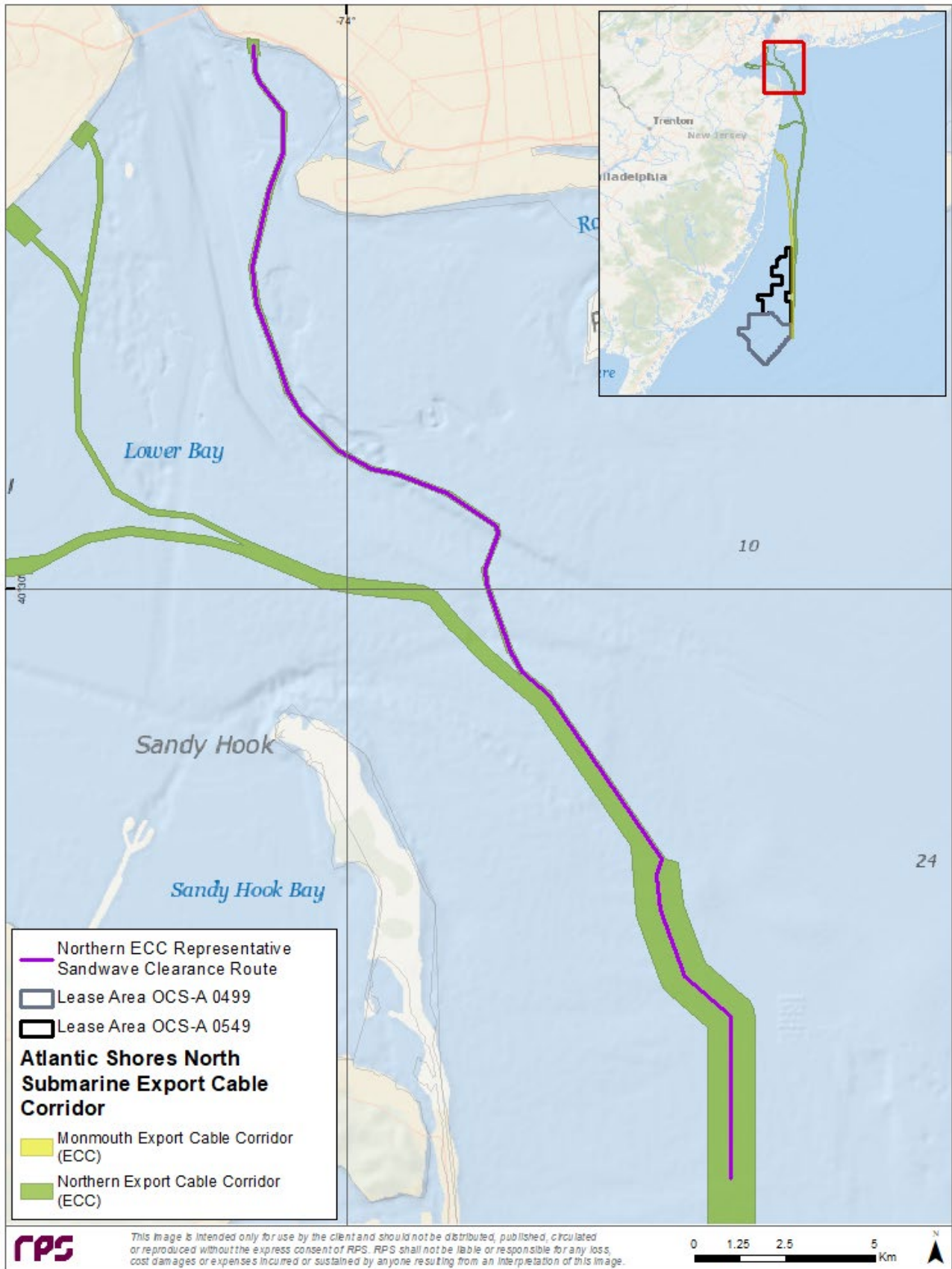


Figure 3-4: Modeled Northern ECC Representative Sandwave Clearance Route.

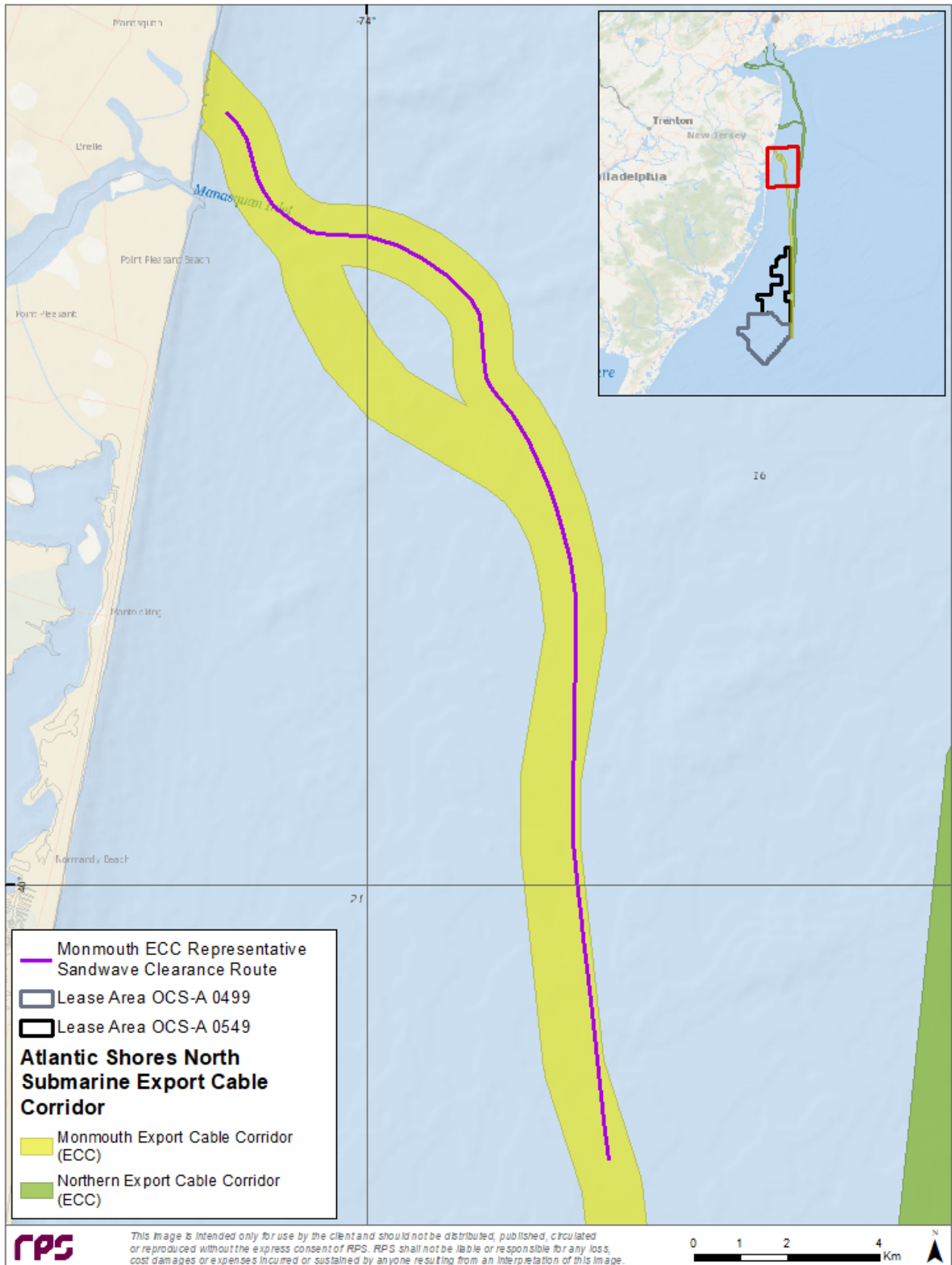


Figure 3-5: Modeled Monmouth ECC Representative Sandwave Clearance Route.



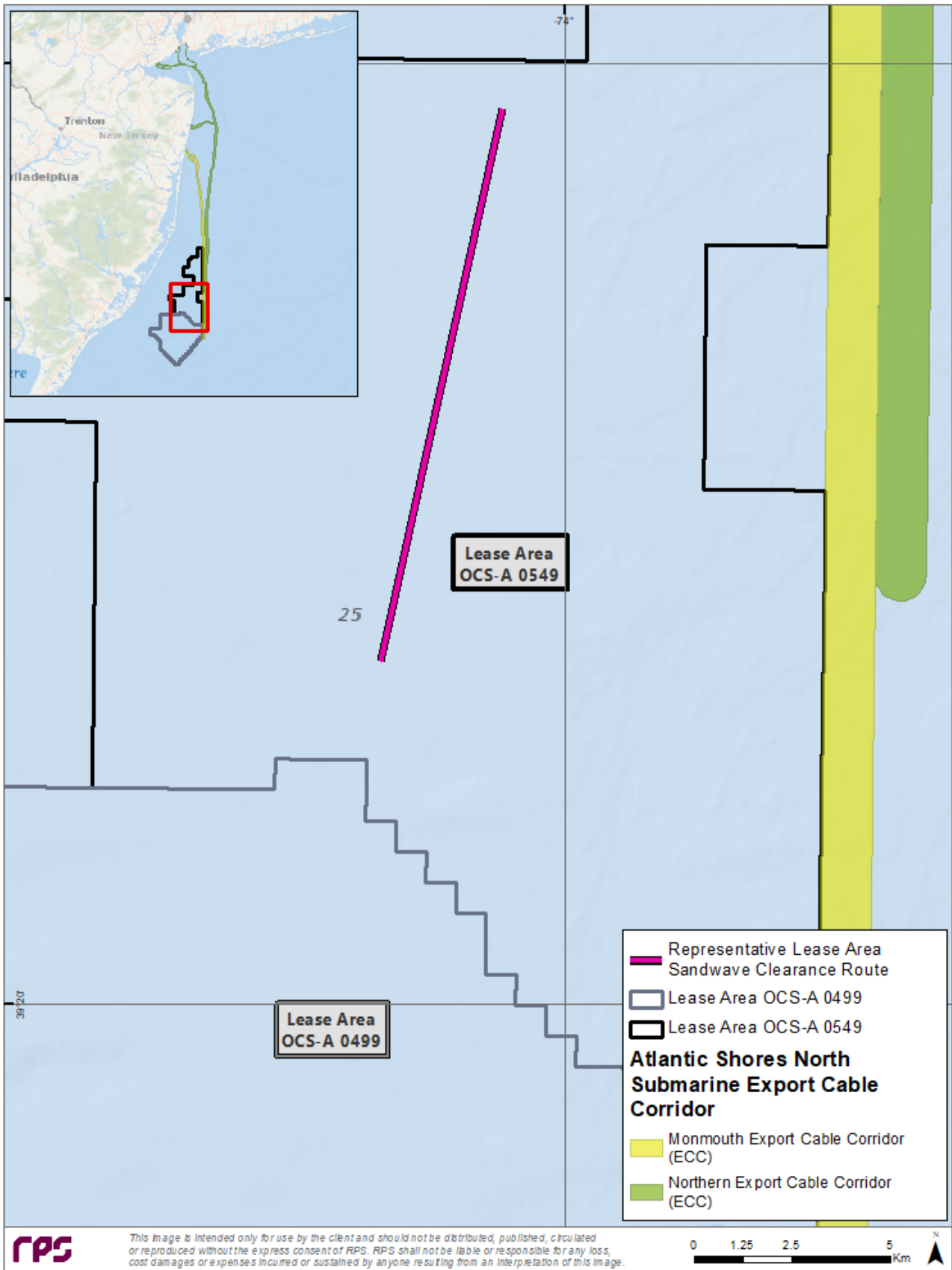


Figure 3-6: Modeled Representative Lease Area Sandwave Clearance Route.

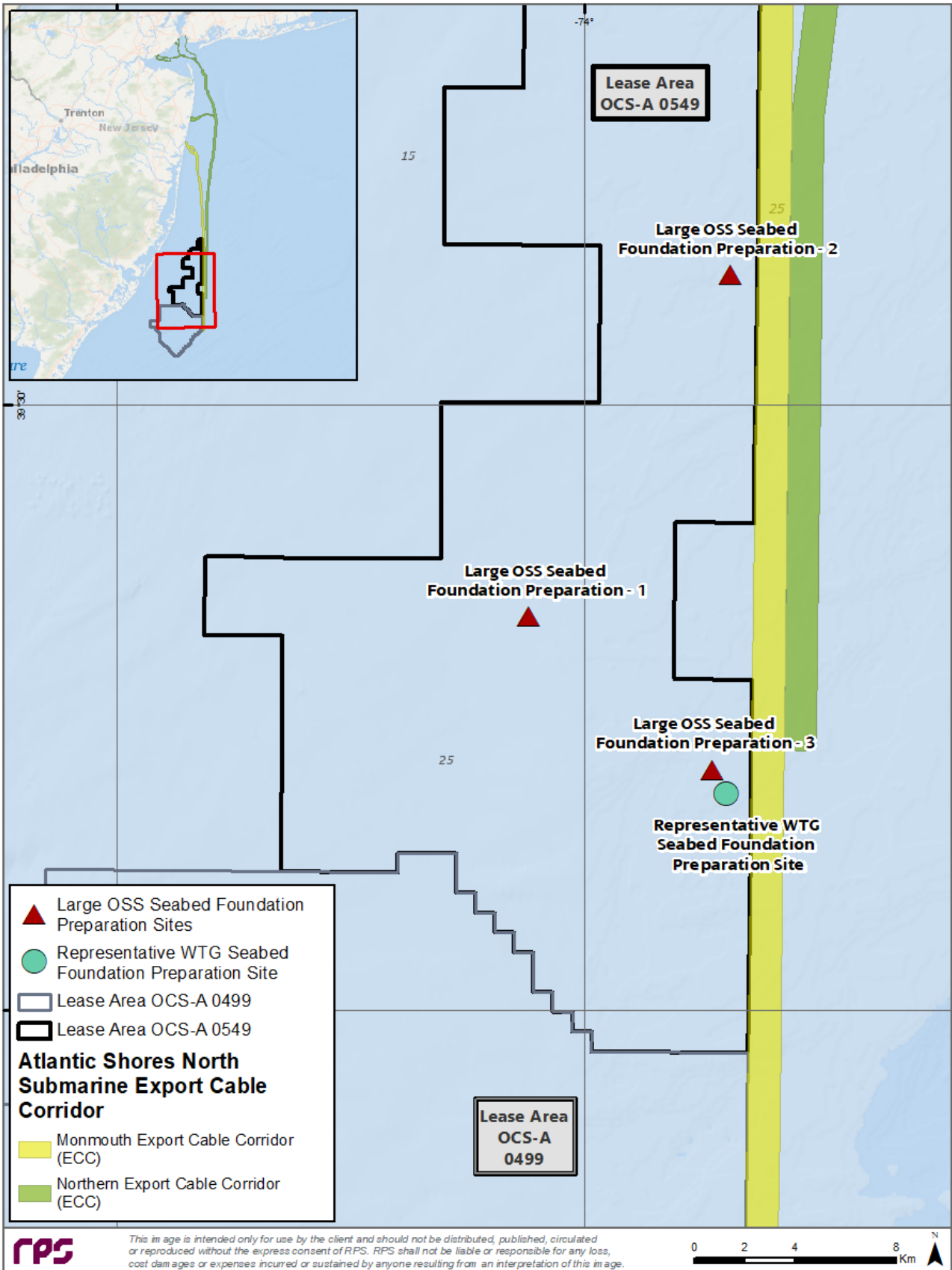


Figure 3-7: Modeled Seabed Preparation Locations at a Representative WTG Foundation Site and Three Large OSS Foundation Sites.

**Cable Installation & Landfall Approaches:**

An individual representative IAC route (Figure 3-8) that passed through a region of finer sediment was modeled as a conservative assessment of potential impacts from cable installation within the WTA. Fine sediments (e.g., clays, silts) tend to last longer in the water column, whereas coarse sediment (e.g., fine sand, coarse sand) will settle at a faster rate. To evaluate the influence of equipment type on sediment dispersion, two possible equipment types were assessed for IAC installation: jet trencher and mechanical trencher.

The modeled offshore export cable scenarios included representative routes along the full length of the Monmouth (Figure 3-11) and Northern (Figure 3-10) ECCs. As described in Section 1.1, the Monmouth ECC diverges nearshore then converge to reach their respective landfall site. To account for the divergence (“branch”), a total of two Monmouth ECC scenarios were modeled. The Northern ECC and Monmouth ECC parallel the eastern boundary of the Lease Area and extend north towards their respective landfall sites. The Asbury, NJ landfall approach was not modeled as it is in proximity to the Monmouth landfall and experiences similar hydrodynamic forcing conditions and resulting effects from the cable installation and landfall activities would be on the same order of magnitude as those for Monmouth. Variability in results for the Asbury landfall approach would primarily be due to the sediment composition, which consists primarily of coarse material but has intermittent sections that contain clay and fine sand prior to landfall.

The Northern ECC has multiple landfall approaches, so one of the longest routes (Gowanus – South Beach Approach), within the most complex hydrodynamic conditions was selected and modeled in this assessment. Being one of the longer routes corresponds to the largest potential volume of resuspended sediment, and because it resides in an area of complex hydrodynamics the potential suspended sediment plume is subject to higher current velocities transporting it further from the source. Herein, this simulation will be referred to as the representative Northern ECC route as it provides a conservative approach and results can be considered representative of the other approach options in its proximity. While multiple landfall approaches are proposed, one landfall approach for the Northern ECC was simulated; it can be considered representative of other landfall approaches in proximity to the ECC landfall locations. The sediment composition closest to shore for all of the potential landfall approaches associated with the Northern ECC consisted of relatively high fractions of coarse material (e.g., sands). As with the Northern ECC cable installation modeling, the representative landfall location selected for simulating the HDD pit excavation and backfill was determined based on hydrodynamic conditions as the sediment compositions were similar.

The modeled landfall approaches included representative HDD pits along both the Monmouth (Figure 3-12) and Northern (Figure 3-9) ECCs. Only the excavation (assuming side cast) of the HDD pits was modeled but can be considered representative of backfill as this operation would take place on the order of hours to days after excavation. Additionally, only one HDD pit location was modeled within each ECC but can be considered representative of the other potential landfalls due to the proximity of the landfall locations, similar sediment characteristics, and similar or weaker hydrodynamic forcing conditions.

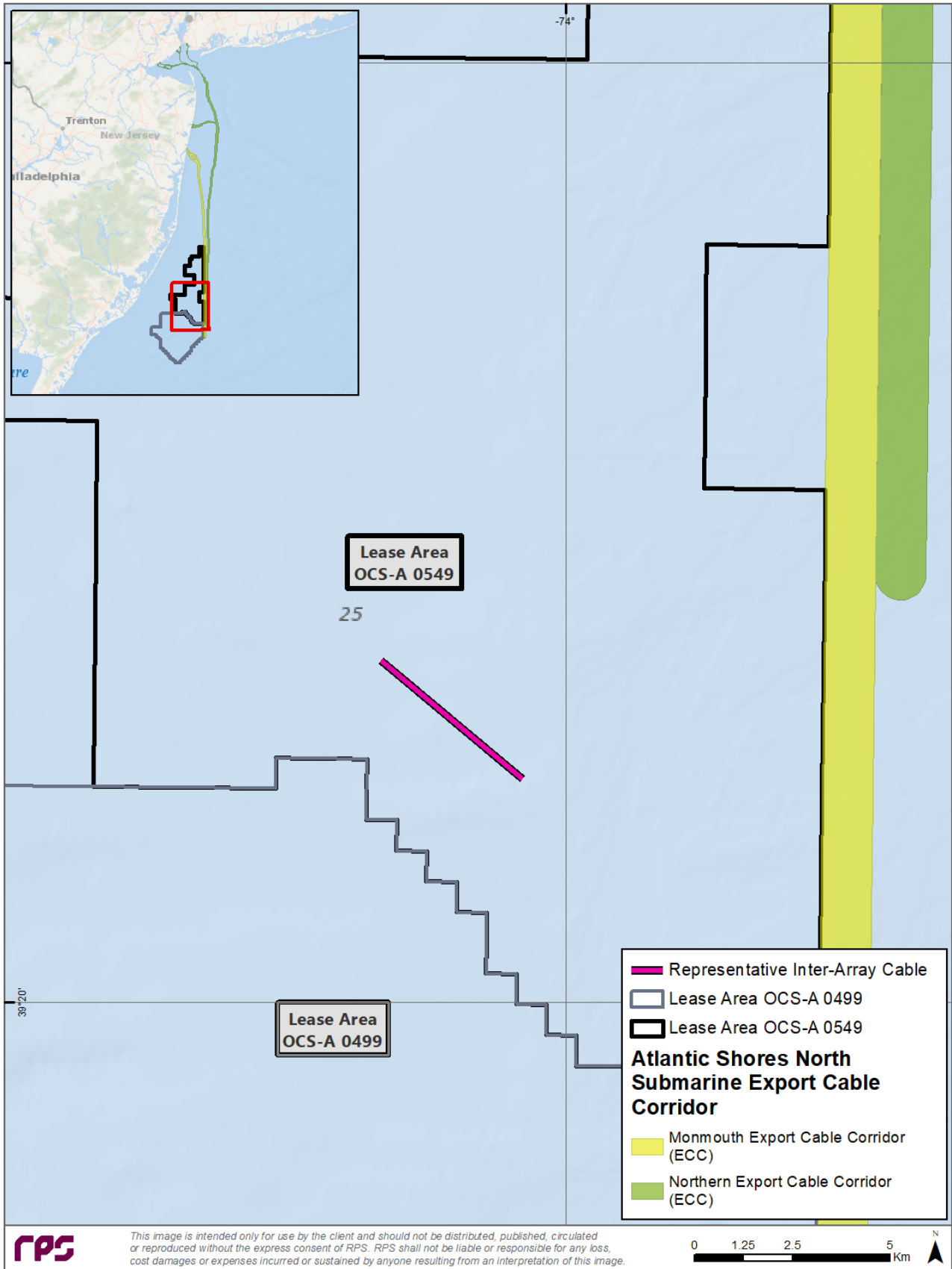


Figure 3-8: Modeled Representative Inter-Array Cable Route.

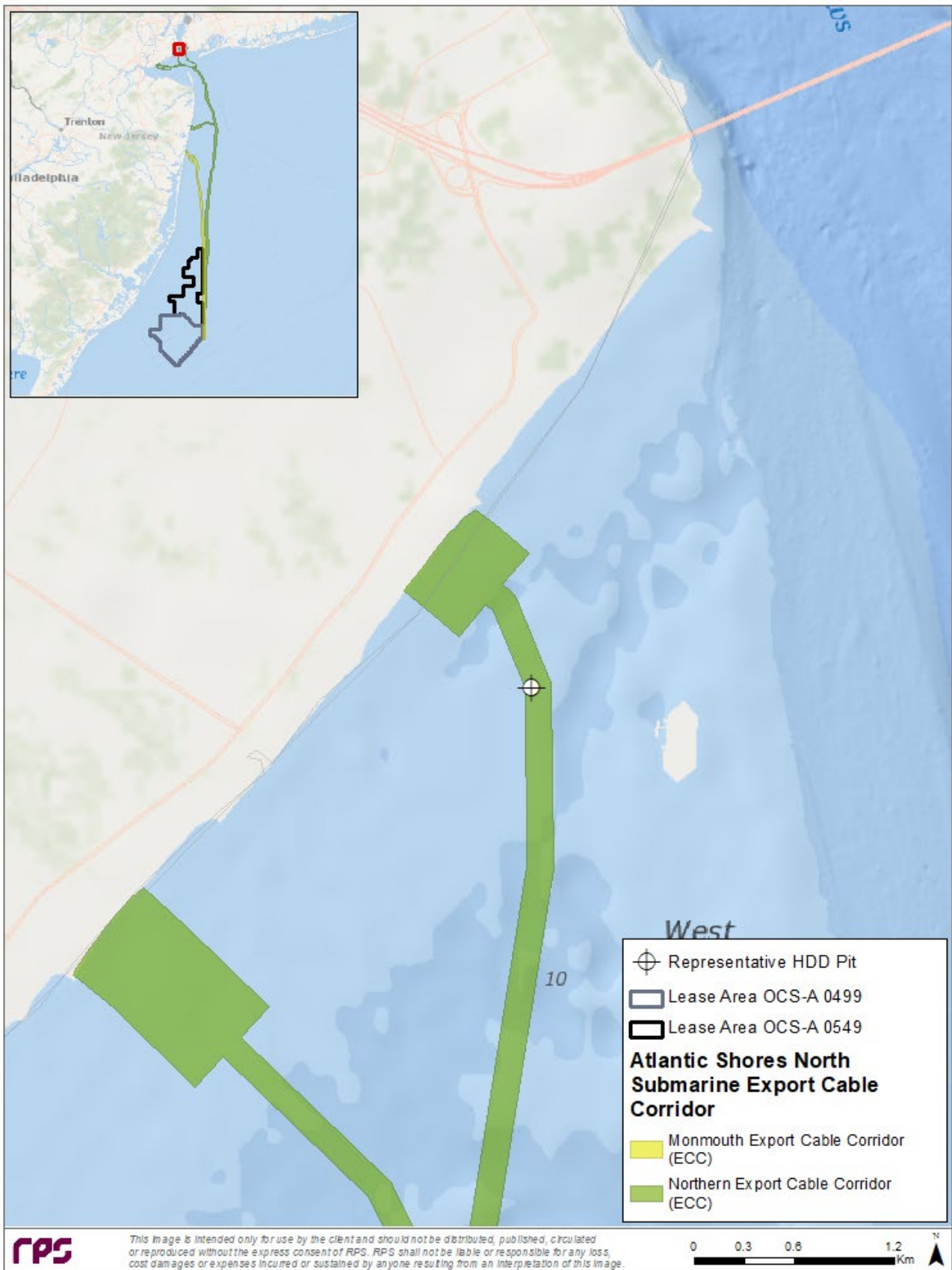


Figure 3-9: Modeled Northern ECC Representative Landfall Approach.

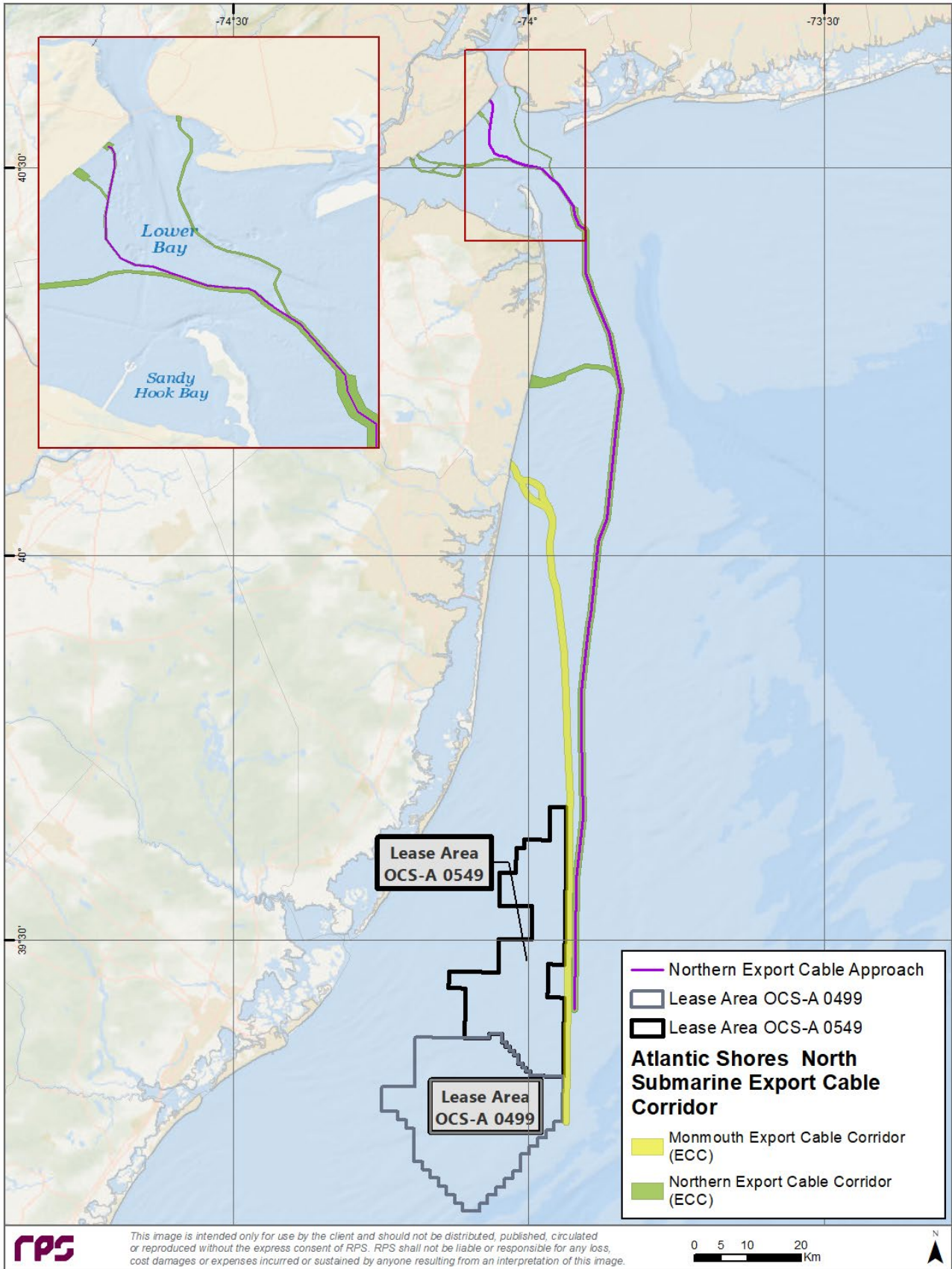


Figure 3-10: Modeled Northern ECC Approach.

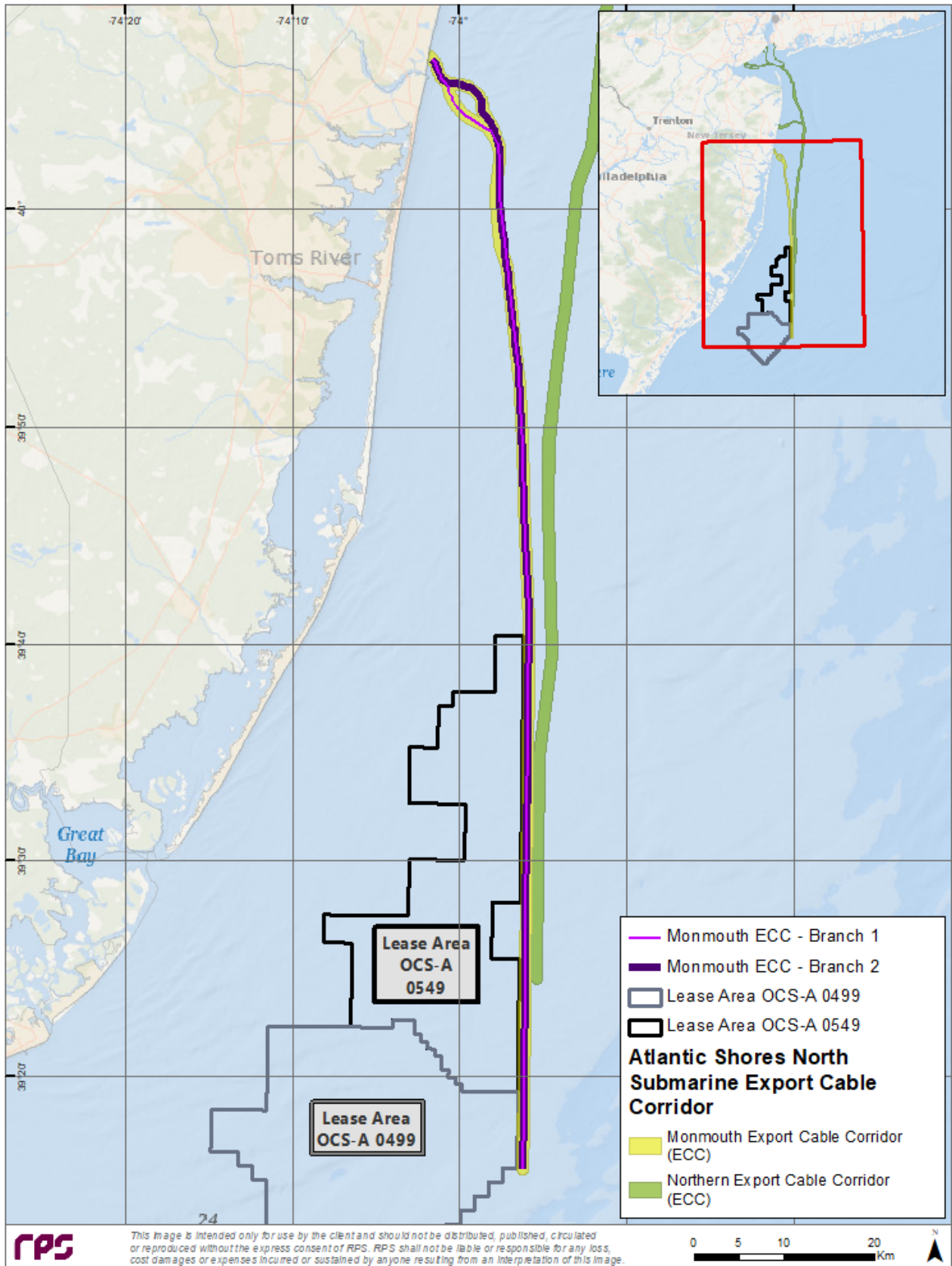


Figure 3-11: Modeled Monmouth Export Cable, Branch 1 and Branch 2.

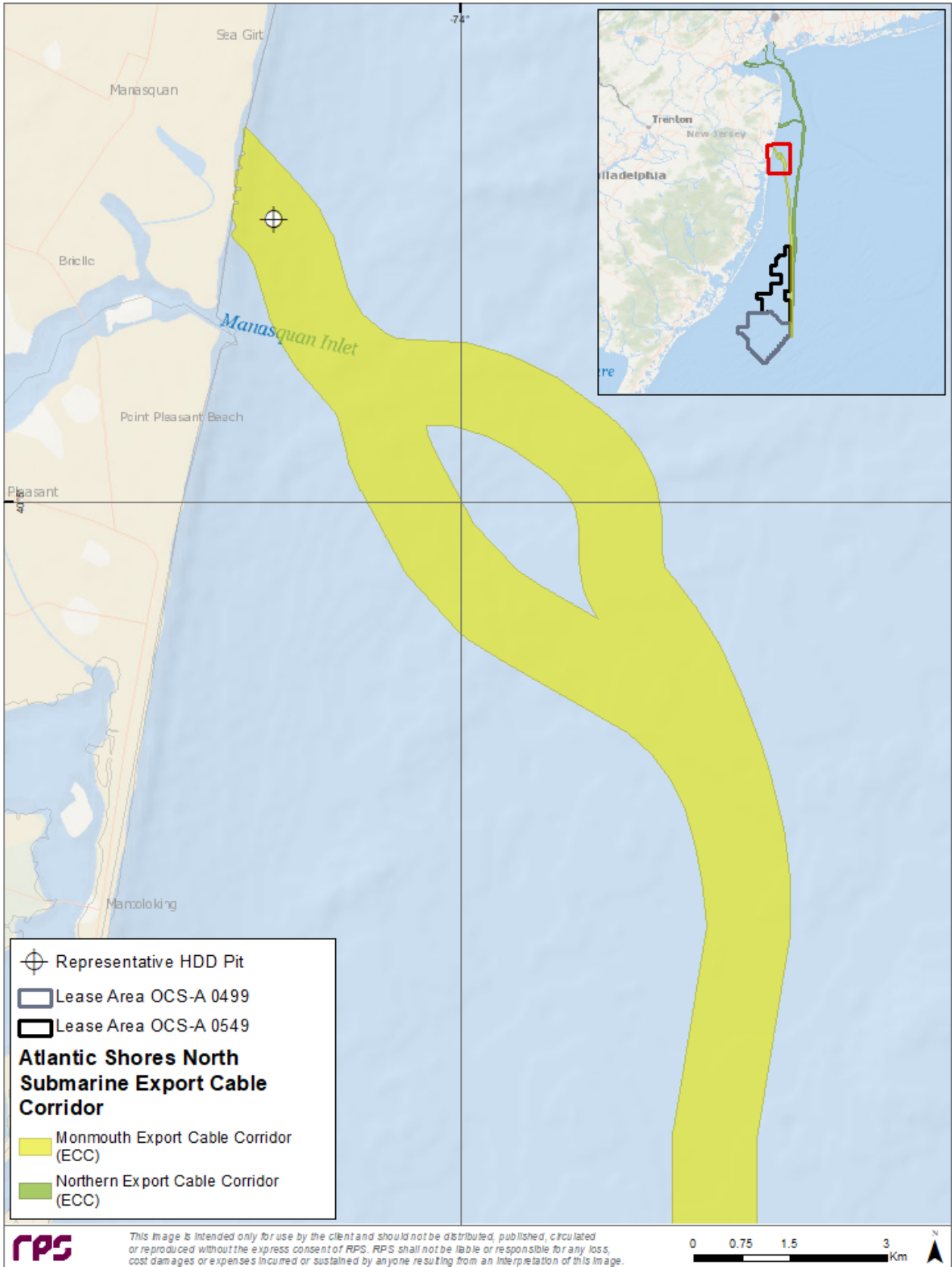


Figure 3-12: Modeled Monmouth ECC Representative Landfall Approach.



### 3.2.4 Source & Sediment Load Characterization

Sandwave clearance activities were modeled using TSHD, conservative equipment parameters; average sandwave dimensions found along the route were used to estimate the clearance volume. For the Northern ECC and Lease Area sandwave clearance simulations, 20% of the fine sediment (e.g., clays, silts) were released at the surface to simulate overflow and the remaining 80% of the material was dumped approximately 5 m below the surface. This was slightly different than the Monmouth ECC sandwave clearance approach because it was performed using a sediment composition that was primarily fine material so all of the sediment (i.e., 100%) was released at the surface. Whereas the Northern ECC and Lease Area had spatially varying sediment compositions that contained more coarse material, so to better represent reality, settling of the coarse material within the hopper and the subsequently dumped below the water surface by the TSHD was captured and reproduced in this modeling assessment (Table 3-3). For all TSHD simulations, it was assumed that sediment disturbed by the drag arm was negligible compared to overflow and dumping operations.

As the Large OSS and WTG seabed foundation preparation sites were located within the Lease Area, the same approach of overflow at the surface using 20% of fine material and the remaining 80% was dumped 5 m below the surface as was used for sandwave clearance in the Lease Area. Although operations of dredging would be continuous until the region is cleared, the introduction of sediments to the water column was intermittent and occurred when the hopper reached capacity. Hopper capacity was assumed to be 15,000 m<sup>3</sup> for all seabed preparation scenarios. The frequency of dumping and overflow were estimated using the hopper capacity and the production rate (Table 3-3). Based on the total dredge volumes applied in this modeling assessment, dumping and overflow were predicted to occur three times for the Large OSS sites and once for the representative WTG site.

For the WTG foundations, the realistic depth of disturbance varies between zero and 3 m. In extreme circumstances this depth may range up to 6 m, however, that is not expected and was not applied in this assessment because it does not represent a realistic situation that would likely occur in the field. Therefore, the average depth across all foundations was estimated to be approximately 0.53 m deep and was applied for the representative WTG seabed foundation preparation simulation. For the OSS foundations, the average seabed preparation depth is slightly larger, and was modeled assuming an average depth of 1 m. Cable installation activities that will suspend sediments in the water column include IAC burial within the Lease Area, cable burial within the ECCs, and HDD pit activity for the landfall approaches. Inter-array and offshore export cable installation may be achieved through various methods, which may be combined interchangeably.

Based on a preliminary assessment performed in support of Atlantic Shores' COP for Lease Area OCS-A 0499, the sensitivity of equipment type and the rate of installation on the fate and transport of suspended sediments was evaluated. Three burial techniques (jet trenching, jet ploughing, and mechanical trenching) and two installation rates (fast and slow) were used in this sensitivity analysis. Jet trenching and mechanical trenching were selected for use in the final modeling because the results predicted higher impacts associated with those equipment types when compared to jet ploughing. For example, simulations with jet trenching and mechanical trenching were predicted to have: 1) larger areas exceeding TSS concentration thresholds (25, 50, 100, or 200 mg/L), 2) deposition above thresholds (1 or 5 mm) extending further away from the route centerline, 3) larger areas exceeding depositional thickness thresholds (1, 5, 20, or 100 mm), 4) higher maximum TSS concentrations, and 5) larger maximum depositional thicknesses. For the jet trenching and mechanical trenching simulations, a slower installation rate resulted in larger areas exposed to TSS concentrations for longer durations when compared with the faster installation rate. To reflect the maximum design cases (i.e., largest impacts associated with TSS concentrations and deposition for installation equipment and parameters), the results from the sensitivity analysis informed this assessment as well and jet trenching and mechanical trenching techniques were selected for use in final modeling and the slow installation rates were assumed to bound the potential effects associated with cable installation activities.

The jet trenching scenario, using the slower installation rate, was determined to be the maximum design case and was used for final modeling efforts for the ECCs. Assuming the slower installation rate for both, jet trenching and mechanical trenching methods were used to model the representative IAC scenarios. The cable installation method was simulated using installation parameters that reflect a conservative estimate of typical

installation speed and trench depth. Based on the equipment type, 25% of the sediment was mobilized into the water column near the seabed for inter-array and offshore export cable installation. Anticipated conservative HDD pit dimensions along each ECC were modeled using one equipment type (excavator). For HDD pit excavation, 100% of the sediment was mobilized and introduced at the water surface.

For all of these scenarios, a conservative approach was used by assuming no mitigation techniques (e.g., cofferdam, silt screen) would be deployed during construction activities. A summary of the seabed preparation, IAC installation, offshore export cable installation, and HDD pit construction parameters are provided in Table 3-3.

**Table 3-3: Construction Activity Modeling Parameters**

Component	Equipment Type	Trench Width (m)	Trench Depth (m)	Trench Cross-Sectional Area (m <sup>2</sup> )	Pit Volume (m <sup>3</sup> )	Advance Rate (m/hr)	Production Rate (m <sup>3</sup> /hr)	Percent Mobilized (%)
Northern ECC Sandwave Clearance*	TSHD	30	0.9	27	-	68	1850	100
Monmouth ECC Sandwave Clearance	TSHD	30	0.9	27	-	68	1850	100
Representative IAC Sandwave Clearance*	TSHD	30	0.9	27	-	68	1850	100
Large OSS Seabed Foundation Preparation – 1*	TSHD	-	1	-	34,344	68	1850	100
Large OSS Seabed Foundation Preparation – 2*	TSHD	-	1	-	34,344	68	1850	100
Large OSS Seabed Foundation Preparation – 3*	TSHD	-	1	-	34,344	68	1850	100
Representative WTG Seabed Foundation Preparation*	TSHD	-	0.53	-	5,483	68	1850	100
Representative IAC	Mechanical Trencher	0.56	1.8	1.0	-	150	450	25
Representative IAC	Jet Trencher	0.56	1.8	1.0	-	250	450	25
Northern ECC Landfall Approach, Representative HDD Pit	Excavator	20	3.0	60	600	-	60	100
Northern ECC	Jet Trencher	0.56	1.8	1.0	-	250	450	25
Monmouth ECC Landfall Approach, Representative HDD Pit	Excavator	N/A	3.0	N/A	600	N/A	60	100
Monmouth ECC – Branch 1	Jet Trencher	0.9	2.0	1.8	-	250	450	25
Monmouth ECC – Branch 2	Jet Trencher	0.9	2.0	1.8	-	250	450	25
Monmouth ECC Landfall Approach, Representative HDD Pit	Excavator	20	-	-	600	-	60	100

\*Of the 100% of material released, 20% of the fine material (e.g., clays, silts) were released at the surface and the remaining 80% of material was released approximately 5 m below the water surface to simulate overflow and dumping operations, respectively.

### 3.3 Sediment Modeling Results

SSFATE simulations were performed for each sediment disturbance activity. Sediment concentrations were computed on grids with varying resolutions in the horizontal and vertical dimensions to capture the unique results of each scenario. Model-predicted concentrations are considered above ambient or “excess” concentrations above background (i.e., a concentration of 0 mg/L is assumed for the ambient concentration). Results from the model runs are presented through a discussion of the results and tables showing the predictions of suspended sediment concentration and relative thickness of sediment deposition expected to occur along the proposed ECCs and Lease Area as a result of construction activities. For all dredging and cable installation scenarios, sediment concentrations were computed on a grid with resolution of 30 m x 30 m or 50 m x 50 m in the horizontal, while landfall scenarios used a smaller horizontal grid (10 m x 10 m) to capture complex coastal hydrodynamic processes. Depending on the length of the simulation and the depth of sediment disturbing activities the vertical dimensions were either 0.5 m or 1 m.

Results from the model runs are presented through a set of figures and tables showing the predictions of suspended sediment concentration and relative thickness of sediment deposition expected to occur along the proposed ECC’s and Lease Area as a result of construction activities. Maps of instantaneous above-ambient TSS concentrations; maximum above-ambient TSS concentrations; durations of time for which above-ambient TSS of  $\geq 10$  mg/L occur; and seabed deposition (in mm) are provided. Tables quantifying the maximum extent to concentration and depositional thresholds for each installation technique; the modeled area exceeding TSS thresholds for specific durations, as well as areas of seabed deposition exceeding thickness thresholds, are summarized for each scenario.

Additional information about standard graphical outputs for each scenario are provided below:

- **Maps of Instantaneous TSS Concentrations:** These maps show an example snapshot of TSS concentrations at a single moment in time; thus, conveying the spatial and temporal variability of the sediment plume in a way that cannot be depicted by cumulative maps. The plan view shows the maximum concentration throughout the water column at that snapshot time, and the vertical cross-section shows the cross-sectional variability of concentrations along a transect. These instantaneous maps show that the plume is not a continuous blanket of sediment, but rather narrow, heterogeneous patches that individually persist for minutes to hours at a single location.
- **Maps of Time-integrated Maximum TSS Concentrations:** Predicted suspended sediment concentrations are presented as a composite of maximum concentrations predicted to occur during sediment-disturbing activities at all times and locations throughout the model simulation. These map shows the maximum time-integrated water column concentration from the entire water column in scaled plan view, and a non-scaled inset, showing a cross-sectional view of maximum TSS concentrations in the water column. The concentrations are shown as contours using mg/L. The entire area within the contour is at or above the concentration defined by the contour itself. Most importantly, it should be noted that these maps show the maximum TSS concentration that occurred throughout the entire simulation and therefore: (1) these concentrations do not persist throughout the entire simulation and may occur during just one- or several-time steps (time step of five or 10 minutes); and (2) these concentrations do not occur concurrently throughout the entire modeled area but are the time-integrated spatial views of maximum predicted concentrations. It should be emphasized that the maximum predicted sediment plume concentration or extent will not exist at any one time during the installation.
- **Maps of Duration of TSS Concentrations Greater than 10 mg/L:** These maps show the number of hours that the TSS concentrations are expected to be equal to or greater than 10 mg/L.
- **Maps of Seabed Deposition:** These maps show the predicted deposition on the seabed that would occur once the activity has been completed. The thickness levels are shown as contours (in mm) and the entire area within the contour is at or above the thickness defined by the contour itself. The contours have been delineated at levels either tied to biological significance (i.e., 1 mm and 2 mm) or to facilitate viewing the results.

### 3.3.1 Results Summary Tables

Results from all modeled scenarios were analyzed to determine the spatial area, generally not contiguous, and maximum extents of TSS concentration, duration, and deposition thresholds. The time-integrated results provide a sum of all individual concentration grid cells that exceeded a threshold anywhere in the water column. The values reported and discussed reflect the scenario predicted to have the maximum effect (i.e., maximum effects scenario) for the Monmouth ECC branches.

Post-processing included calculations of areas above multiple TSS concentration thresholds and duration thresholds (Table 3-4 to Table 3-7). The areas in these tables are the total areas from the entire simulation, and therefore reflect the sum of different, non-contiguous instances of smaller areas throughout the entire route (i.e., the threshold exceedances do not occur simultaneously). The tables illustrate that areas exposed to above-ambient TSS concentrations were largest when assessing concentrations above 10 mg/L, and that the areas rapidly decreased in size as the concentration threshold or duration increased. For example, the Monmouth ECC scenario had a total area throughout the entire route of 33.73 km<sup>2</sup> ≥10 mg/L for more than 2 hours, but only 0.02 km<sup>2</sup> of this area was ≥200 mg/L for more than 2 hours (Table 3-4). Above-ambient TSS concentrations also decreased with time. For the same example scenario (i.e., Monmouth ECC), concentrations ≥10 mg/L decreased from 33.73 km<sup>2</sup> for 2 hours (Table 3-4), to 11.33 km<sup>2</sup> for 4 hours (Table 3-5), to 3.17 km<sup>2</sup> for 6 hours (Table 3-6), and 0.04 km<sup>2</sup> for 12 hours (Table 3-7). Additionally, TSS concentrations ≥50 mg/L did not endure for periods >12 hours. Similar trends of rapid decrease of area with increasing time and/or increasing threshold are noted for all other routes presented.

**Table 3-4: Areas over Above-Ambient TSS Threshold Concentrations for Longer than 2 Hours for Each Scenario.**

Scenario	Concentration Thresholds in mg/L					
	10	25	50	100	200	650
	Areas Above Concentration Threshold (km <sup>2</sup> )					
Representative Northern ECC– Sandwave Clearance	15.62	9.40	4.83	2.62	1.49	0.84
Representative Sandwave Clearance, Monmouth ECC	16.44	10.42	6.45	3.39	1.34	0.18
Representative IAC – Sandwave Clearance	25.48	16.52	12.49	8.84	4.99	1.03
Large OSS Seabed Foundation Preparation – 1	4.76	4.19	3.67	3.05	2.59	1.85
Large OSS Seabed Foundation Preparation – 2	4.62	3.55	2.84	2.10	1.69	1.15
Large OSS Seabed Foundation Preparation – 3	4.85	3.71	2.95	2.47	2.12	1.43
Representative WTG Seabed Foundation Preparation	1.00	0.91	0.84	0.75	0.63	0.38
Representative IAC – Mechanical Trencher	4.94	1.47	0.54	0.22	0.01	N/A
Representative IAC – Jet Trencher	2.78	1.01	0.42	0.08	N/A	N/A
Northern ECC Landfill Approach, Representative HDD Pit	0.14	0.03	0.01	<0.01	<0.01	<0.01
Representative Northern ECC– Jet Trencher	42.45	12.84	3.25	0.06	N/A	N/A
Monmouth Export Cable – Jet Trencher*	33.73	15.43	6.42	1.32	0.02	N/A
Monmouth ECC Landfall Approach, Representative HDD Pit	1.13	0.28	0.14	0.07	0.03	<0.01

\*Both branches of this ECC were modeled and results were very similar. Of the two modeled ECC branches, only results from the maximum effect scenario were reported for simplicity and to be conservative.

**Table 3-5: Areas over Above-Ambient TSS Threshold Concentrations for Longer than 4 Hours for Each Scenario.**

Scenario	Concentration Thresholds in mg/L					
	10	25	50	100	200	650
	Areas Above Concentration Threshold (km <sup>2</sup> )					
Representative Northern ECC– Sandwave Clearance	2.78	0.54	0.14	0.04	N/A	N/A
Representative Sandwave Clearance, Monmouth ECC	5.97	3.00	1.37	0.47	0.05	N/A
Representative IAC – Sandwave Clearance	13.39	5.41	3.30	1.75	0.61	0.02
Large OSS Seabed Foundation Preparation – 1	1.87	1.42	1.08	0.83	0.59	0.27
Large OSS Seabed Foundation Preparation – 2	1.68	1.19	0.83	0.61	0.44	0.27
Large OSS Seabed Foundation Preparation – 3	1.35	0.95	0.64	0.44	0.28	0.13
Representative WTG Seabed Foundation Preparation	0.25	0.15	0.08	0.05	0.03	0.01
Representative IAC – Mechanical Trencher	2.14	0.41	0.14	N/A	N/A	N/A
Representative IAC – Jet Trencher	0.85	0.24	0.03	N/A	N/A	N/A
Northern ECC Landfill Approach, Representative HDD Pit	0.04	0.01	<0.01	<0.01	<0.01	<0.01
Representative Northern ECC– Jet Trencher	16.30	1.68	0.05	N/A	N/A	N/A
Monmouth Export Cable – Jet Trencher*	11.33	3.48	0.79	0.10	N/A	N/A
Monmouth ECC Landfall Approach, Representative HDD Pit	0.41	0.15	0.07	0.03	0.01	<0.01

*\*Both branches of this ECC were modeled and results were very similar. Of the two modeled ECC branches, only results from the maximum effect scenario were reported for simplicity and to be conservative.*

**Table 3-6: Areas over Above-ambient TSS Threshold Concentrations for Longer than 6 Hours for Each Scenario.**

Scenario	Concentration Thresholds in mg/L					
	10	25	50	100	200	650
	Areas Above Concentration Threshold (km <sup>2</sup> )					
Representative Northern ECC– Sandwave Clearance	0.32	0.07	0.04	0.01	N/A	N/A
Representative Sandwave Clearance, Monmouth ECC	2.05	0.56	0.22	0.05	N/A	N/A
Representative IAC – Sandwave Clearance	7.12	1.43	0.48	0.18	0.07	N/A
Large OSS Seabed Foundation Preparation – 1	0.65	0.45	0.33	0.18	0.04	N/A
Large OSS Seabed Foundation Preparation – 2	0.60	0.38	0.30	0.21	0.14	0.03
Large OSS Seabed Foundation Preparation – 3	0.50	0.33	0.20	0.08	0.02	N/A
Representative WTG Seabed Foundation Preparation	N/A	N/A	N/A	N/A	N/A	N/A
Representative IAC – Mechanical Trencher	0.45	0.14	0.04	N/A	N/A	N/A
Representative IAC – Jet Trencher	0.23	0.05	N/A	N/A	N/A	N/A
Northern ECC Landfill Approach, Representative HDD Pit	0.01	<0.01	<0.01	<0.01	<0.01	<0.01
Representative Northern ECC– Jet Trencher	5.92	0.14	0.01	N/A	N/A	N/A
Monmouth Export Cable – Jet Trencher*	3.17	0.62	0.16	N/A	N/A	N/A
Monmouth ECC Landfall Approach, Representative HDD Pit	0.17	0.08	0.04	0.02	0.01	<0.01

*\*Both branches of this ECC were modeled and results were very similar. Of the two modeled ECC branches, only results from the maximum effect scenario were reported for simplicity and to be conservative.*

**Table 3-7: Areas over Above-ambient TSS Threshold Concentrations for Longer than 12 Hours for Each Scenario.**

Scenario	Concentration Thresholds in mg/L					
	10	25	50	100	200	650
	Areas Above Concentration Threshold (km <sup>2</sup> )					
Representative Northern ECC– Sandwave Clearance	N/A	N/A	N/A	N/A	N/A	N/A
Representative Sandwave Clearance, Monmouth ECC	<0.01	N/A	N/A	N/A	N/A	N/A
Representative IAC – Sandwave Clearance	0.24	N/A	N/A	N/A	N/A	N/A
Large OSS Seabed Foundation Preparation – 1	N/A	N/A	N/A	N/A	N/A	N/A
Large OSS Seabed Foundation Preparation – 2	<0.01	N/A	N/A	N/A	N/A	N/A
Large OSS Seabed Foundation Preparation – 3	N/A	N/A	N/A	N/A	N/A	N/A
Representative WTG Seabed Foundation Preparation	N/A	N/A	N/A	N/A	N/A	N/A
Representative IAC – Mechanical Trencher	N/A	N/A	N/A	N/A	N/A	N/A
Representative IAC – Jet Trencher	N/A	N/A	N/A	N/A	N/A	N/A
Northern ECC Landfill Approach, Representative HDD Pit	N/A	N/A	N/A	N/A	N/A	N/A
Representative Northern ECC– Jet Trencher	0.30	N/A	N/A	N/A	N/A	N/A
Monmouth Export Cable – Jet Trencher*	0.04	N/A	N/A	N/A	N/A	N/A
Monmouth ECC Landfall Approach, Representative HDD Pit	0.02	<0.1	N/A	N/A	N/A	N/A

*\*Both branches of this ECC were modeled and results were very similar. Of the two modeled ECC branches, only results from the maximum effect scenario were reported for simplicity and to be conservative.*

The maximum extents of the 10 mg/L and 100 mg/L concentrations, as measured perpendicular to the route centerline, and the maximum duration of TSS exposure >10 mg/L and >100 mg/L for each scenario, are listed in Table 3-8. When reviewing Table 3-8 it is important to note that the estimated duration of water column concentrations exceeding the thresholds of 10 and 100 mg/L includes the time associated with the construction activity. The reported durations of water column concentrations >10 and >100 mg/L are cumulative over the entire duration of the simulation and do not represent the duration it takes for water column concentrations to return to ambient after the construction activities cease. For example, based on the total volume and the production rate, the duration of dredging for the representative Large OSS sites requires approximately 18.6 hours. Results from the modeling assessment (Table 3-8) predict it will take between 8.9 and 12.1 hours for water column concentrations to be below 10 mg/L. Because the release of sediment was intermittent throughout the “active” dredging operations some of the time coincided with the dredging activity and did not require an additional 8.9 to 12.1 hours for water column concentrations to fall below 10 mg/L. The representative WTG seabed foundation preparation simulation was estimated to take 4.9 hours to return to ambient concentrations with a maximum extent to the 10 mg/L TSS threshold of 1.11 km.

For the sandwave clearance scenarios, water column concentrations were predicted to dissipate to less than 10 mg/L within 8.7 hours, 12.5 hours, and 14.3 hours for the Northern ECC, Monmouth ECC, and IAC simulations, respectively. The maximum extent of the plume to the 10 mg/L contour was largest for the Northern ECC, followed by the IAC, and Monmouth ECC scenarios. The larger extent associated with the Northern ECC can be contributed to the swift currents transporting the plume farther from the source which caused the plume to dissipate faster than the other two representative sandwave scenarios. In addition to the

magnitude of the subsurface currents, the magnitude and extent of the plume is controlled by the orientation of the route with respect to the currents and the sediment composition within the disturbance areas.

Based on the model results, the two representative IAC installation scenario extents are relatively similar, and that the Monmouth ECC cable installation activities are predicted to have plumes >10 mg/L and >100 mg/L that extend further than the Northern ECC activities. The Monmouth ECC scenario’s larger plume extent can be attributed to the route orientation, timing of the currents, advance rate, larger volume of disturbed sediment, and higher fraction of fine sediment, causing the sediments to take longer to settle. The plumes depicted throughout this report are not expected to be of these sizes contiguously from the release; rather these model results show the potential trajectories the sediment plumes may follow.

**Table 3-8: Maximum Extent to the 10 mg/L and 100 mg/L TSS Contours from the Route Centerline and Maximum Duration of Exposure to TSS >10 mg/L and >100 mg/L for Each Scenario.**

Scenario	Maximum Duration (hrs) of TSS >10 mg/L	Maximum Distance (km) to 10 mg/L Contour	Maximum Duration (hrs) of TSS >100 mg/L	Maximum Distance (km) to 100 mg/L Contour
Representative Northern ECC– Sandwave Clearance	8.7	4.47	7.0	1.29
Representative Sandwave Clearance, Monmouth ECC	12.5	3.20	7.0	2.1
Representative IAC – Sandwave Clearance	14.3	3.89	8.3	3.24
Large OSS Seabed Foundation Preparation – 1	11.9	2.37	7.6	2.26
Large OSS Seabed Foundation Preparation – 2	12.1	2.40	9.1	2.33
Large OSS Seabed Foundation Preparation – 3	8.9	2.60	7.2	2.18
Representative WTG Seabed Foundation Preparation	4.9	1.11	4.4	1.05
Representative IAC – Mechanical Trencher	8.7	2.71	3.8	0.60
Representative IAC – Jet Trencher	8.0	2.16	2.5	0.80
Northern ECC Landfill Approach, Representative HDD Pit	10.3	1.85	10.2	0.18
Representative Northern ECC– Jet Trencher	17.7	2.42	3.0	0.36
Monmouth ECC – Jet Trencher*	12.8	2.60	6.0	1.5
Monmouth ECC Landfall Approach, Representative HDD Pit	12.3	3.30	11	0.4

*\*Both branches of this ECC were modeled and results were very similar. Of the two modeled ECC branches, only results from the maximum effect scenario were reported for simplicity and to be conservative.*

The areas affected by sediment deposition over various thickness thresholds are summarized in Table 3-9. For both cable installation simulations within the Lease Area, the model did not predict any areas exceeding 1 mm thickness thresholds to be greater than >0.01 km<sup>2</sup>. This was because of the high fraction of fine material and the orientation of the route to the currents which advected the released sediment way from the source. For all seabed preparation scenarios (sandwave and foundation preparation), deposition was predicted to exceed 100 mm. This is due to the relatively large volume introduced during overflow and dumping, over a short period of time, and the assumption that 100% of the dredged sediment would be released back to the environment once the hopper reached capacity. The larger extents to the deposition thresholds for the Large OSS foundation preparation scenarios occurs because the sediment was introduced at the same location multiple times. For the sandwave clearances, sediment was introduced intermittently along the length of the route.



The Monmouth ECC cable installation scenarios resulted in a maximum thickness between 10-20 mm. The Northern ECC cable installation scenarios resulted in a maximum thickness between 1-5 mm. Both representative HDD Pit construction simulations predicted depositional thicknesses to exceed 10 mm, with the Northern ECC HDD pit excavation estimated to exceed 100 mm thicknesses. However, these areas are very small (<0.01 km<sup>2</sup>) and are contained around the pit location. The representative Monmouth ECC HDD pit excavation was predicted to have a larger extent to the ≥1 mm and ≥10 mm thickness thresholds compared to the representative Northern ECC HDD Pit excavation simulation. The area impacted was also slightly larger for the representative Monmouth ECC HDD pit excavation, because it contained higher percentages of fine material which took slightly longer to settle and therefore travelled further from the source due to the currents.

Table 3-9: Deposition over Thresholds for Each Scenario.

Scenario	Max Extent (km) of Deposition ≥1 mm	Max Extent (km) of Deposition ≥10 mm	Area (km <sup>2</sup> ) over Deposition Threshold				
			1 mm	5 mm	10 mm	20 mm	100 mm
Representative Northern ECC– Sandwave Clearance	0.58	0.20	5.17	3.46	2.91	1.73	1.15
Representative Sandwave Clearance, Monmouth ECC	0.86	0.17	5.20	2.86	2.34	1.90	1.06
Representative IAC – Sandwave Clearance	1.22	0.15	3.47	1.06	0.83	0.64	0.36
Large OSS Seabed Foundation Preparation – 1	2.10	0.76	2.55	0.89	0.40	0.22	0.03
Large OSS Seabed Foundation Preparation – 2	2.18	0.97	2.68	0.86	0.47	0.23	0.03
Large OSS Seabed Foundation Preparation – 3	2.03	0.82	2.75	0.83	0.45	0.17	0.03
Representative WTG Seabed Foundation Preparation	0.86	0.37	0.60	0.16	0.08	0.03	0.01
Representative IAC – Mechanical Trencher	N/A	N/A	N/A	N/A	N/A	N/A	N/A
Representative IAC – Jet Trencher	0.05	N/A	<0.01	N/A	N/A	N/A	N/A
Northern ECC Landfill Approach, Representative HDD Pit	0.15	0.07	0.01	<0.01	<0.01	<0.01	<0.01
Representative Northern ECC– Jet Trencher	0.09	N/A	4.45	N/A	N/A	N/A	N/A
Monmouth Export Cable – Jet Trencher*	0.20	0.03	8.32	0.75	0.02	N/A	N/A
Monmouth ECC Landfall Approach, Representative HDD Pit	0.48	0.10	0.09	0.03	0.01	N/A	N/A

\*Both branches of the ECC were modeled and results were very similar. Of the two modeled ECC branches only results from the maximum effect scenario was reported for simplicity and to be conservative.

### 3.3.2 Seabed Preparation: Sandwave Clearance

#### Representative Northern ECC – Sandwave Clearance

The instantaneous map illustrates that the plume is patchy throughout the water column; as it is transported by subsurface currents, the concentrations dissipate and settle (Figure 3-13). Sandwave clearance along the Northern ECC route was predicted to result in plumes that extended vertically throughout the water column, with higher fractions of fine material lingering longer in the water column. In regions where there were higher percentages of fine material, and where the current was both faster (e.g., within the channel in northern section) and not in-line with the route, the extent of the plume tended to be larger (Figure 3-14). This was primarily due

to the finer sediment being more easily transported away from the dump sites. In contrast, the coarse material which was dumped settled relatively quickly to the seabed, depositing around the release sites. The map of time integrated maximum water column concentration (Figure 3-14) revealed that relatively higher concentrations (e.g.,  $\geq 650$  mg/L) were predicted closer to the dump sites, with lower concentrations (10-25 mg/L) spanning northwest and southeast of the route with respect to the current action at the time of release.

All TSS concentrations are predicted to return to ambient concentrations within approximately 8.7 hours (Table 3-8). Longest durations of water column concentrations  $\geq 10$  mg/L correspond to areas with fine material and hydrodynamic forcing that caused the plume to compound on itself (e.g., northern portion of the route; Figure 3-15).

After being released near the surface during overflow, or just below the surface when dumping, the coarse sediment settles first to the seabed creating a depositional footprint centered around the dump sites with deposition extending diagonally due to the influence of oscillating subsurface currents (Figure 3-16). The thickest deposits (i.e., deposition  $>100$  mm) remain near the release location, with thinner deposits (i.e., deposition between 1 and 5 mm) extending laterally from the release location (Figure 3-16). The maximum extent to the 1 mm and 10 mm contours was predicted to be approximately 0.58 km and 0.20 km, respectively (Table 3-9).

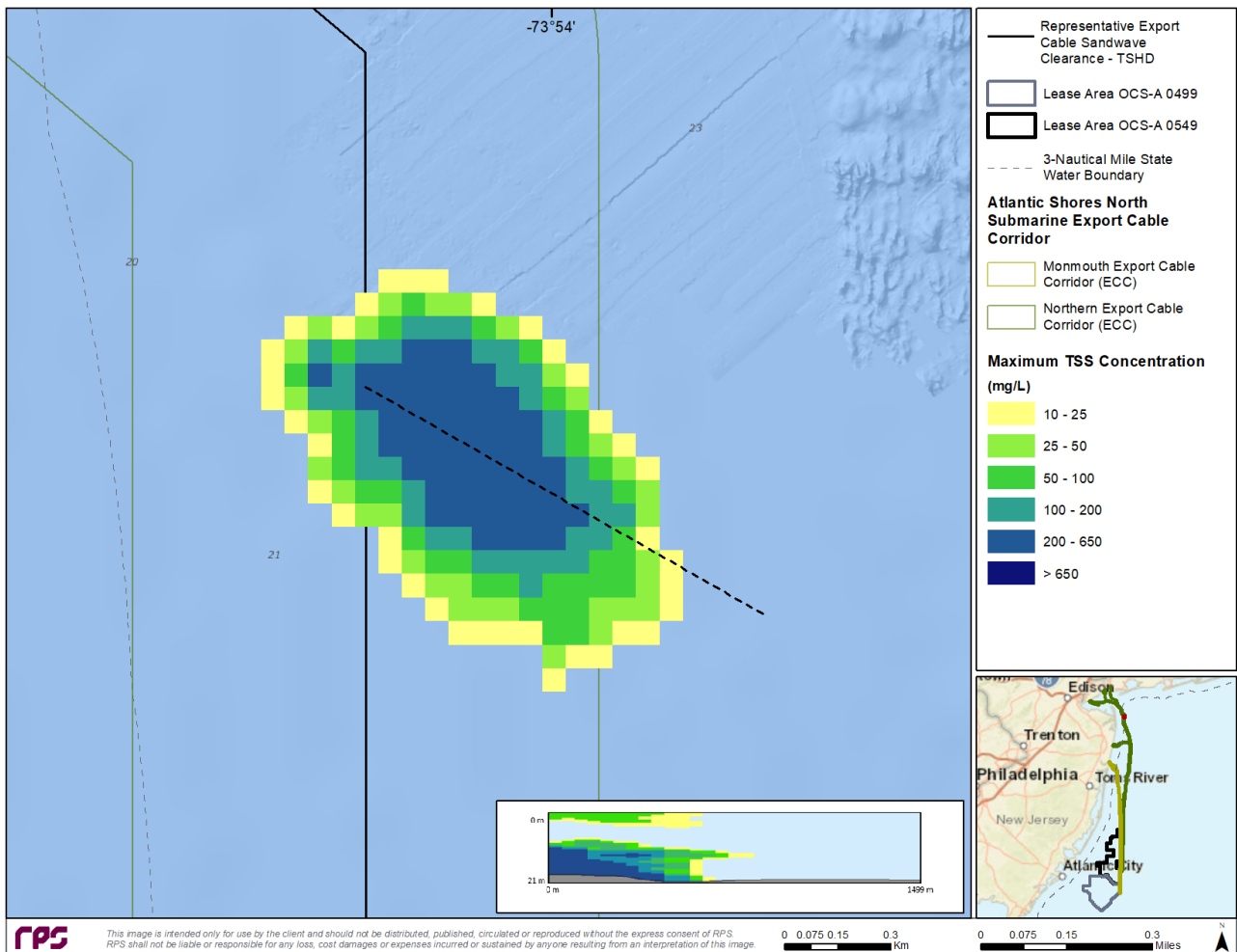


**Figure 3-13: Snapshot of instantaneous TSS concentrations for a time step during the Representative Northern ECC Sandwave Clearance – TSHD simulation.**

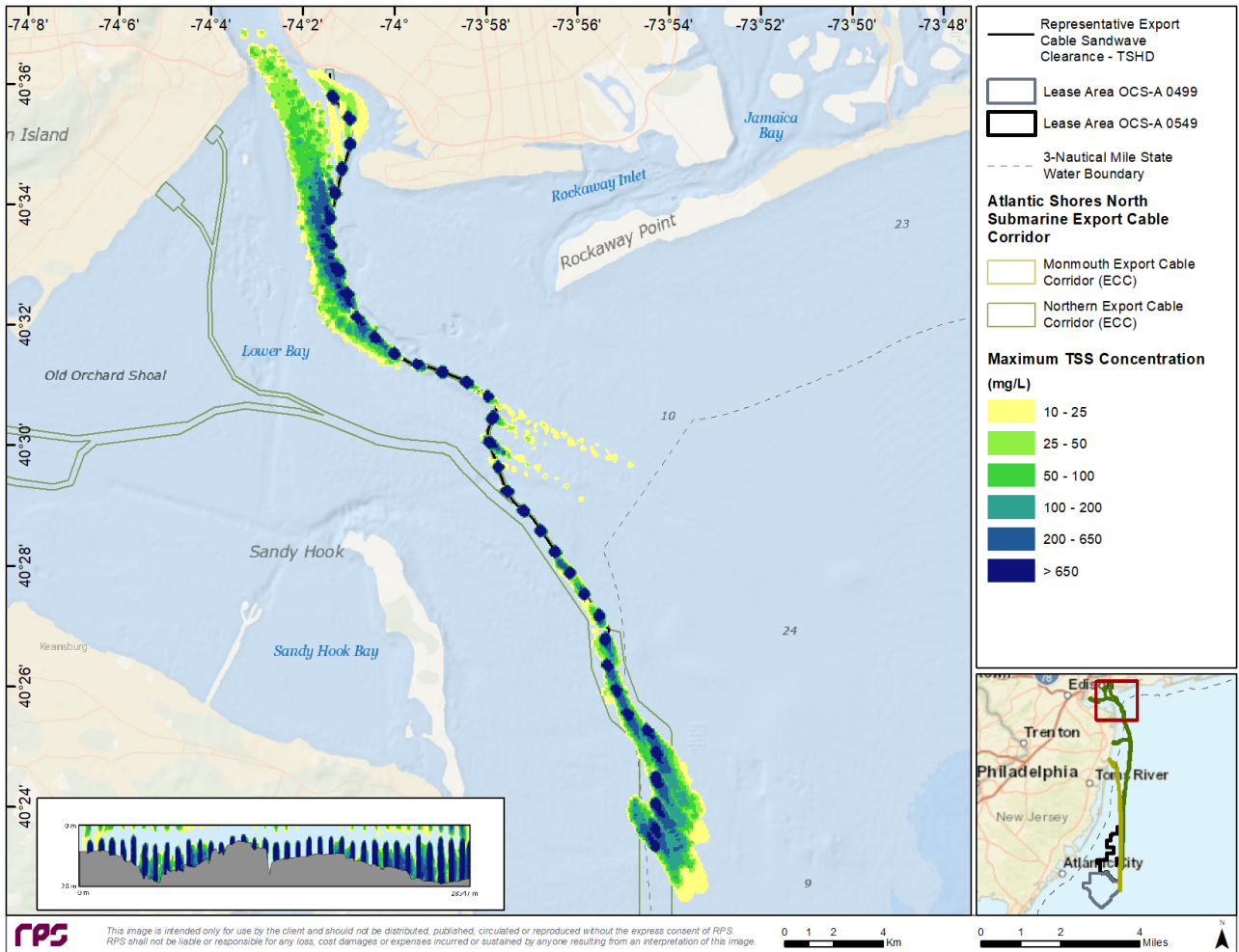


Figure 3-14: Map of time-integrated maximum concentrations associated with the Representative Northern ECC Sandwave Clearance – TSHD simulation.

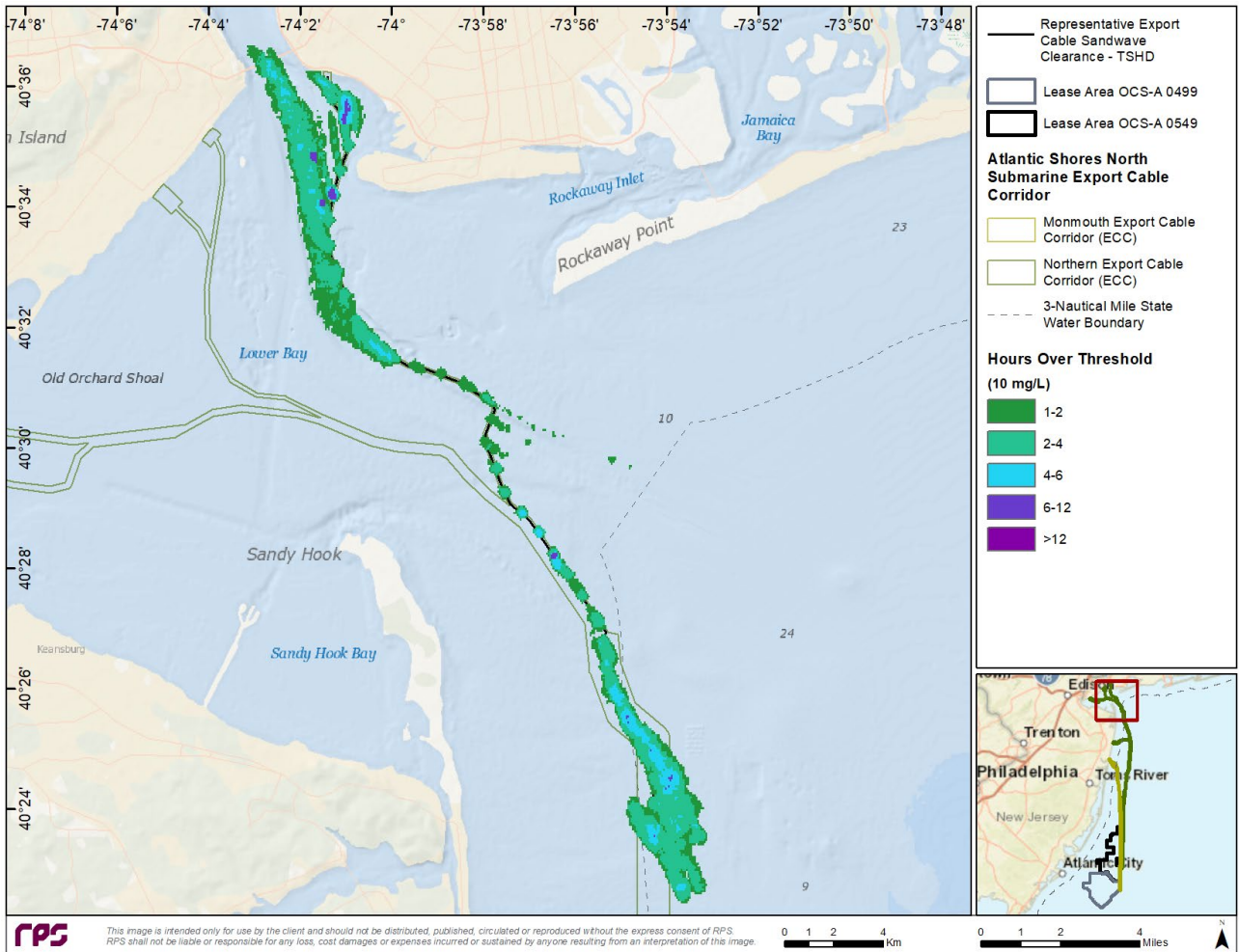


Figure 3-15: Map of duration of TSS ≥ 10 mg/L associated with the Representative Northern ECC Sandwave Clearance – TSHD simulation.

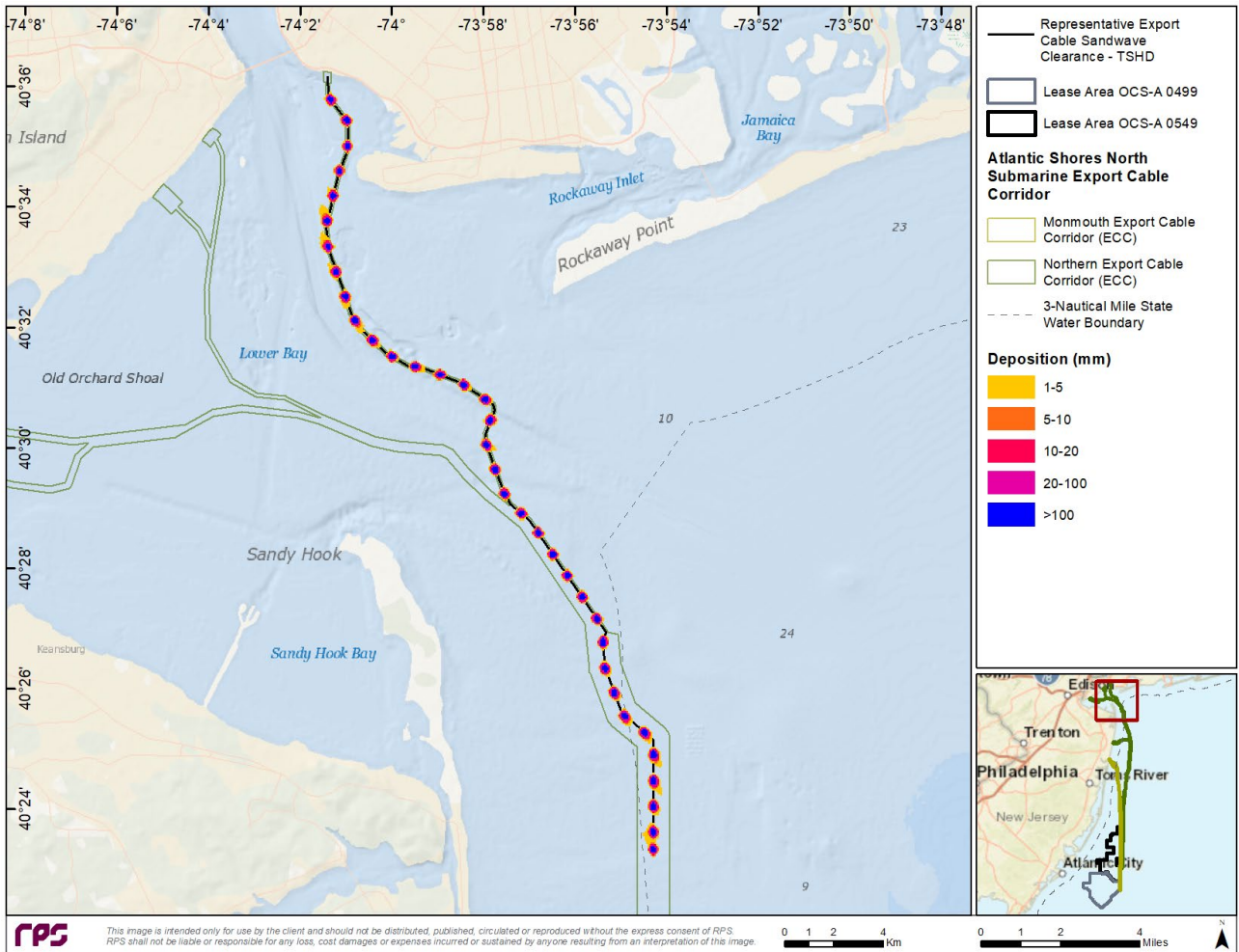


Figure 3-16: Map of deposition thickness associated with the Representative Northern ECC Sandwave Clearance – TSHD simulation.

### **Representative Monmouth ECC – Sandwave Clearance**

A snapshot of the instantaneous concentrations is presented in Figure 3-17 with the vertical cross-section along the route. This figure illustrates that higher concentrations were contained around the route centerline, with lower concentrations biased towards the south due to bottom currents. The cross-section shows that the plume extended throughout the water column due to the sediment being introduced at the surface. The map of maximum time-integrated concentrations is presented in Figure 3-18 with the vertical cross-section along the route, the duration of exposure to TSS  $\geq 10$  mg/L is presented in Figure 3-19, and the seabed deposition is shown in Figure 3-20.

Figure 3-18 illustrates how the plume oscillated with the tides, which is reflective in the oscillatory pattern of the concentrations relative to the route centerline. The oscillatory pattern was less evident in regions where the route was parallel to local currents. In sections where the route was parallel to the currents, the plumes from the periodic dumping locations interacted with each other more than in sections where the currents are perpendicular to the route. The interaction of the plumes resulted in areas with prolonged durations of exposure to TSS concentrations  $\geq 10$  mg/L (Figure 3-19). Concentrations  $\geq 10$  mg/L had a maximum extent of approximately 3.20 km from the route centerline.

The map of duration of exposure to TSS  $\geq 10$  mg/L (Figure 3-19) shows a pattern similar to the maximum concentration, with most locations exposed for less than 12 hours and a small area exposed for a little over 12 hours. Because the sediment is predominantly coarse, which tends to settle out of the water column relatively quickly, the deposition tended to remain close to the route centerline near locations associated with the periodic dumping of sediment at the surface (Figure 3-20). The deposition close to the route centerline was relatively high due to the coarse sediment settling near the source and the large volume of sediment introduced into the water column within a short period of time and within a small area.

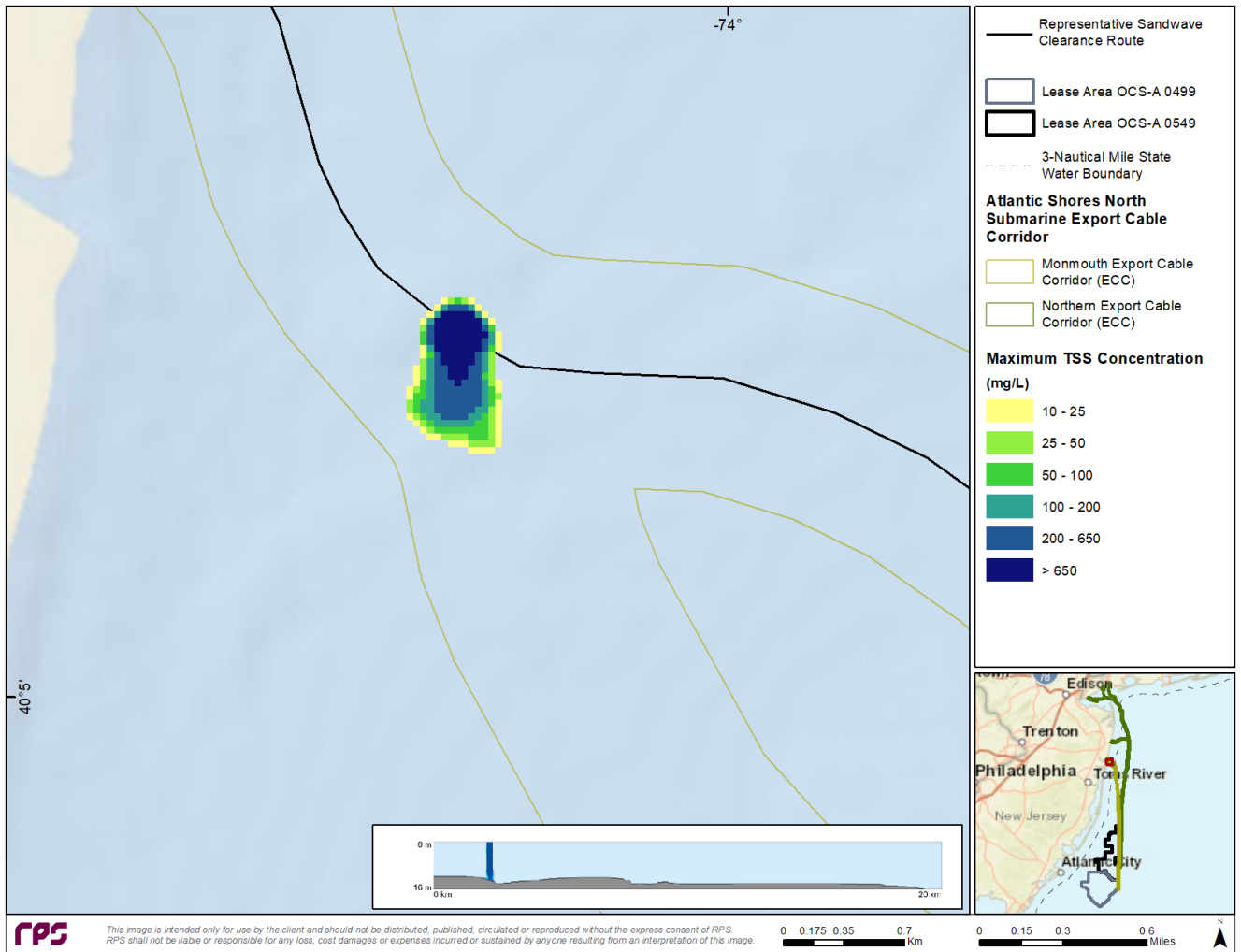


Figure 3-17: Snapshot of Instantaneous TSS Concentrations Associated with Sandwave Clearance along the Monmouth ECC.

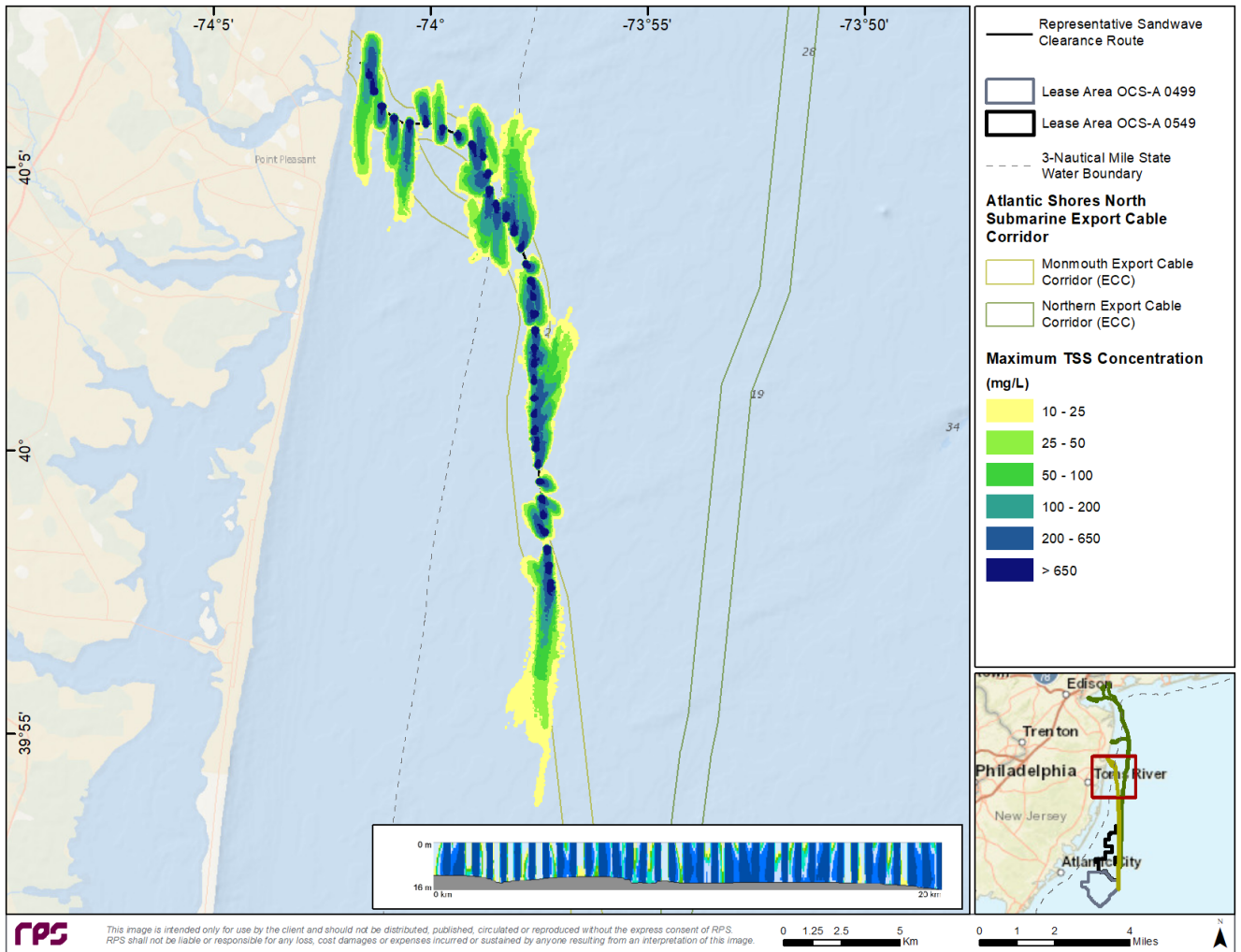


Figure 3-18: Map of Time-Integrated Maximum TSS Concentrations Associated with Sandwave Clearance along the Monmouth ECC.



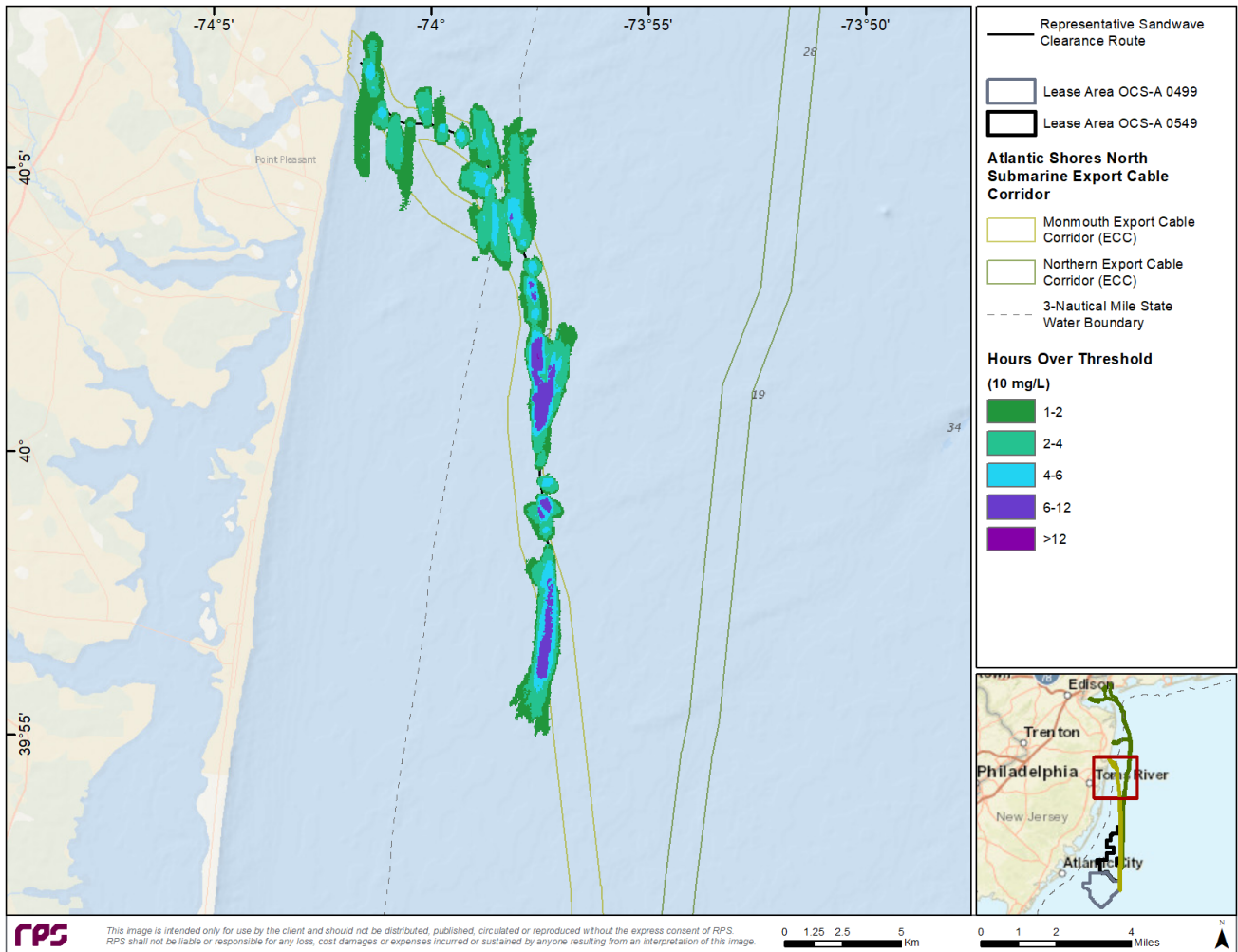


Figure 3-19: Map of Duration of TSS ≥10 mg/L Associated with Sandwave Clearance along the Monmouth ECC.

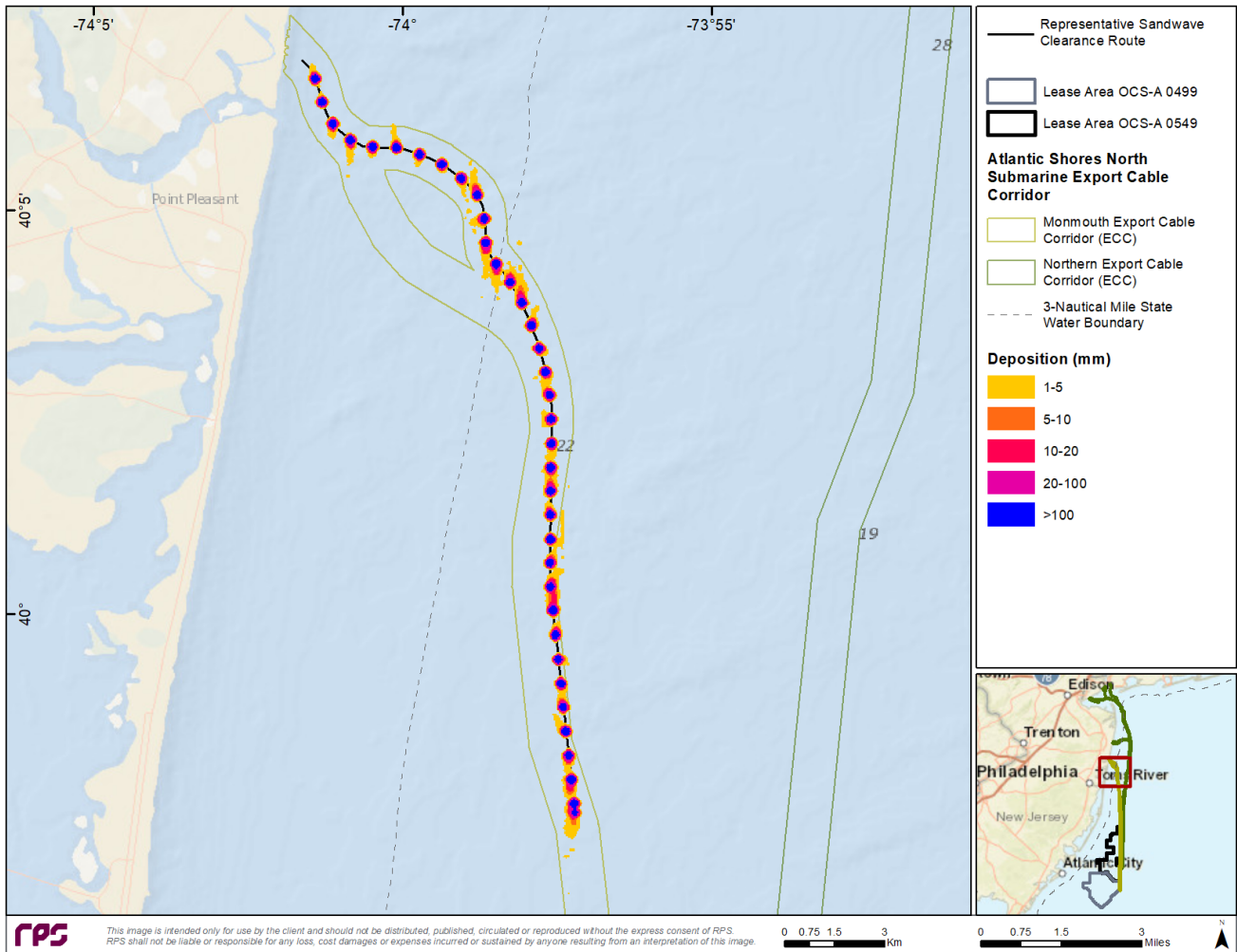


Figure 3-20: Map of Deposition Thickness Associated with Sandwave Clearance along the Monmouth ECC.

**Representative Inter-array Cable in Lease Area – Sandwave Clearance**

Sandwave clearance was simulated within the Lease Area along a representative route that coincided with the longest, continuous section of sandwaves. Based on the simulation timing, the portion of sediment associated with overflow was readily transported by the currents, which resulted in the resulting plumes being transported away from the route. Coarse material released during dumping settled relatively quickly around the dump site. In contrast, finer material was shown to remain within the water column and be transported away from the centerline (Figure 3-22).

A snapshot of the instantaneous concentrations from the representative sandwave clearance within the Lease Area (Figure 3-21) showed the dump and overflow plume was patchy throughout the water column, with the highest concentrations at the seabed and lowest concentrations closer to the water surface. This snapshot of an area with a relatively high percentage of fine material was taken following the overflow operations that were predicted to be furthest from the route centerline. The time-integrated maximum water column concentration map (Figure 3-22) contains an inset that shows the cross-sectional view of the plume extending from the water surface to the seabed.

TSS concentrations extend laterally and orthogonally from the IAC centerline (Figure 3-22). This can be attributed to strong current action within the Lease Area that transported the sediment suspended within the water column. As with the maximum concentration maps, the maps of the duration of water column TSS concentrations  $\geq 10$  mg/L (Figure 3-23) follow a similar pattern and display the influence of subsurface currents on the duration of sediment concentrations exceeding thresholds. TSS concentrations that exceed 650 mg/L were predicted to dissipate between 4 to 6 hours (Table 3-5 and Table 3-6). TSS concentrations  $\geq 10$  mg/L are predicted to persist for approximately 14.3 hours (Table 3-8; Figure 3-23). The results show, in any given location, the total TSS exposure  $\geq 10$  mg/L is typically between one to six hours, with regions closest to the route generally dissipating within six to 12 hours.

Seabed deposition for this scenario (Figure 3-24) exceeded 100 mm near the dump location, with thickness between 1 and 5 mm extending orthogonally from the dump site. Depositional thicknesses at the dredge locations in association with drag arm disturbances were mostly  $>1$  mm with smaller patches of  $>5$  mm thicknesses (Figure 3-24). The maximum distance to the 1 mm and 10 mm contour is predicted to extend approximately 1.22 km and 0.15 km, respectively (Table 3-9).

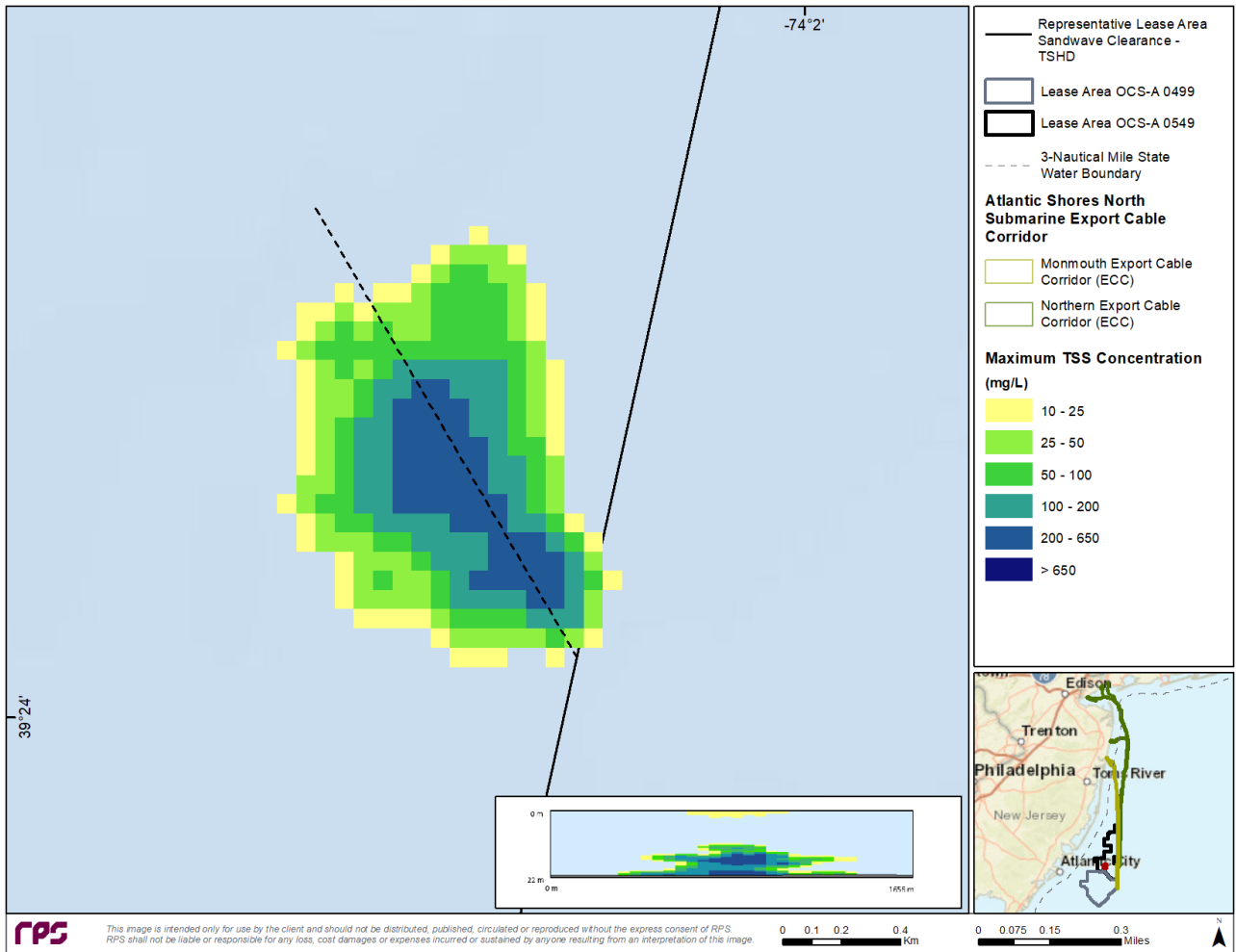


Figure 3-21: Snapshot of instantaneous TSS concentrations for a time step during the Representative Inter-array Cable Sandwave Clearance – TSHD simulation.

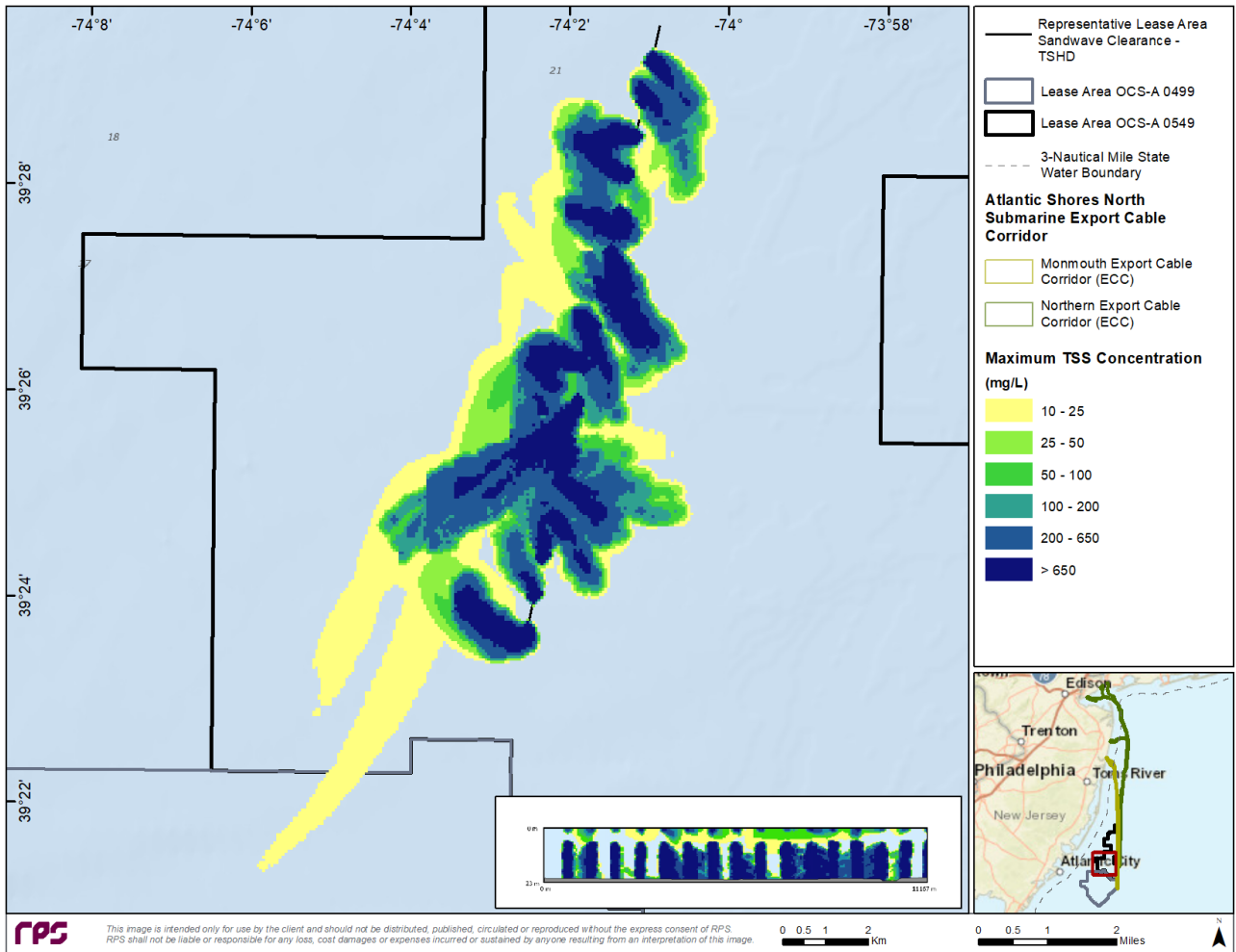


Figure 3-22: Map of time-integrated maximum concentrations associated with the Representative Inter-array Cable Sandwave Clearance – TSHD simulation.

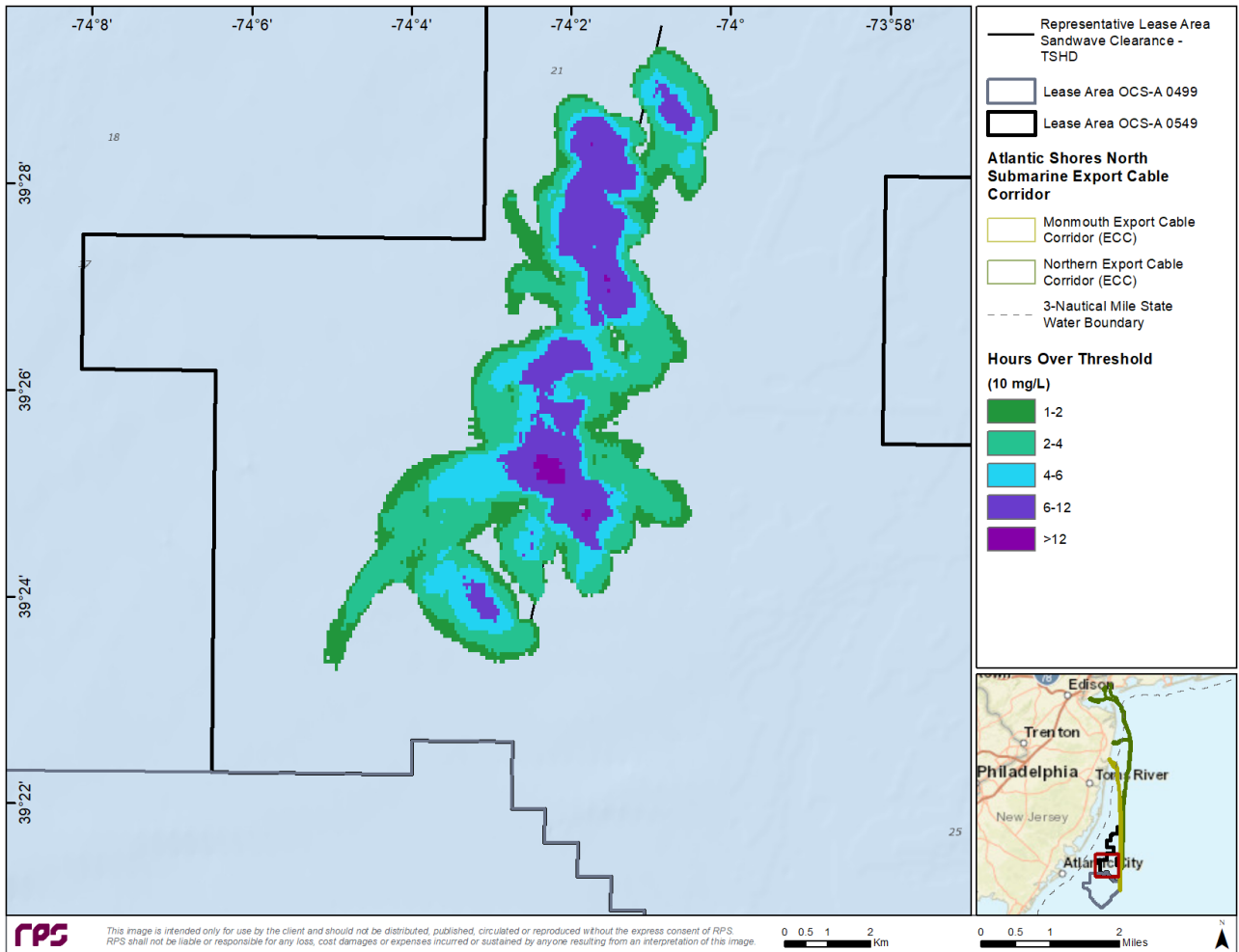


Figure 3-23: Map of duration of TSS ≥ 10 mg/L associated with the Representative Inter-array Cable Sandwave Clearance – TSHD simulation.

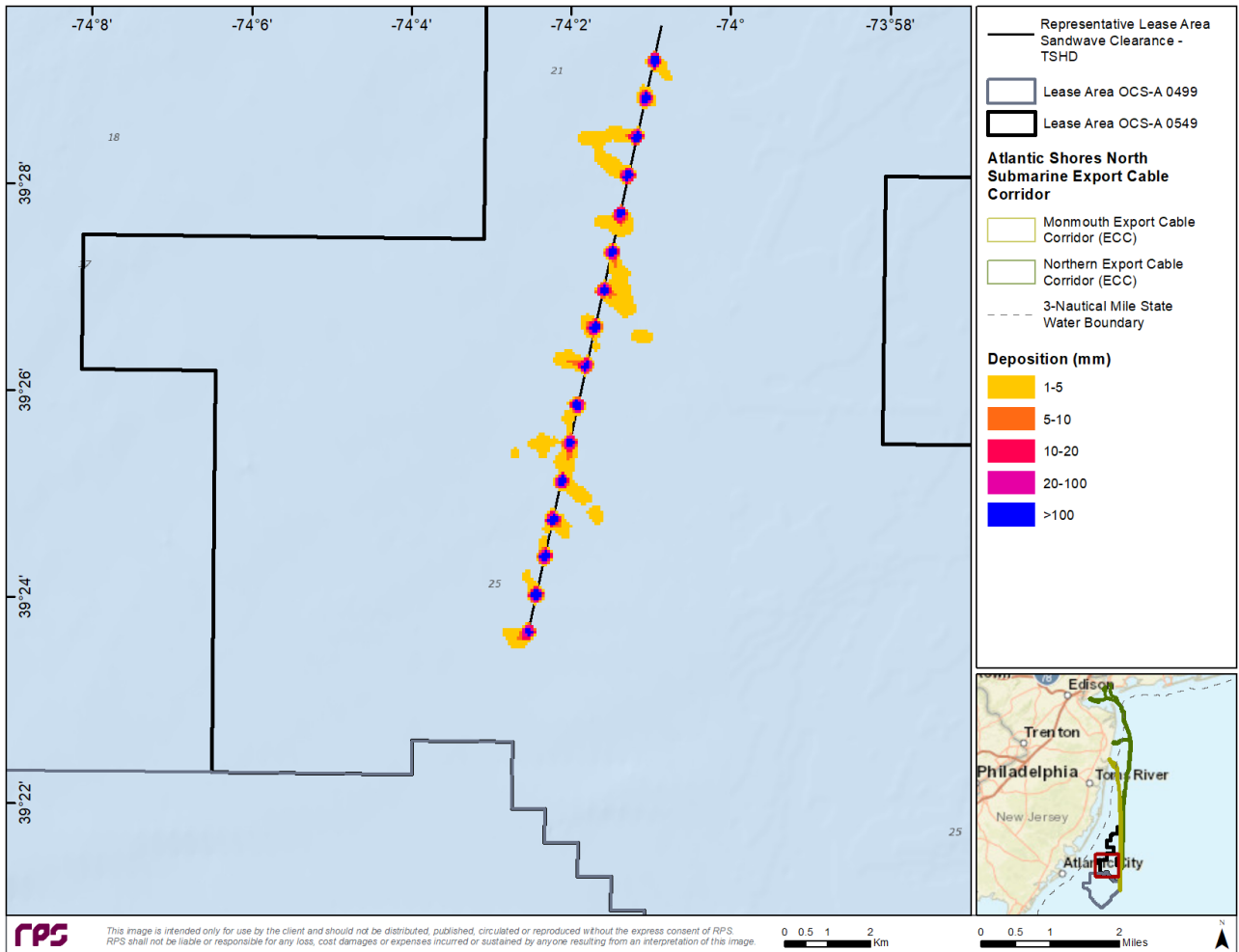


Figure 3-24: Map of deposition thickness associated with the Representative Inter-array Cable ECC Sandwave Clearance – TSHD simulation.

### 3.3.3 Seabed Preparation: Large OSS & WTG Foundations

The three Large OSS seabed foundation preparation simulations are presented separately as it is anticipated that clearance of these foundations would occur at different times. Therefore, the plumes from the three distinct sites are not anticipated to interact and can be considered independent when viewing the mapped results.

#### **Large OSS Seabed Foundation Preparation – Site 1**

The instantaneous water column concentration map (Figure 3-25) depicts two plumes: one south of the release site, released during the second overflow and dump operation, and the other plume near the source represents the third dump and overflow. The southern plume consists of lower concentrations because it was dispersed by subsurface currents and settled over time, as indicated by the cross-section (Figure 3-25). The plume with higher concentrations near the source spans the entire water column because overflow and dumping operations were simulated just prior to the instantaneous snapshot (Figure 3-25). The time-integrated maximum water column concentration map illustrates that the concentrations span the entire water column near the source, but as the sediment settles the vertical distribution in the water column becomes more biased towards the seabed (Figure 3-26). Based on the timing of the currents and of the dumping and overflow operations, the first plume was initially transported north and was swept south as the tides oscillated. This caused the first and second plume to compound prior to the first plume fully dissipating. The second plume was transported southeast and dissipated before the third overflow and dump. The third plume was carried north of the release location and circled east around the Large OSS Site 1 as it was settling and dispersing.

As shown in the duration of water column concentrations  $\geq 10$  mg/L map (Figure 3-27), the majority of the plume returned to ambient within 4 to 6 hours, with the plume entirely dissipating to less than 10 mg/L within 11.9 hours (Table 3-8). The region associated with durations of 6 to 12 hours correspond to the locations of the compounding plumes (Figure 3-27) and highlight the influence of current direction at the time of overflow and dumping. Based on the location of the Large OSS – Site 1, it is important to note that the *in-situ* sediment grain size contains more coarse sand and less clay than was modeled in this assessment. The grain size used in this simulation likely produced a plume with higher concentrations that take longer to settle and resulted in a plume that was transported farther from the source than may occur during the actual construction operations.

The depositional footprint followed the trajectory of the plume and primarily extended north and south of the site (Figure 3-28). Patches of depositional thicknesses between 1 and 5 mm extended east of the source and contained intermittent patches of deposition with thicknesses between 5 and 10 mm. The thickest deposits ( $>100$  mm) were centered around the Large OSS, with thicknesses ranging between 20 and 100 mm spanning north and south of the site. The maximum extent to the 1 mm and 10 mm contours was predicted to be approximately 2.10 km and 0.76 km, respectively (Table 3-9).



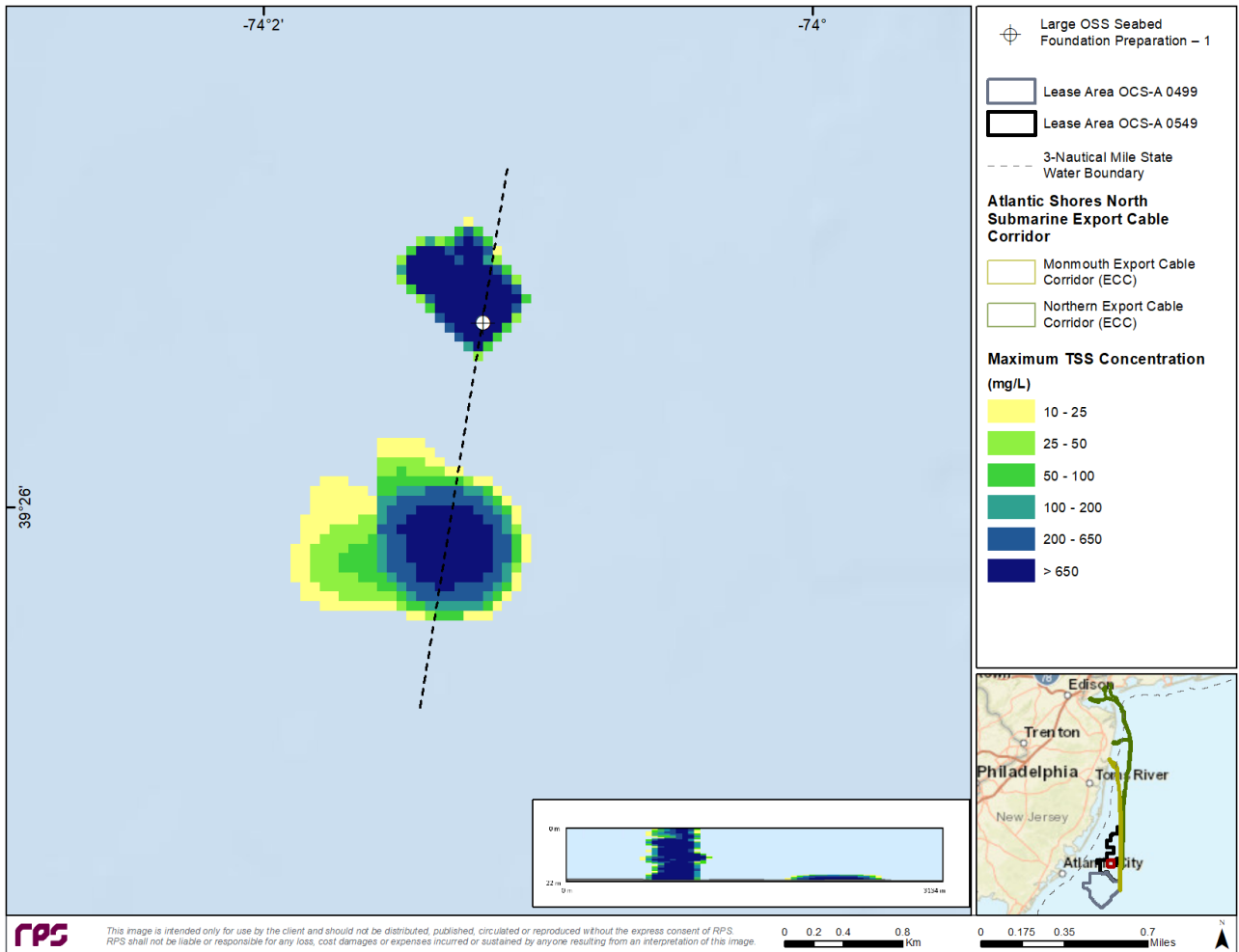


Figure 3-25: Snapshot of instantaneous TSS concentrations for a time step during the Large OSS Seabed Foundation Preparation simulation using TSHD at Site 1.

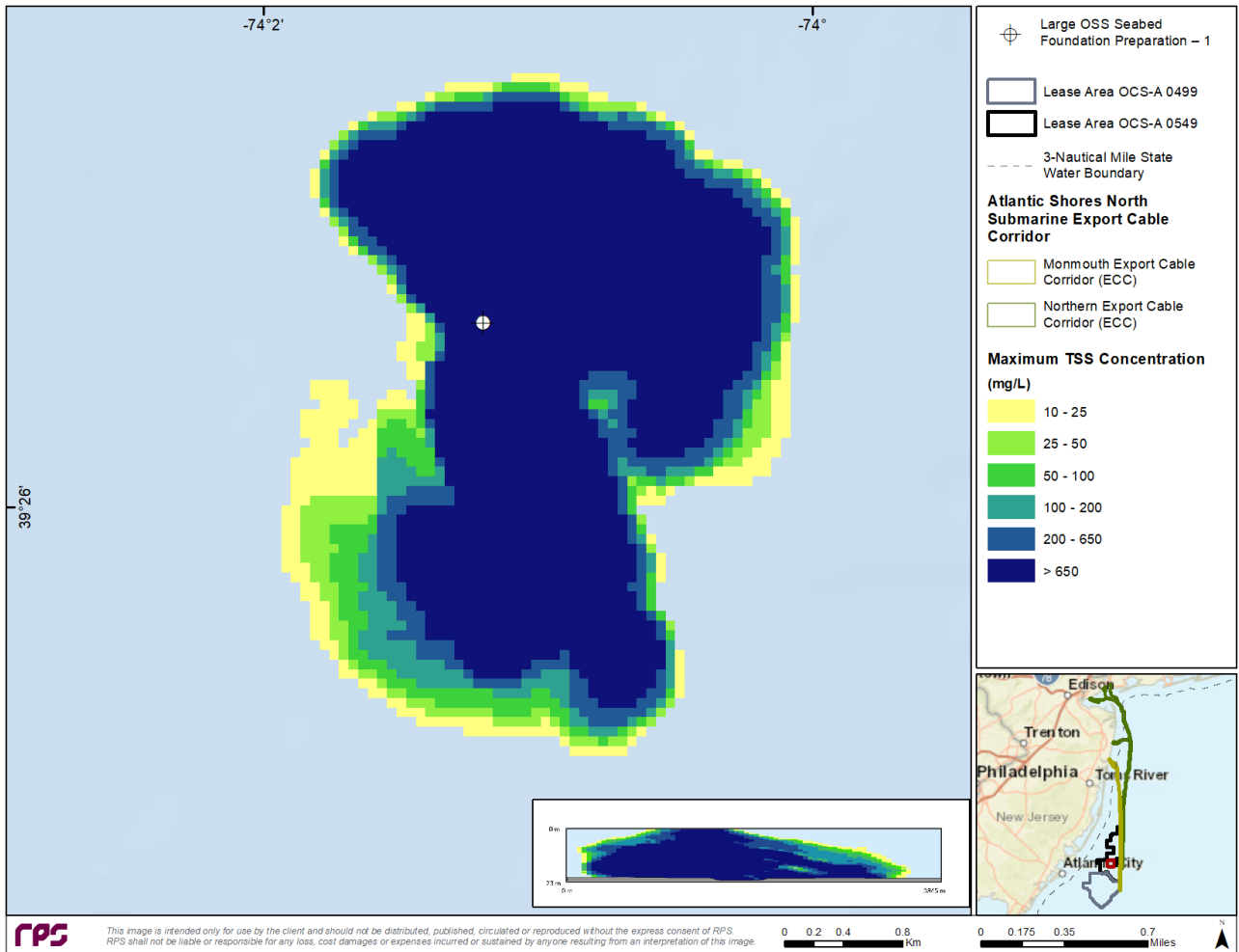


Figure 3-26: Map of time-integrated maximum concentrations associated with the Large OSS Seabed Foundation Preparation simulation using TSHD at Site 1. Note that the cross-section spans north to south along the plume.

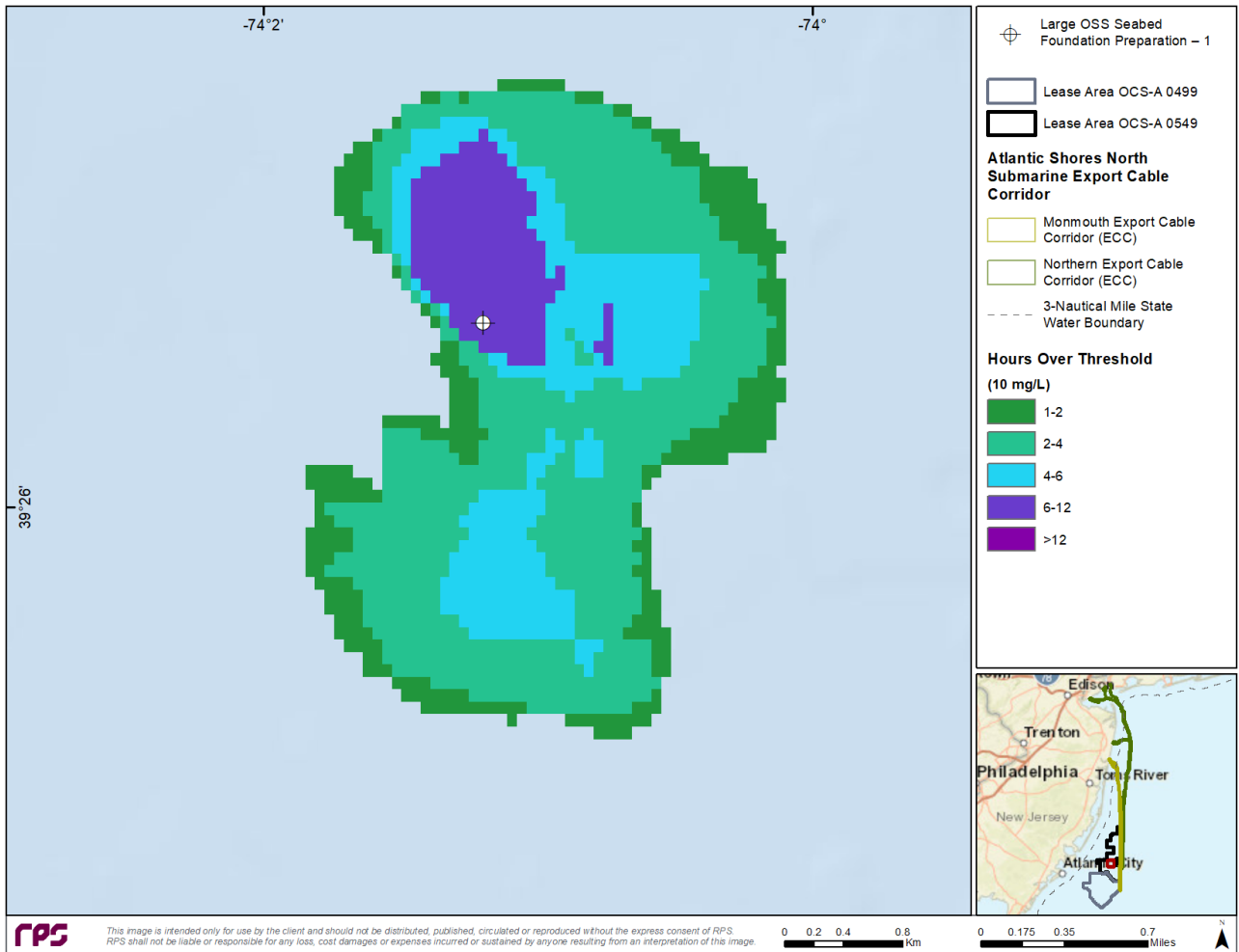


Figure 3-27: Map of duration of TSS  $\geq$  10 mg/L associated with the Large OSS Seabed Foundation Preparation simulation using TSHD at Site 1.

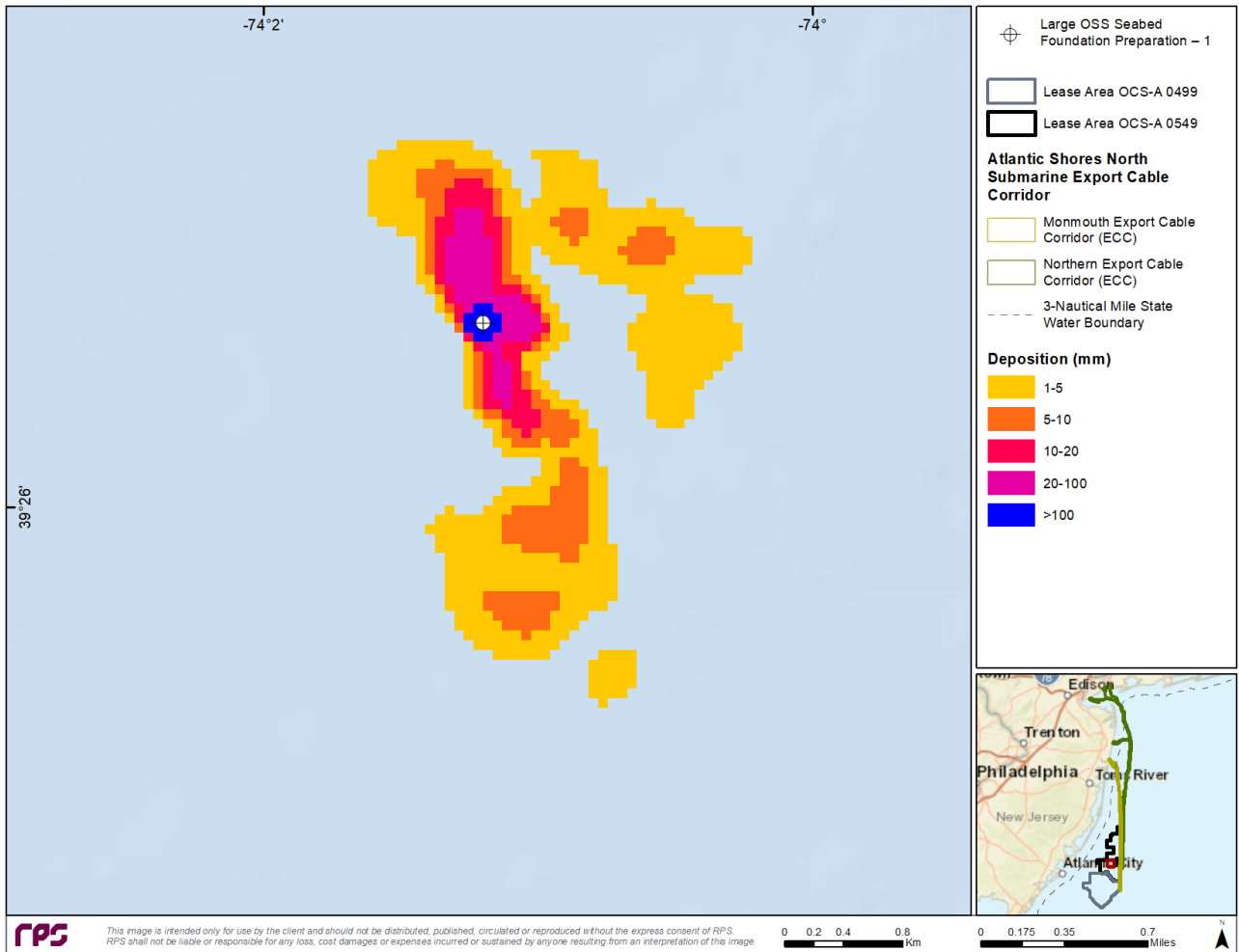


Figure 3-28: Map of deposition thickness associated with the Large OSS Seabed Foundation Preparation simulation using TSHD at Site 1.

### **Large OSS Seabed Foundation Preparation – Site 2**

Seabed foundation preparation at the Large OSS – Site 2 was similar in magnitude and extent when compared with results from Site 1. The differences are due to the geographic location as all other conditions were held constant and can be contributed to the slight variation in the subsurface currents. The instantaneous snapshot of water column concentrations (Figure 3-29) illustrates two plumes: the plume south of the release corresponds to the second overflow and dump while the plume north of the site corresponds to the third overflow and dump. The snapshot was taken slightly after the third release thus illustrating the vertical distribution associated with overflow and dumping. The southern portion of the plume settled over time which resulted in the plume being local to the seabed as it transported and dispersed with subsurface currents.

The time-integrated maximum water column concentration footprint (Figure 3-30) was slightly smaller than what was predicted for Site 1, with smaller areas predicted to exceed water column concentrations for longer than 2 hours for all TSS thresholds (Table 3-4). However, the durations associated with water column concentrations >10 and >100 mg/L were predicted to be longer for Site 2 than at Site 1. This is due to the slightly different forcing from subsurface currents which shifted the trajectory, resulting in a plume with higher concentrations that required slightly more time to dissipate to less than 10 mg/L. The map of duration of water column concentrations  $\geq 10$  mg/L (Figure 3-31) illustrates two distinct regions that require 6 to 12 hours to dissipate to less than 10 mg/L. Additionally, just north of the site, a small area (<0.01 km<sup>2</sup>) was predicted to take approximately 12.1 hours to fully dissipate. Note that based on the location of the Large OSS – Site 2, the *in-situ* sediment composition would be primarily coarse sand but was modeled with a mixture of fine and coarse sand to be conservative. Coarse sand would settle faster, thus reducing the overall magnitude and extent of the subsurface TSS plume. Additionally, it is anticipated that it would take less than 12.1 hours for water column concentrations to fall below 10 mg/L.

As predicted by the model, the depositional footprint for the Large OSS – Site 2 had thicknesses >1 mm extending north/northwest and south/southeast of the site (Figure 3-32). A small area with depositional thickness >100 mm was predicted around the source. The magnitude and extent of deposition was similar for Sites 1 and 2, with slightly larger areas estimated with thicknesses >1 mm for Site 2. The maximum extent to the 1 mm and 10 mm contours was predicted to be approximately 2.18 km and 0.97 km, respectively (Table 3-9).

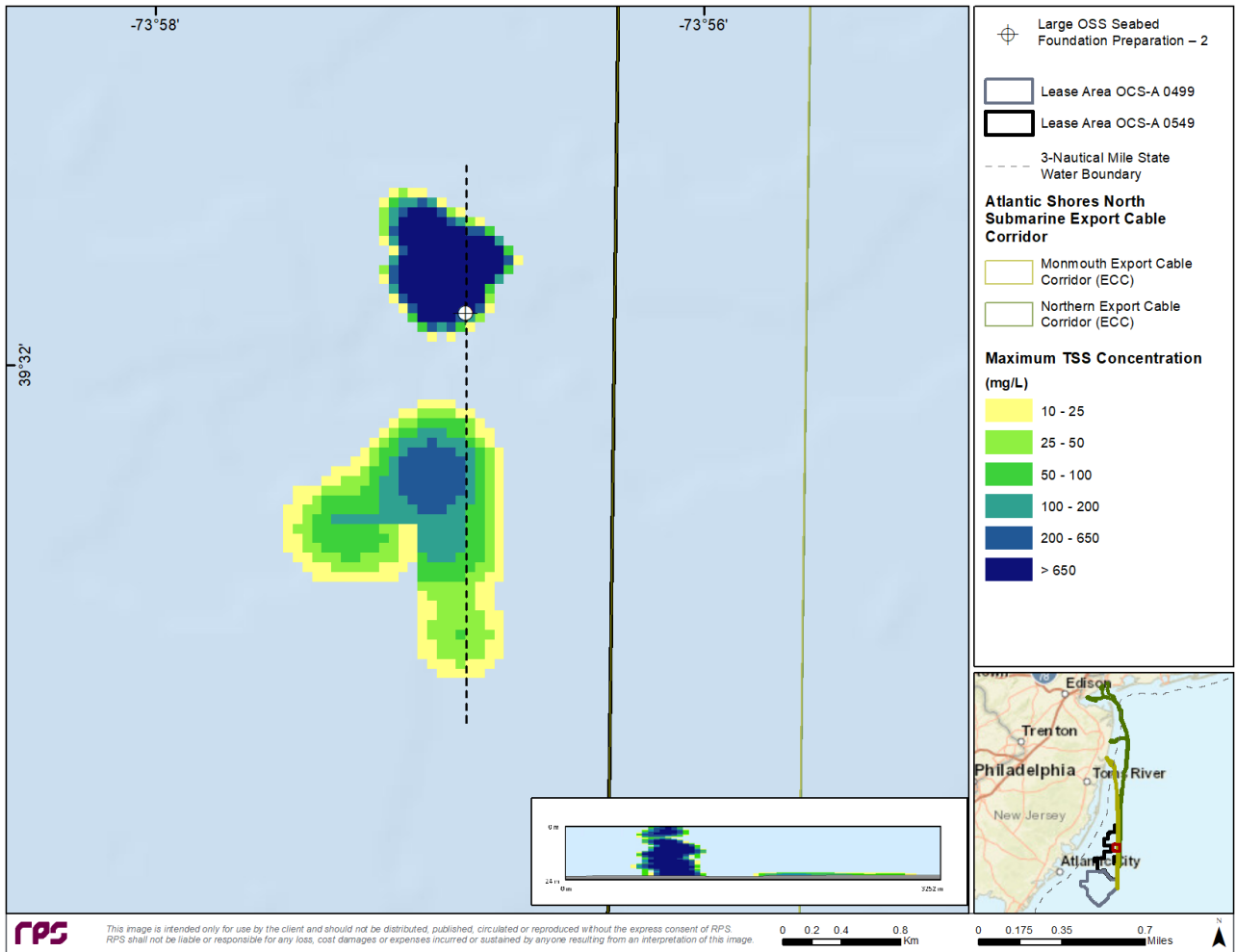


Figure 3-29: Snapshot of instantaneous TSS concentrations for a time step during the Large OSS Seabed Foundation Preparation simulation using TSHD at Site 2.

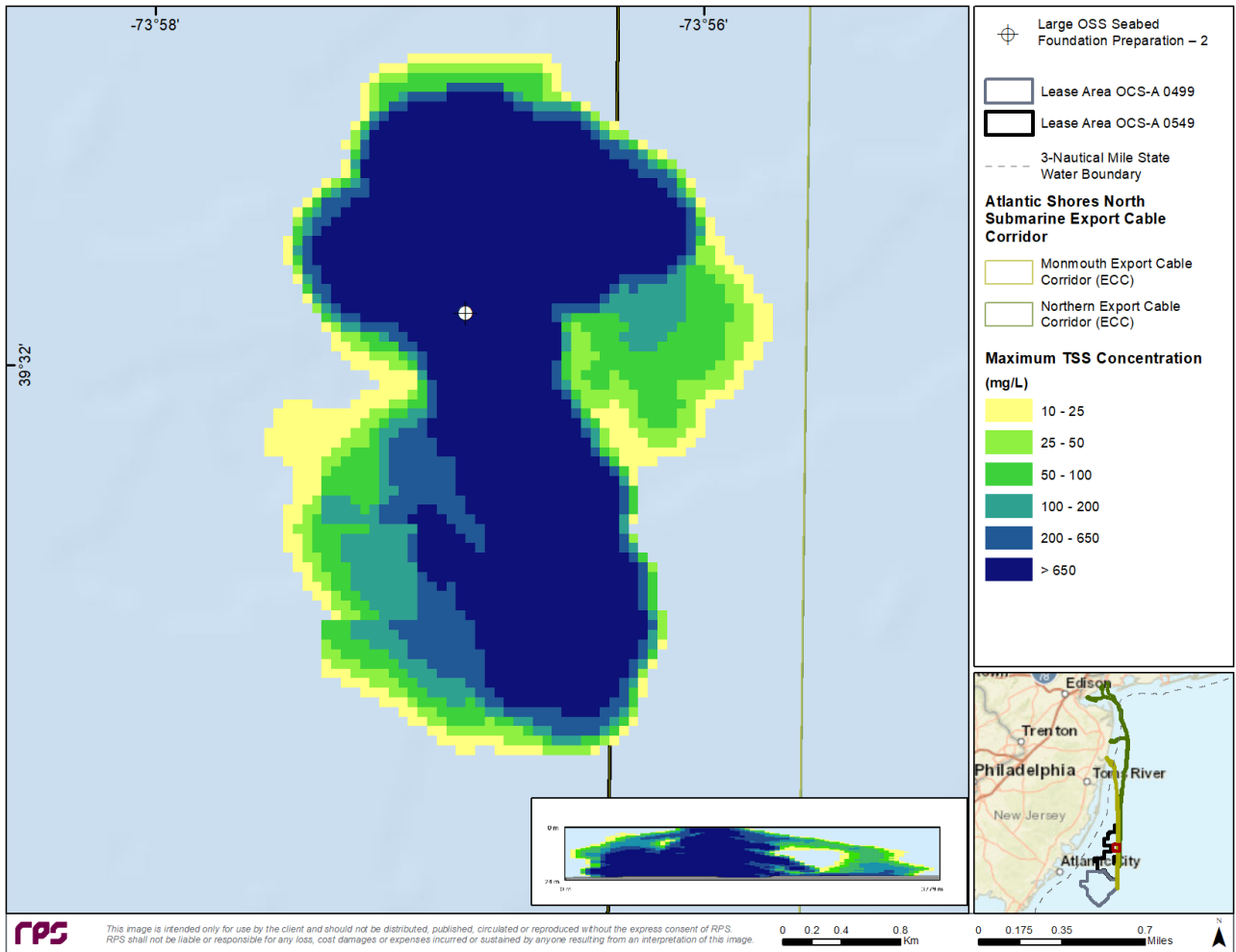


Figure 3-30: Map of time-integrated maximum concentrations associated with the Large OSS Seabed Foundation Preparation simulation using TSHD at Site 2. Note that the cross-section spans north to south along the plume.

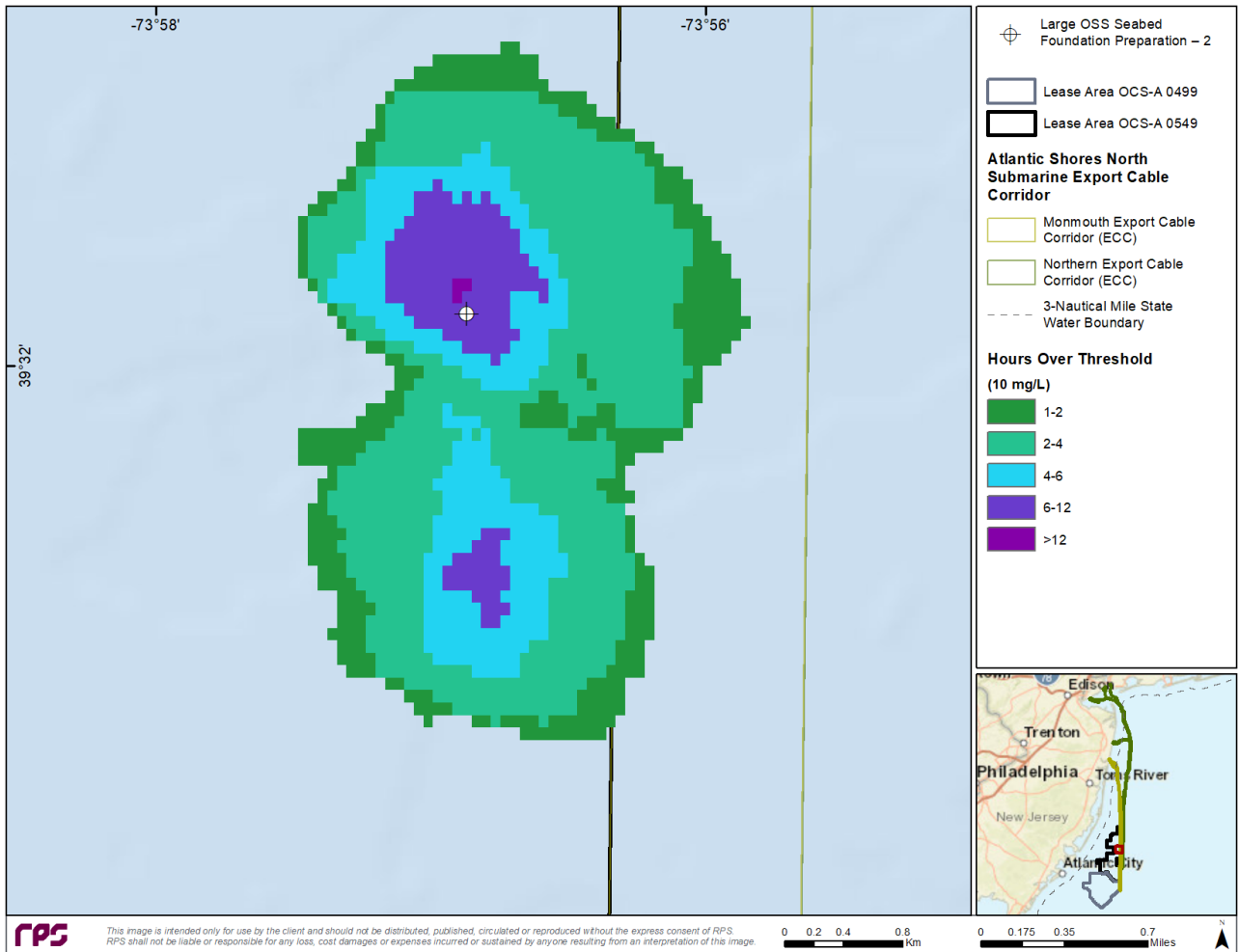
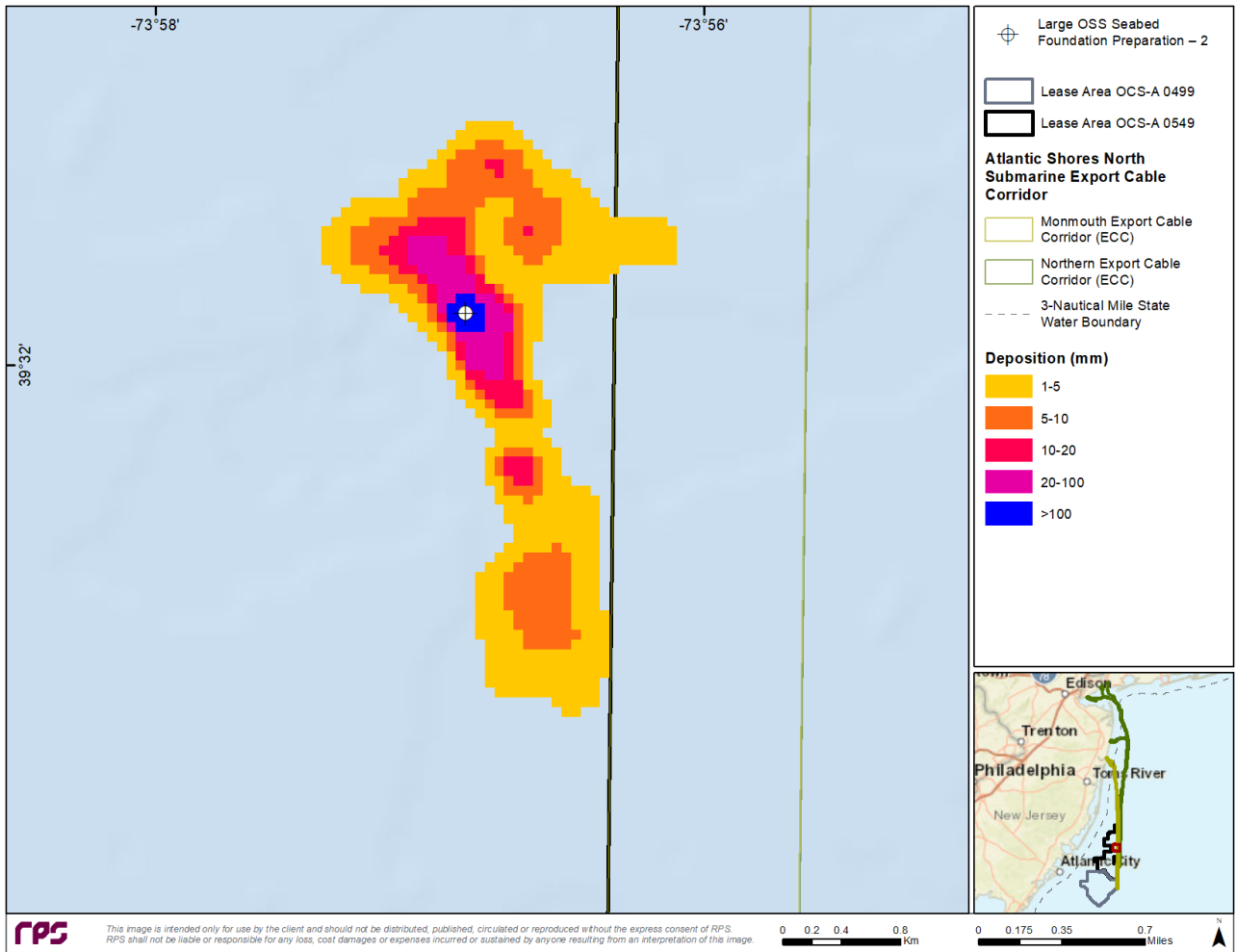


Figure 3-31: Map of duration of TSS ≥ 10 mg/L associated with the Large OSS Seabed Foundation Preparation simulation using TSHD at Site 2.





**Figure 3-32: Map of deposition thickness associated with the Large OSS Seabed Foundation Preparation simulation using TSHD at Site 2.**

### **Large OSS Seabed Foundation Preparation – Site 3**

The variation in results across the three different seabed foundation preparation simulations at the Large OSS sites highlights the influence of environmental forcing on the fate of the suspended sediment plume. The timing and volume of the releases were the same across all three sites, however, the plume was predicted to dissipate faster at the Large OSS – Site 3. The slightly faster currents and the direction of the currents at the time of the release reduced the overlap between the first and second overflow and dump. As indicated by the instantaneous snapshot of water column concentrations (Figure 3-33), the southern plume (second overflow and dump) consists of lower concentrations than those shown for Sites 1 and 2 which were captured at the same instant in time. The faster subsurface currents reduced the water column concentrations quicker than occurred at Sites 1 and 2.

The time-integrated maximum concentration map and cross-sectional view (Figure 3-34) illustrates a plume similar to Sites 1 and 2; with nuanced differences notable only in the summary tables (Table 3-4). As with the other sites the water column concentrations extend throughout the water column close to the source but become more localized to the seabed with increased distance from the source. The map of duration of TSS  $\geq 10$  mg/L (Figure 3-35) shows a similar footprint to the time-integrated maximum water column concentration map. The longest durations (6 to 12 hours) with concentrations  $\geq 10$  mg/L were predicted in proximity to the source and north of the source. Of the three Large OSS sites, Site 3 was predicted to have water column concentrations dissipate to less than 10 mg/L fastest (i.e., in 8.9 hours; Table 3-8). Alternatively, the maximum extent to the 10 mg/L contour at Site 3 was predicted to be the largest across all three sites. All of which can be contributed to the direction and magnitude of the subsurface currents at the time of dump and overflow.

The depositional footprint at Site 3 (Figure 3-36) was similar in size and extent to Site 2. Model results predicted slightly larger areas with thicknesses  $\geq 1$  mm for Site 3 than was predicted at Sites 1 and 2. The thickest deposits ( $>100$  mm) were centered around the release location with thicknesses between 10-100 mm biased by subsurface currents northwest and southeast of the site. The maximum extent to the 1 mm and 10 mm contours was predicted to be approximately 2.03 km and 0.82 km, respectively (Table 3-9).

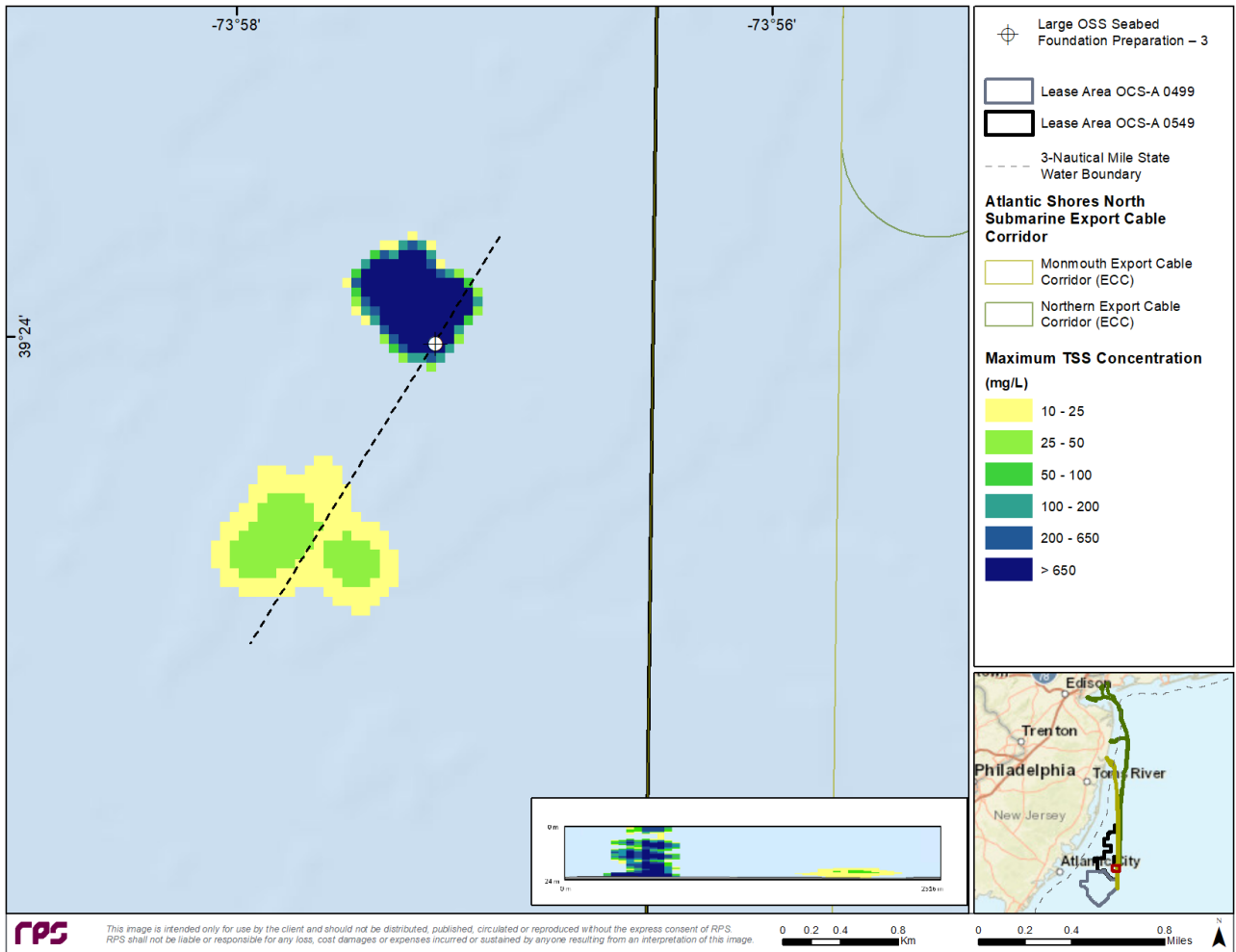


Figure 3-33: Snapshot of instantaneous TSS concentrations for a time step during the Large OSS Seabed Foundation Preparation simulation using TSHD at Site 3.

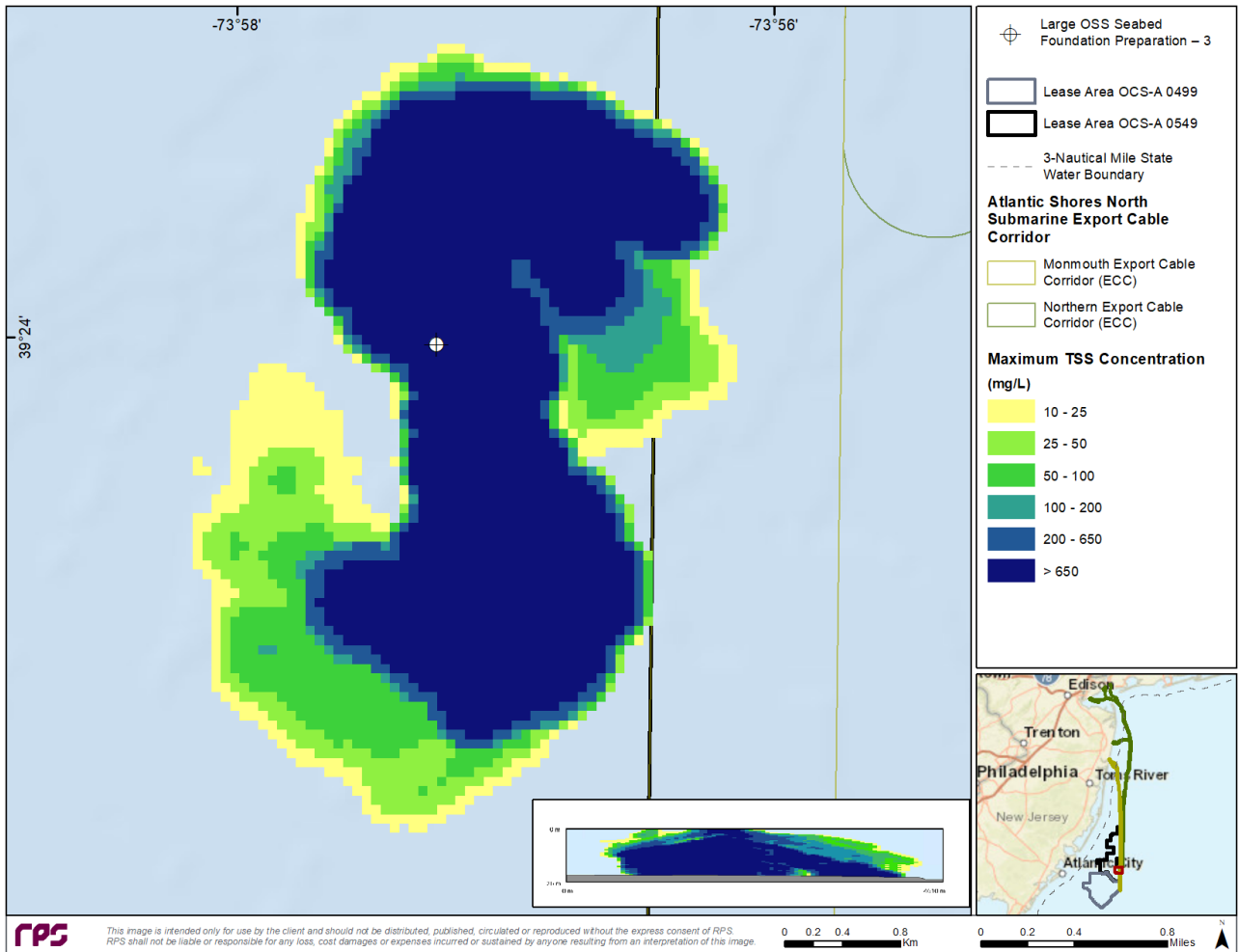


Figure 3-34: Map of time-integrated maximum concentrations associated with the Large OSS Seabed Foundation Preparation simulation using TSHD at Site 3. Note that the cross-section spans north to south along the plume.

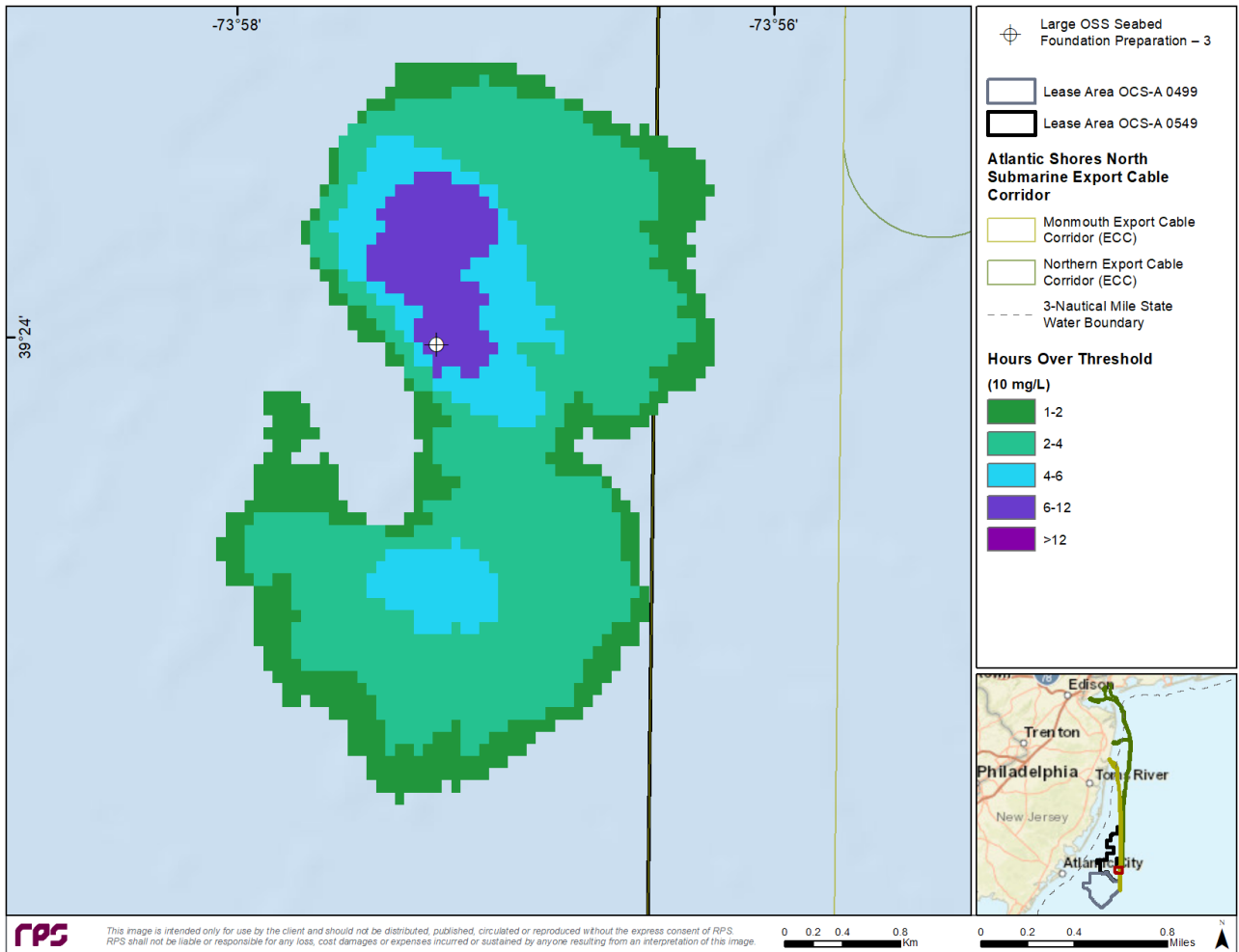
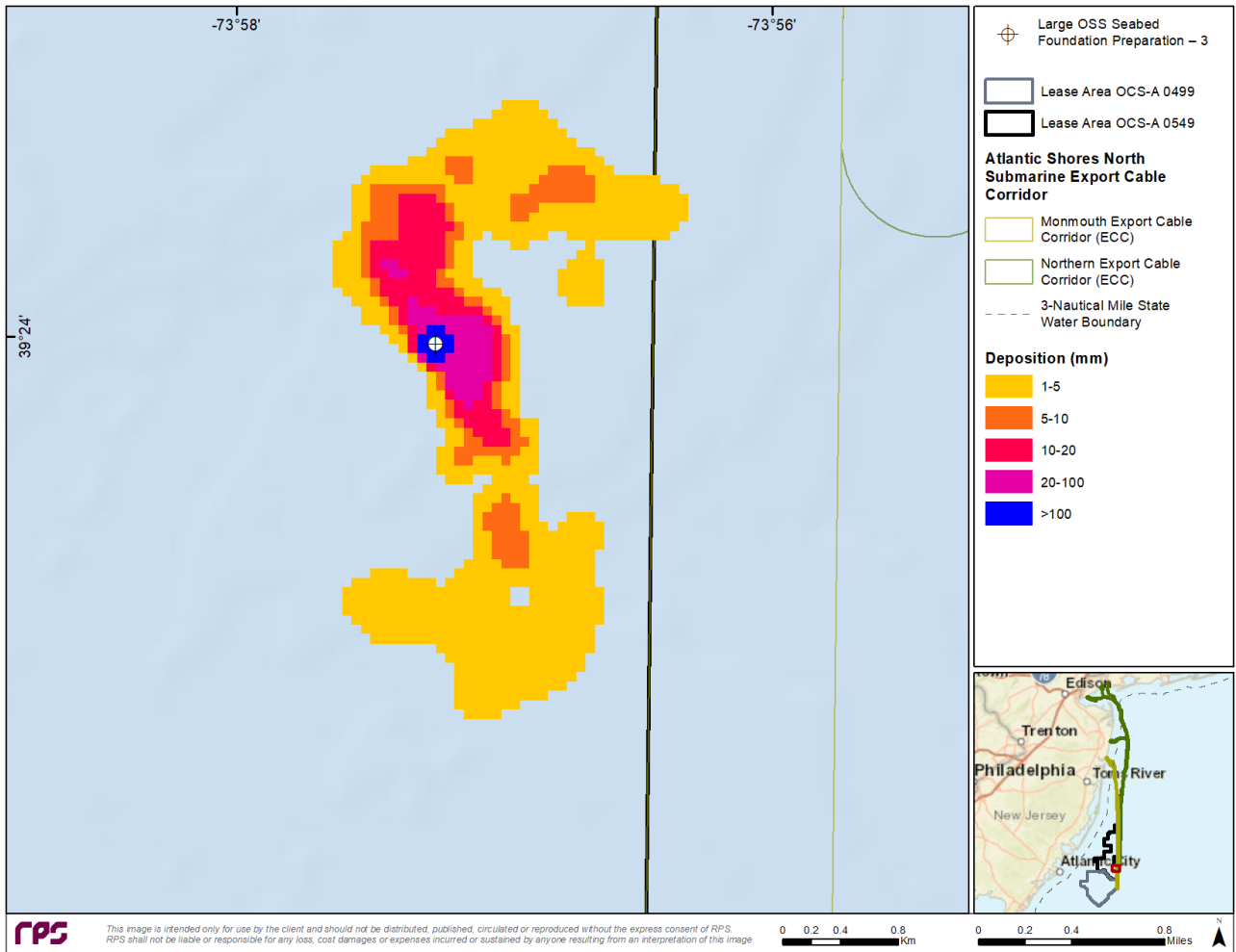


Figure 3-35: Map of duration of TSS ≥ 10 mg/L associated with the Large OSS Seabed Foundation Preparation simulation using TSHD at Site 3.



**Figure 3-36: Map of deposition thickness associated with the Large OSS Seabed Foundation Preparation simulation using TSHD at Site 3.**

### **Representative WTG Seabed Foundation Preparation**

The instantaneous water column concentration snapshot (Figure 3-37) was selected because it shows the plume when it covers the largest area at one timestep throughout the simulation. As the plume is transported by subsurface currents, the water column concentrations are spread laterally as they dissipate. Throughout the advection process the plume is also settling over time, thus resulting in a plume that occupies the lower half of the water column rather than the entire water column (Figure 3-37).

As shown in the time-integrated maximum water column concentration map and cross-section (Figure 3-38), the plume initially extends the entire water column just after dump and overflow operations are simulated. The water column concentrations become more local to the seabed as distance increases from the source due to the sediment settling. The timing of the release coincided with a period of slower current speeds (e.g., slack tide) forcing the plume northwest and then switched to the south as the tides changed. Therefore, the plume was not dispersed as quickly as would occur if dump and overflow coincided with a full flood or ebb tide. The duration of TSS  $\geq 10$  mg/L map (Figure 3-39) illustrates the regions around the WTG site and northwest of the site that were estimated to take 4 to 6 hours to fully dissipate. More specifically, the maximum duration for water column concentrations  $>10$  mg/L were predicted to last approximately 4.9 hours (Table 3-8).

The depositional footprint (Figure 3-40) consists primarily of thicknesses between 1 and 5 mm, with thicker deposits (5 to 20 mm) predicted to occur northwest and east of the representative WTG site. A small area ( $\sim 0.01$  km<sup>2</sup>) directly under the release location was predicted to have depositional thicknesses  $>100$  mm. The maximum extent to the 1 mm and 10 mm contours was predicted to be approximately 0.86 km and 0.37 km, respectively (Table 3-9).

This modeling provides a very conservative estimate of the WTG seabed foundation preparation induced plume as it used the largest anticipated dredge area and volume corresponding to the Suction Bucket Jacket approach, the sediment distribution contained high fractions of fine material, and simulations were performed at a period with relatively slow subsurface currents. The combination of these factors resulted in a plume that took longer to disperse than would likely occur during actual construction operations. These results provide an exceptionally conservative estimate of environmental impacts associated with WTG foundation preparation and in reality, the plume's magnitude and extent would likely be smaller. Therefore, if multiple WTG foundations are prepared in a single day and depending on the prevailing currents at the time of dumping, it is unlikely that the plumes would compound or interact. Based on these results, it is expected that there would be sufficient time between foundation preparation at one WTG site such that water column concentrations would return to ambient before construction occurred at a different WTG site. The impacts associated with WTG seabed foundation preparation can be considered independent events separated by time and space.

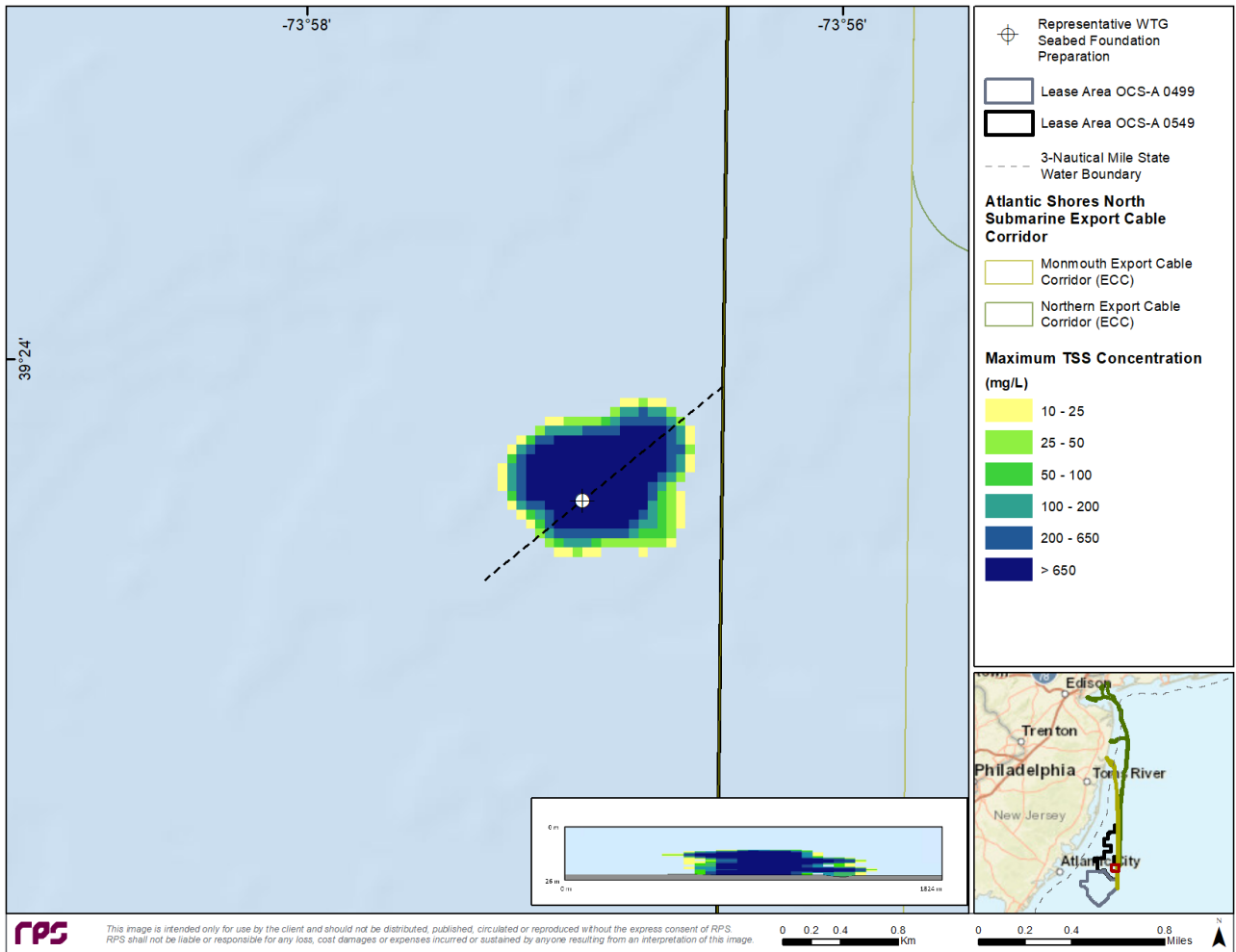


Figure 3-37: Snapshot of instantaneous TSS concentrations for a time step during the Representative WTG Seabed Foundation Preparation simulation using TSHD.



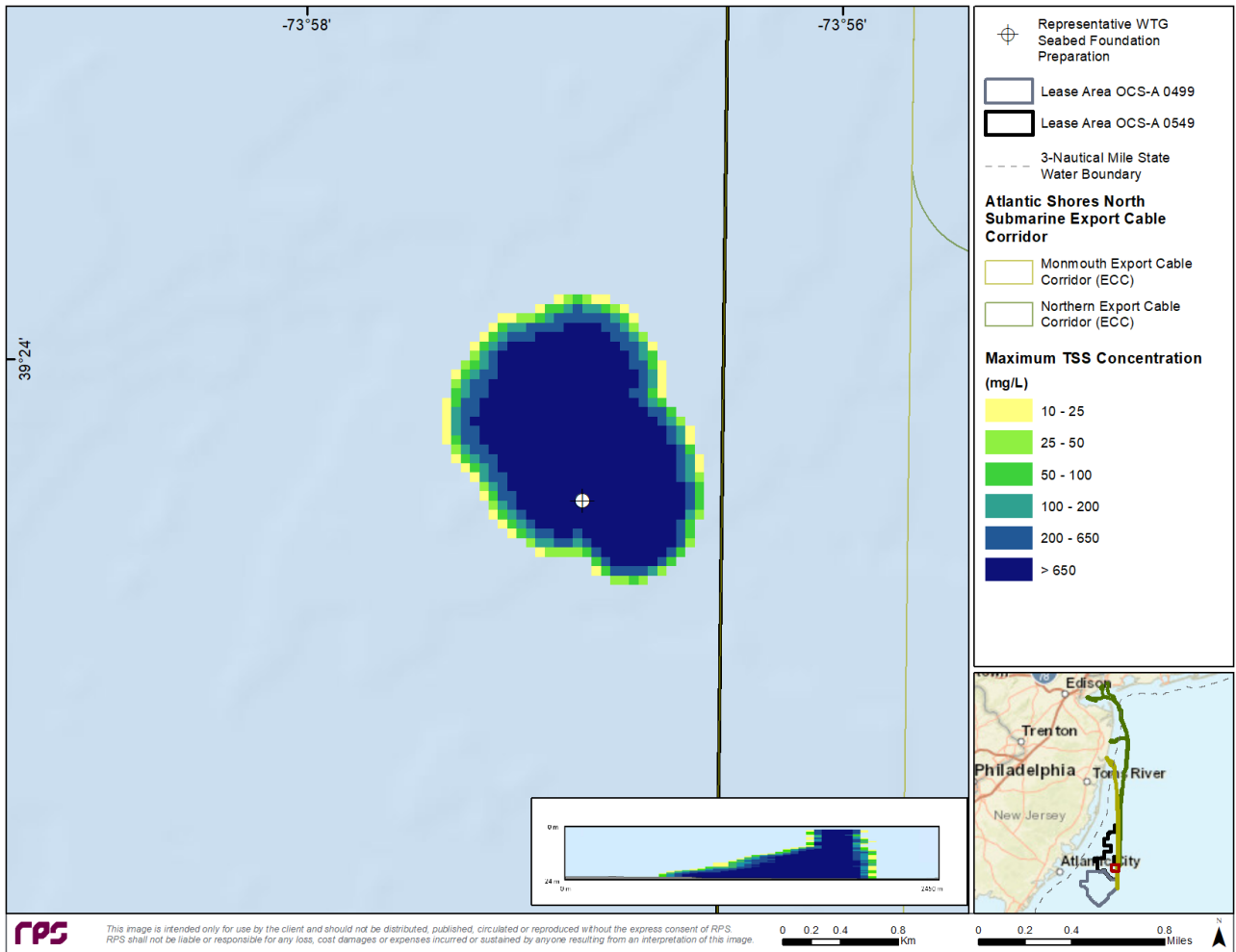


Figure 3-38: Map of time-integrated maximum concentrations associated with the Representative WTG Seabed Foundation Preparation simulation using TSHD.

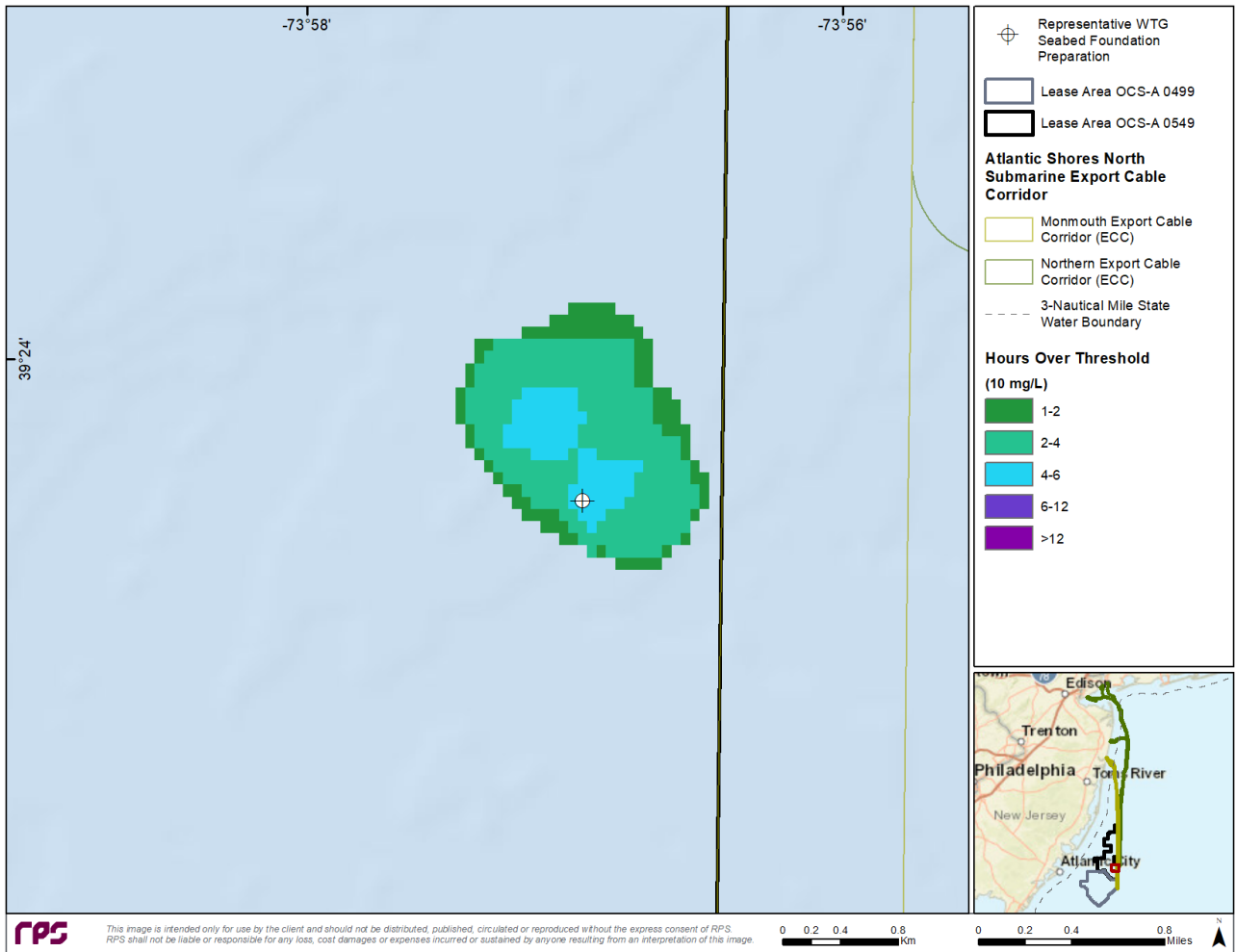
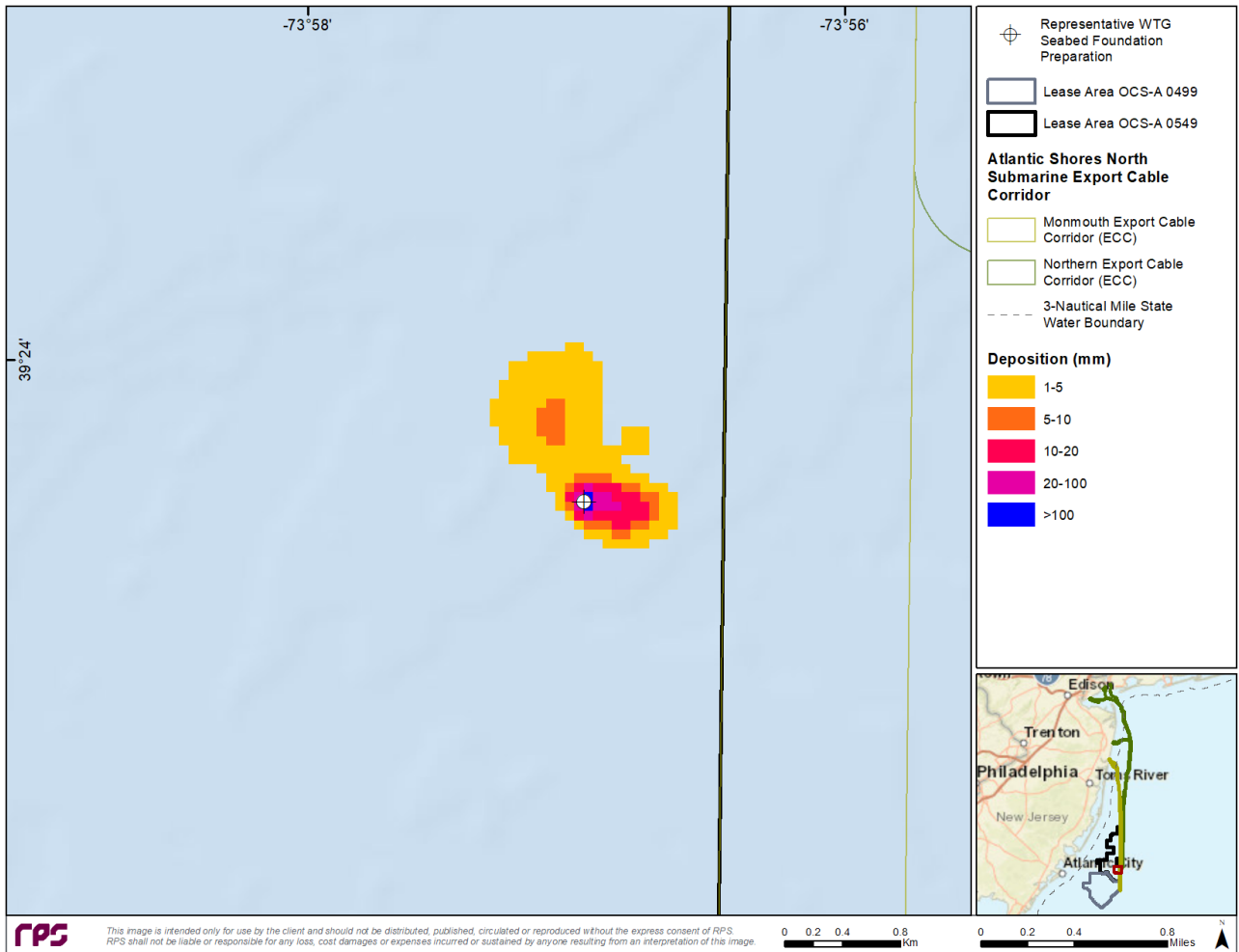


Figure 3-39: Map of duration of TSS  $\geq$  10 mg/L associated with the Representative WTG Seabed Foundation Preparation simulation using TSHD.



**Figure 3-40: Map of deposition thickness associated with the Representative WTG Seabed Foundation Preparation simulation using TSHD.**

### 3.3.4 Lease Area: Cable Installation

#### **Representative Inter-array Cable – Mechanical Trencher & Jet Trencher**

For both the mechanical trencher and jetting technique model results, the highest TSS concentrations were contained around the route centerline, with lower concentrations biased towards the southwest due to hydrodynamic forcing at the time of the simulation (Figure 3-41 and Figure 3-42).

The results for both the jet and mechanical trenching parameters show that in any given location, the total exposure was typically 4 to 6 hours with small, isolated patches of exposure between 6 to 12 hours for the jet trenching scenario and larger, dispersed patches of exposure between 6 and 12 hours for the mechanical trenching scenario (Figure 3-43). Based on the modeling results and regardless of method, the water column concentrations are anticipated to return to ambient within 12 hours.

Model results predict that there was a distinct lack of depositional thickness for both methods of IAC installation (Table 3-9). Neither scenario resulted in areas exceeding 0.01 km<sup>2</sup> of depositional thickness greater than or equal to that of 1 mm. A very small area (~0.0025 km<sup>2</sup>) for the jet trenching simulation was predicted to exceed a thickness of 1 mm (Figure 3-44). This behavior can be attributed to the high percentage of fine sediment and the strong southwest current advecting and dispersing the sediment away from the source so that depositional threshold thicknesses were not exceeded. Deposition below the thresholds of interest were predicted and mimicked a similar footprint as the plume. Deposition exceeding thresholds of interest may occur during the installation of inter-array cables in other areas with higher fractions of coarse sands. In those instances, deposition would likely remain close to the route centerline as occurred for the Northern ECC and Monmouth ECC cable installation simulations.

Model results associated with the cable installation simulation assuming jetting techniques estimated a smaller footprint impacted for slightly less time compared to the mechanical trenching results. This behavior can be attributed to the differences in installation techniques between jetting and mechanical trenching. The mechanical trenching simulation applied a slower installation rate compared with the jetting technique. The same volume of sediment was disturbed, however, it occurred more slowly. This prolonged the total duration of sediment disturbing activities which exposed it to more tidal cycles and inherently increased the duration required for water column concentrations to return to ambient conditions. Elevated TSS was confined to the bottom few meters of the water column, a small fraction of the water column, and water quality impacts from IAC installation are therefore predicted to be short-term and localized.

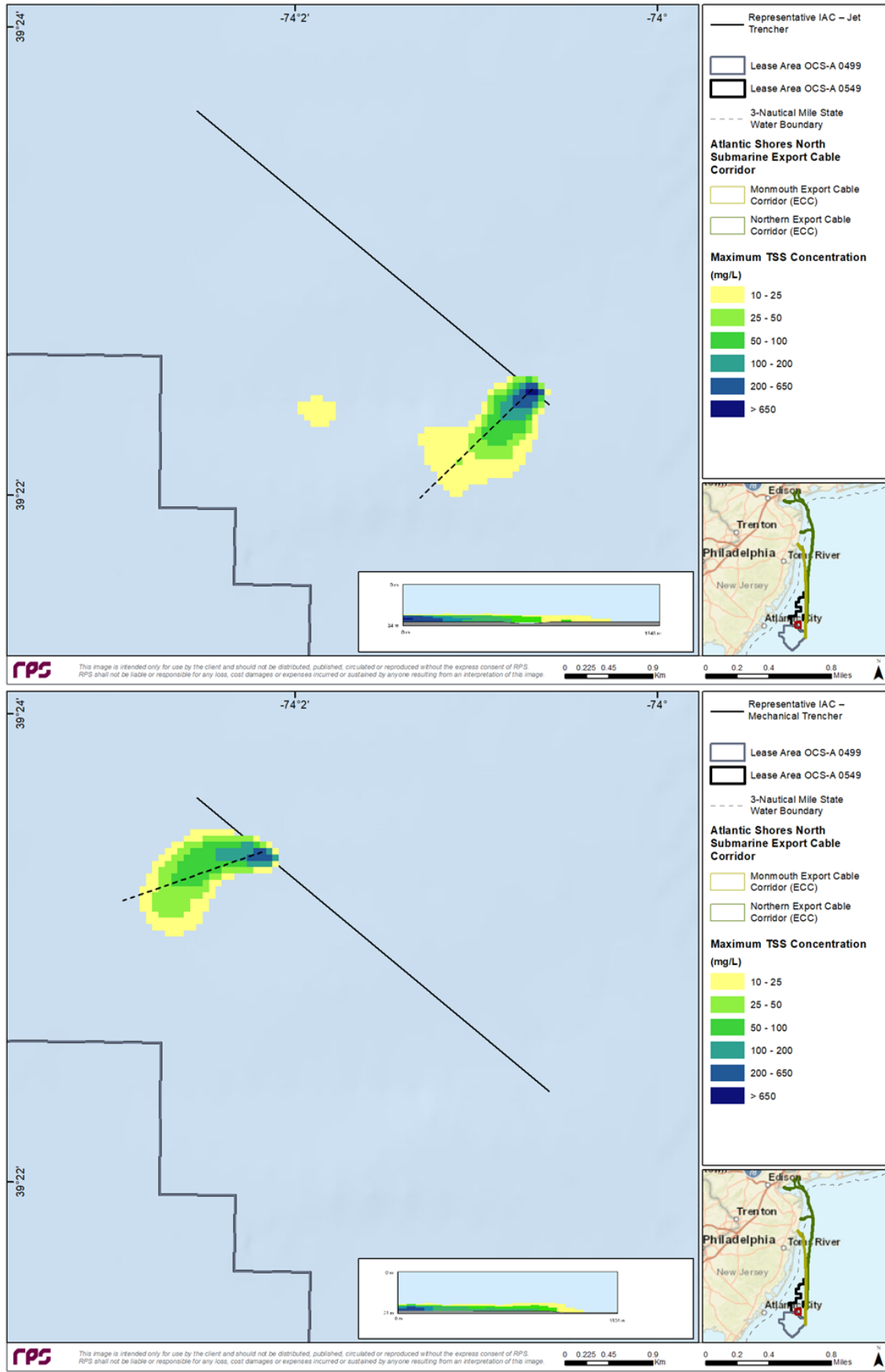


Figure 3-41: Snapshot of instantaneous TSS concentrations for a time step during the Representative IAC Installation simulations using Jet Trenching (top) and Mechanical Trenching (bottom).

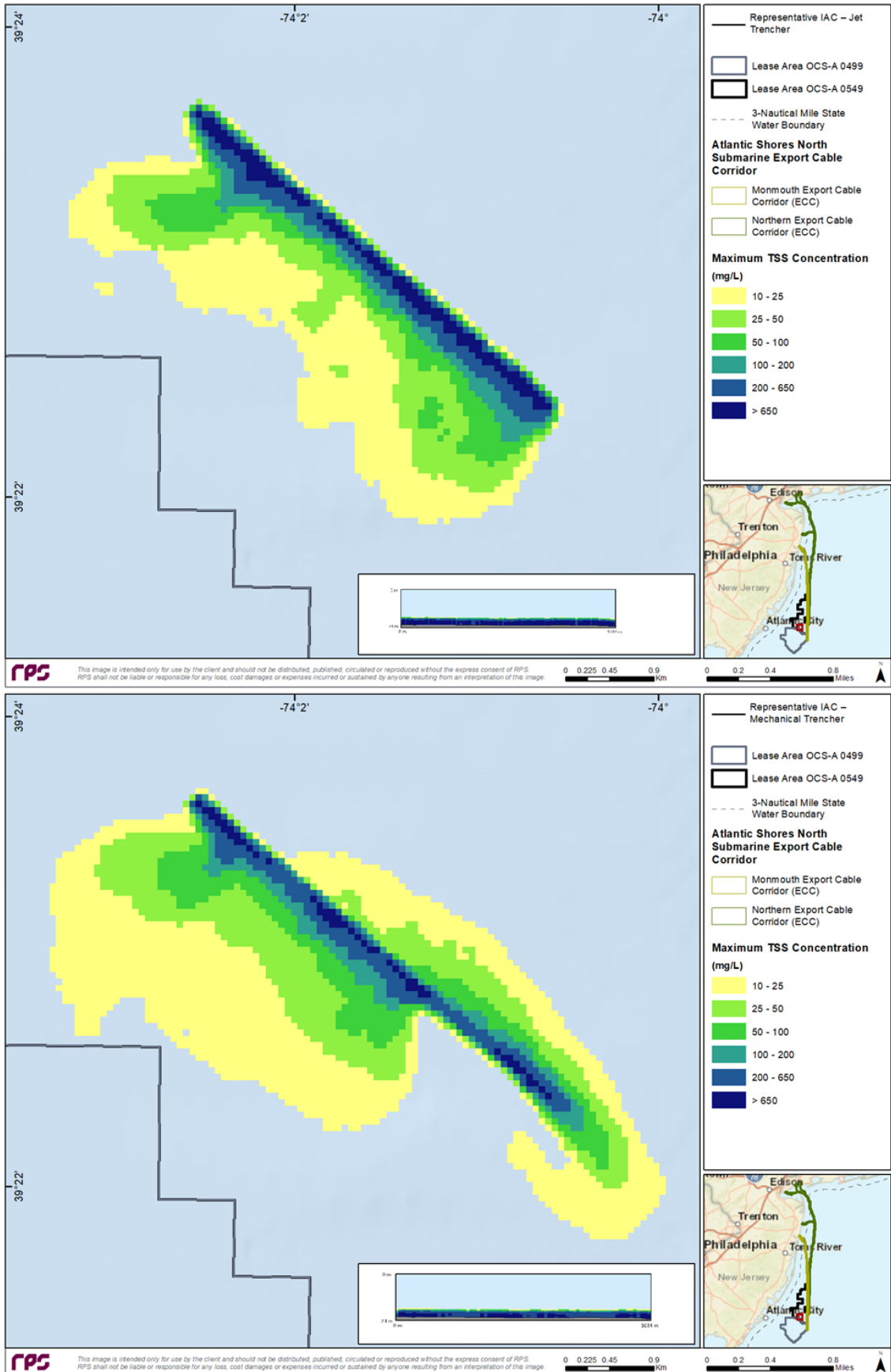


Figure 3-42: Map of time-integrated maximum concentrations associated with the Representative IAC Installation simulations using Jet Trenching (top) and Mechanical Trenching (bottom).

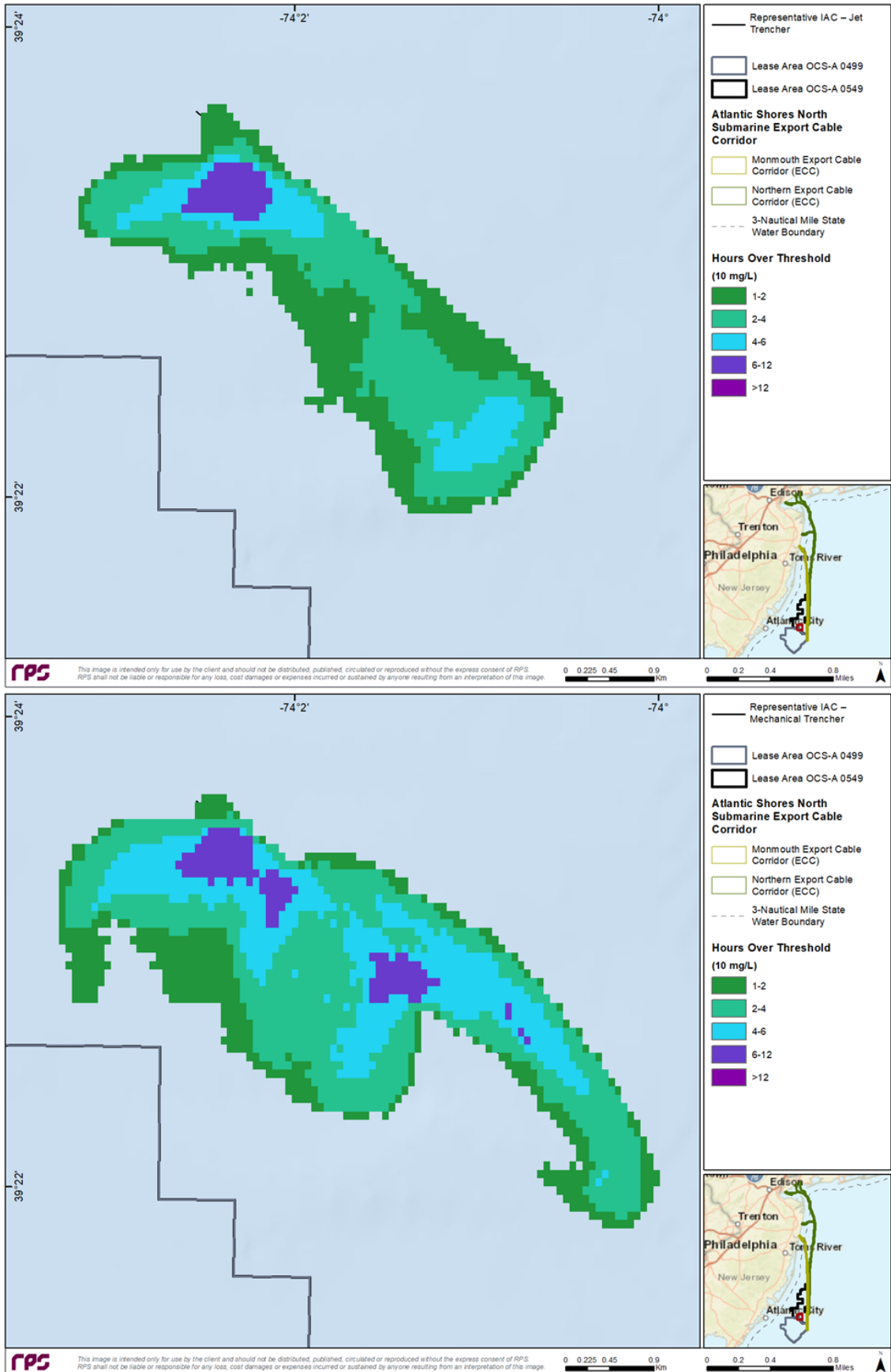


Figure 3-43: Map of duration of TSS  $\geq$  10 mg/L associated with the Representative IAC Installation simulations using Jet Trenching (top) and Mechanical Trenching (bottom).

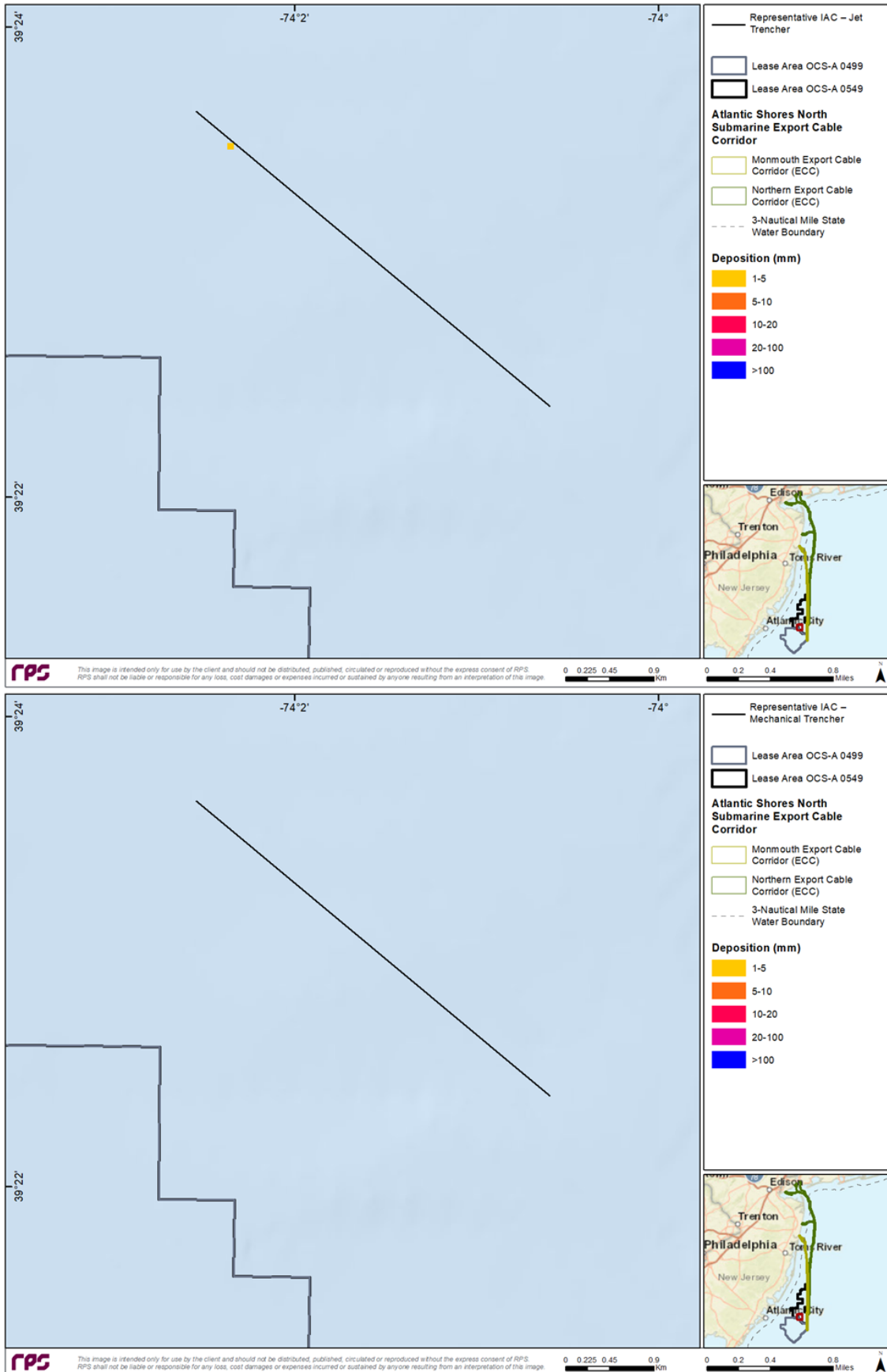


Figure 3-44: Map of deposition thickness associated with the Representative IAC Installation simulations using Jet Trenching (top) and Mechanical Trenching (bottom).



### 3.3.5 Northern ECC and Monmouth ECC: Cable Installation

#### **Representative Northern ECC Cable Installation – Jet Trencher**

Modeling of the representative Northern Export Cable using typical jetting techniques was performed for the entire length of the ECC (i.e., from Lease Area to the representative landfall location). Model results illustrate the transient nature of the plume and how it is influenced by the sediment type and current magnitude and direction at a moment in time. The model results predict the highest concentrations of suspended sediments to occur in the vicinity of the installation device, as expected; however, these higher concentrations then decrease rapidly with distance as the operating device advances along the cable corridor (Figure 3-45 and Figure 3-46). Based on the timing of the simulations and the direction of the current with respect to the ECC, the plume's behavior and footprint changed along the length of the ECC. For the initial 12-13 km of the route, the currents caused the plume to remain centered along the route (Figure 3-47). As the installation progressed north towards landfall, the oscillatory nature of the currents gradually became more evident with the plume extending primarily northwest and southeast. This pattern held true until the route diverged west towards the various landfall approaches. From north of Fort Hancock, NJ to the representative landfall site, the currents were generally parallel to the route which resulted in a suspended sediment plume that stayed along the route centerline.

As sediment characteristics were generally consistent constant along the ECC, the primary factor influencing the suspended sediment concentrations was the forcing of the currents. In some areas with higher fractions of fine material, the plume tended to extend farther away and take longer to settle when currents were perpendicular to the route. TSS concentrations  $\geq 10$  mg/L are predicted to dissipate and return to ambient conditions within 18 hours (Figure 3-47).

The depositional footprint follows along the route centerline with the majority of the footprint falling below any thresholds of interest, with isolated patches along the route predicted to have thicknesses between 1 and 5 mm (Figure 3-48). The pattern of deposition followed the orientation of the currents with respect to the route. In locations when the current was parallel with the route, depositional thicknesses tended to exceed the thresholds of interest because the sediment was not advected away from the source but rather along it.

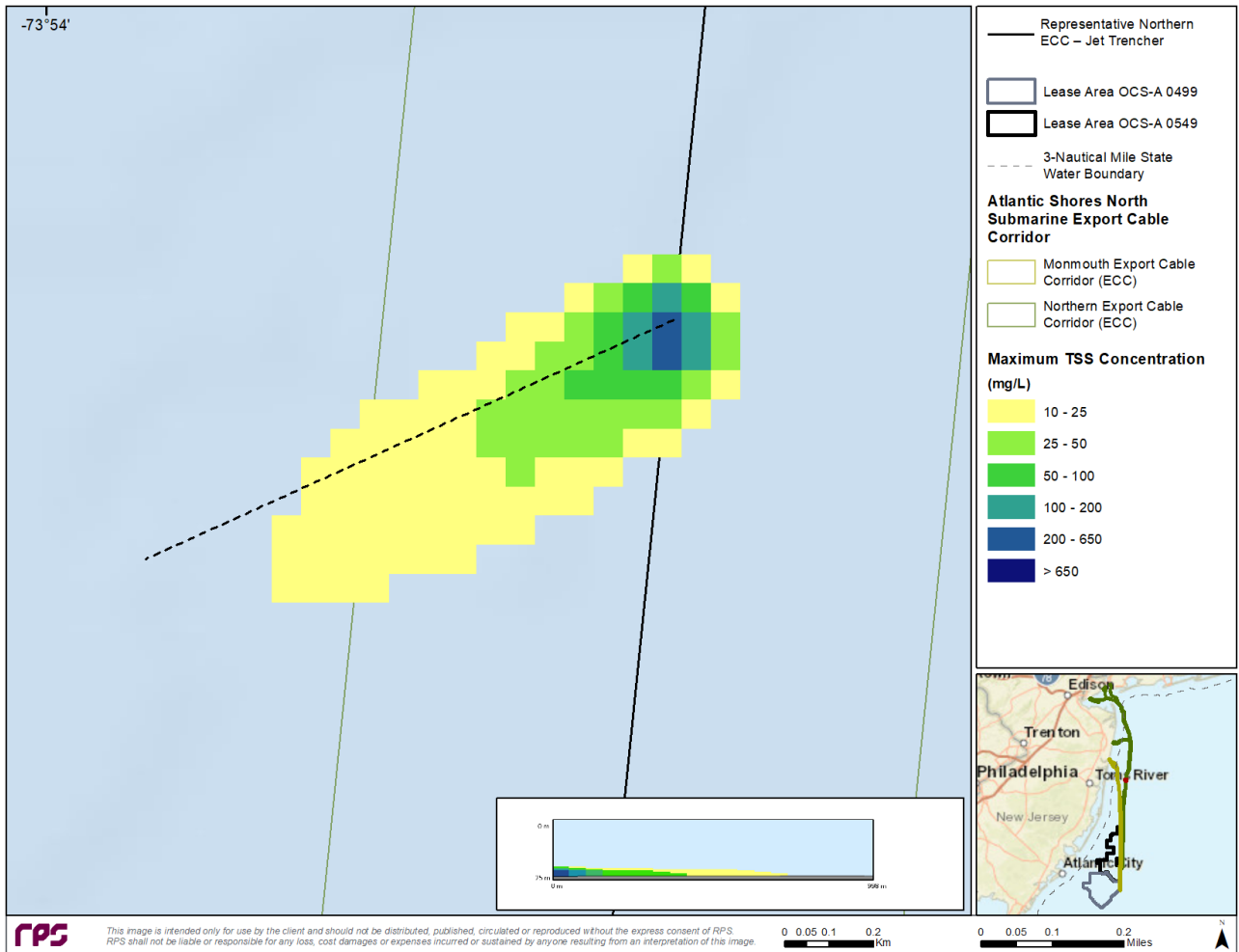


Figure 3-45: Snapshot of instantaneous TSS concentrations for a time step during simulation for the Representative Northern ECC Cable Installation— Jet Trencher simulation.

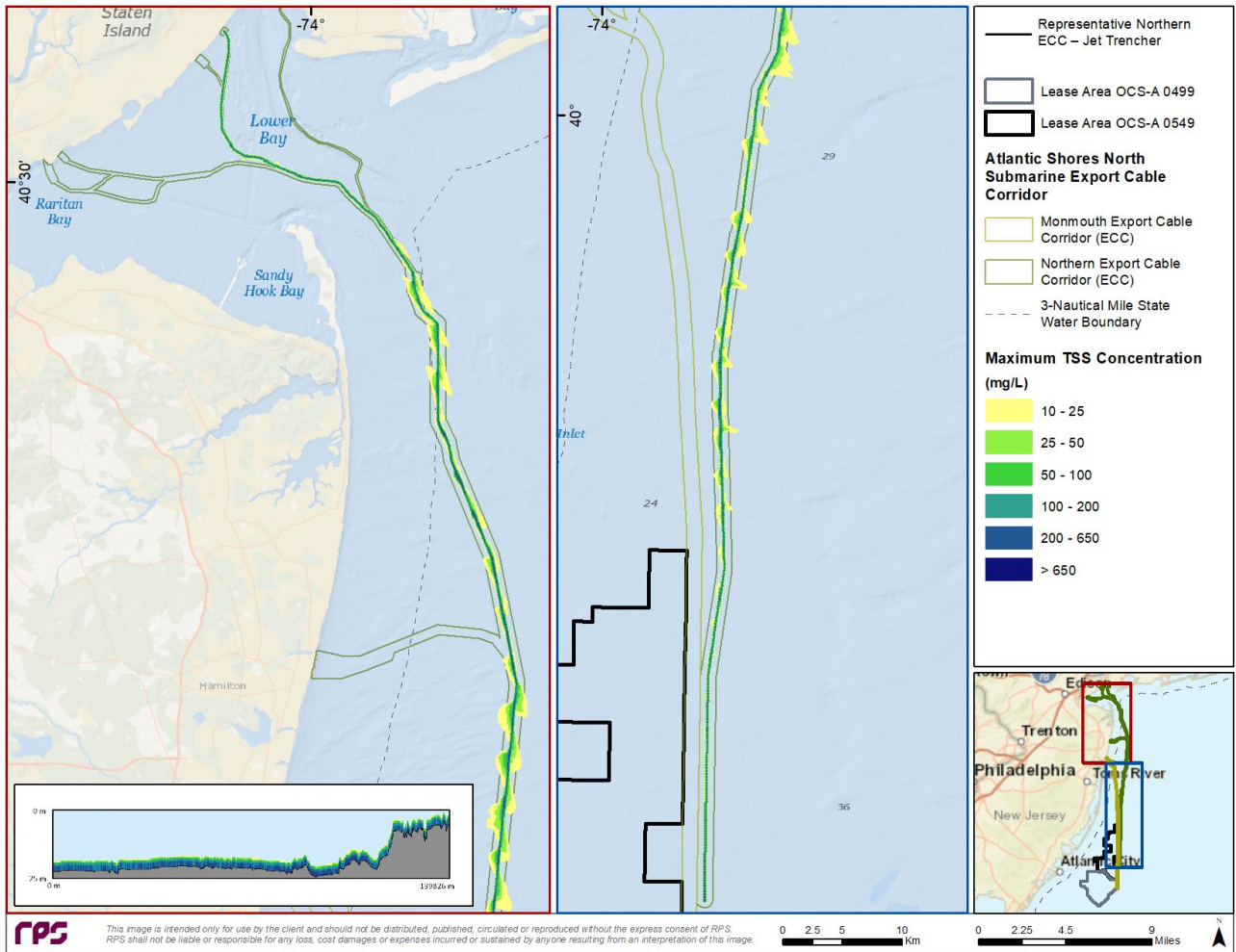


Figure 3-46: Map of time-integrated maximum concentrations associated with the Representative Northern ECC Cable Installation — Jet Trencher simulation.

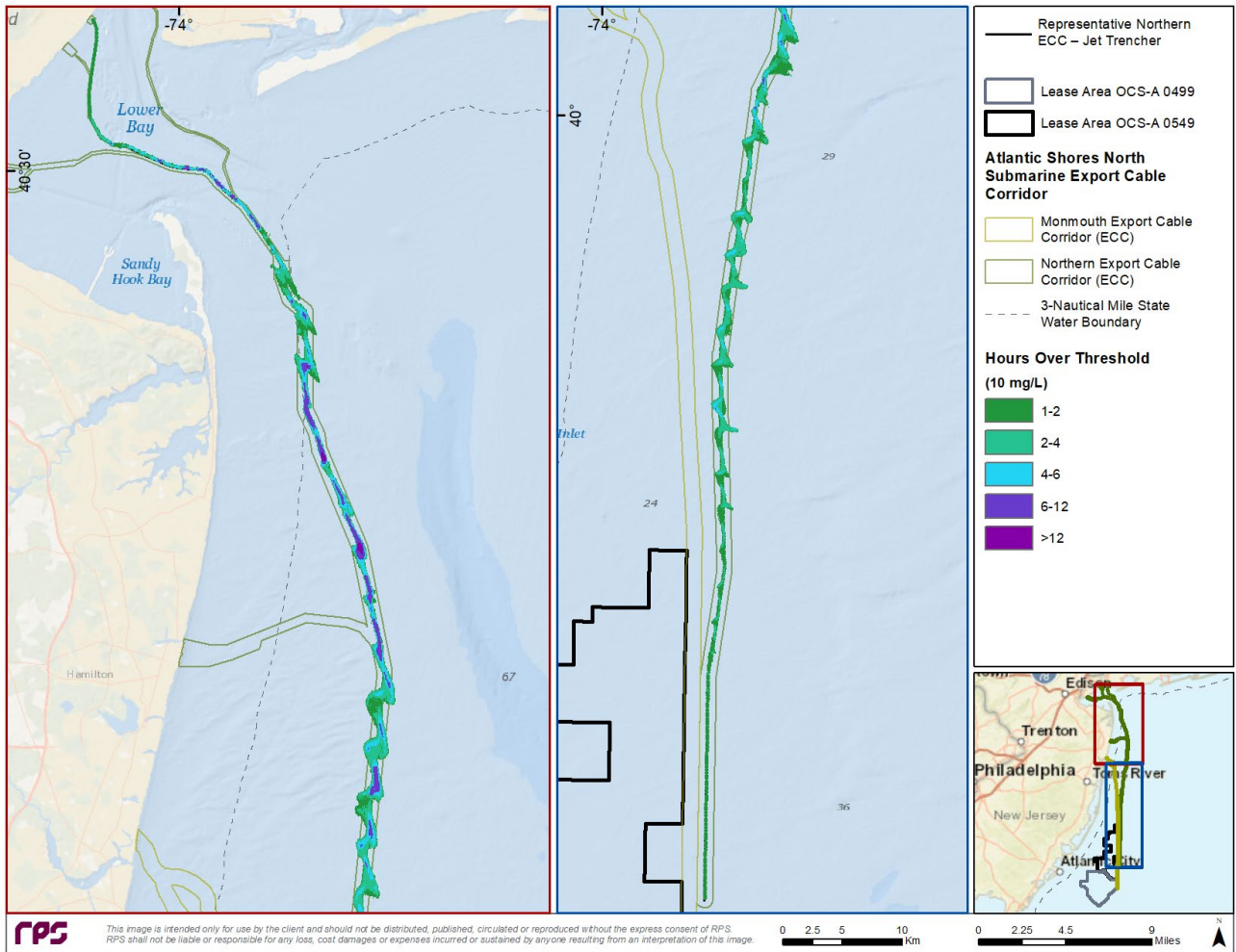


Figure 3-47: Map of duration of TSS ≥ 10 mg/L associated with the Representative Northern ECC Cable Installation — Jet Trencher simulation.

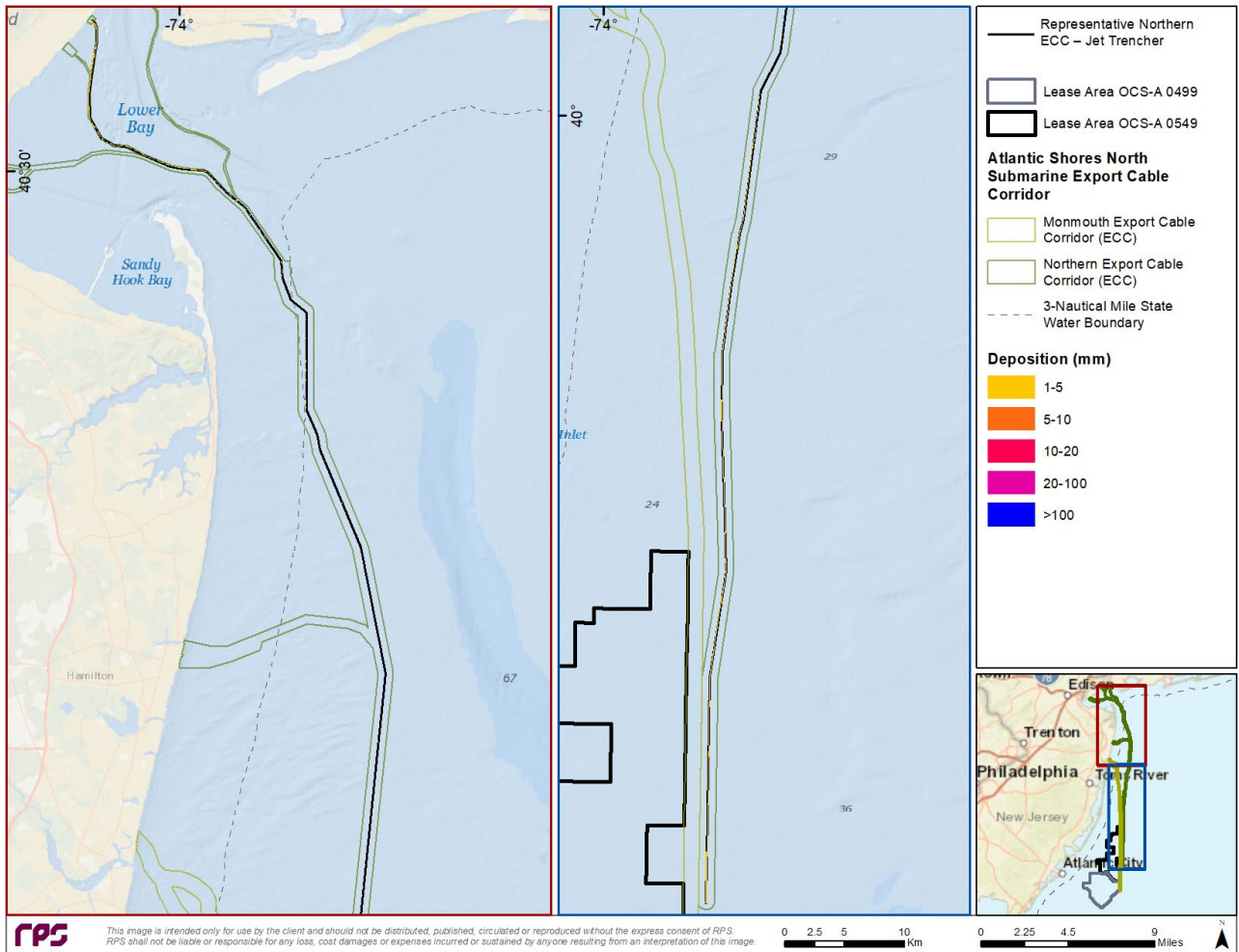


Figure 3-48: Map of deposition thickness associated with Representative Northern ECC Cable Installation — Jet Trencher simulation.

**Representative Monmouth ECC Cable Installation (Branches 1 and 2) – Jet Trencher**

The mapped result figures for the ECC scenarios are presented together because most of the modeled route was the same, with differences occurring after the route diverged to create Branches 1 and 2. Due to the similarity in results for each of the ECC branches, only one value was reported in the summary tables and discussed in the text for the Monmouth ECC cable installation modeling. The values reported and discussed reflect the scenario predicted to have the maximum effect (i.e., maximum effects scenario) for each of the respective ECC branches.

A snapshot of the instantaneous concentrations from the Monmouth ECC – Branch 1 scenario is presented in Figure 3-49 along with the vertical cross-section across the plume. This figure was representative of both branches and illustrates that higher concentrations were contained around the route centerline, with lower concentrations biased towards the west due to bottom currents. The cross-section shows that the plume was localized to the bottom of the water column. The map of maximum time-integrated concentrations with the vertical cross-section across the plume (Figure 3-50), the duration of exposure to TSS above  $\geq 10$  mg/L (Figure 3-51) and the seabed deposition (Figure 3-52) show the entire Monmouth ECC route with zoomed-in extents highlighting results for Branches 1 and 2.

Figure 3-50 illustrates how the plume moved from east to west with the tides, which is reflective in the oscillatory pattern of the concentrations relative to the route centerline. The oscillatory pattern was less evident in regions where the route is parallel to local currents and where the sediment is predominantly coarse because it tends to settle out of the water column relatively quickly and remain close to the route centerline. Concentrations  $\geq 10$  mg/L had a maximum excursion of approximately 2.60 km from the route centerline (Table 3-8). The map of exposure of the water column to TSS concentrations  $\geq 10$  mg/L (Figure 3-51) shows a pattern similar to the maximum concentration, with most locations experiencing exposures of less than 4 hours, while some areas had exposures between 6 and a little over 12 hours. As presented in Figure 3-20, the deposition between 1 and 5 mm tended to stay central to the route centerline, with discontinuous patches between 5 and 10 mm.

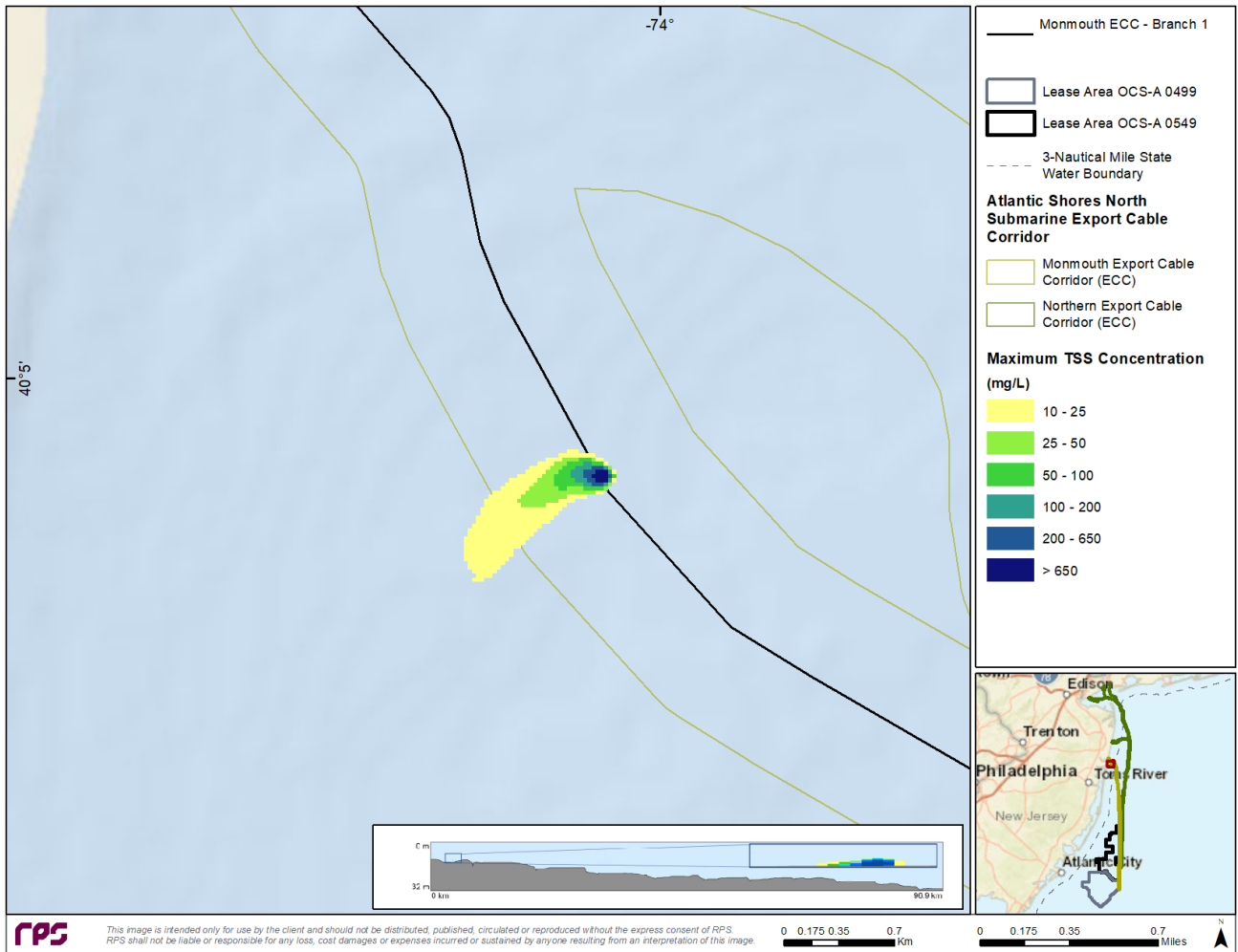


Figure 3-49: Snapshot of Instantaneous TSS Concentrations Associated with Cable Burial along the Monmouth ECC – Branch 1.

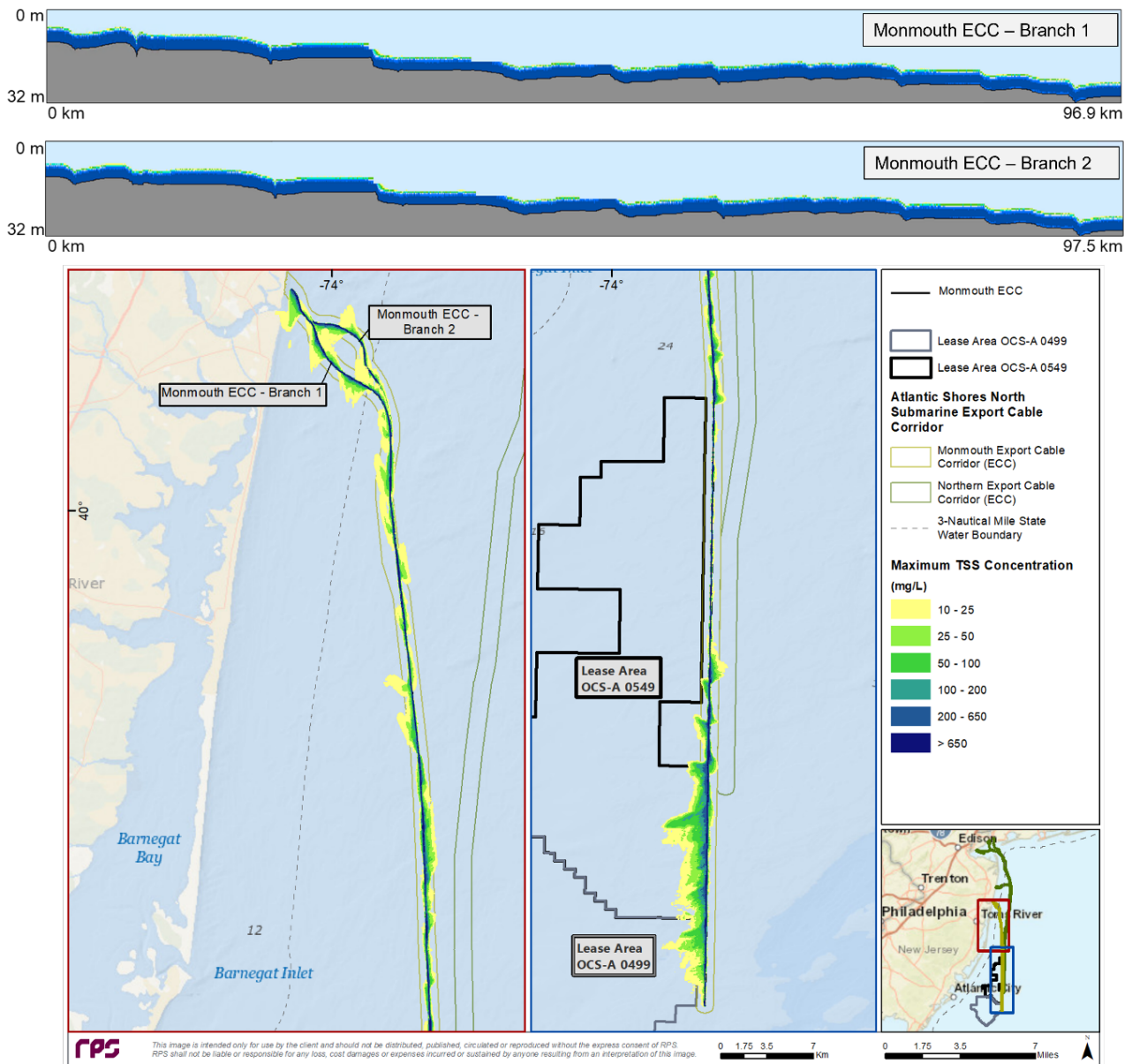


Figure 3-50: Map of Time-Integrated Maximum TSS Concentrations Associated with Cable Burial along the Monmouth ECC for Branch 1 and Branch 2.



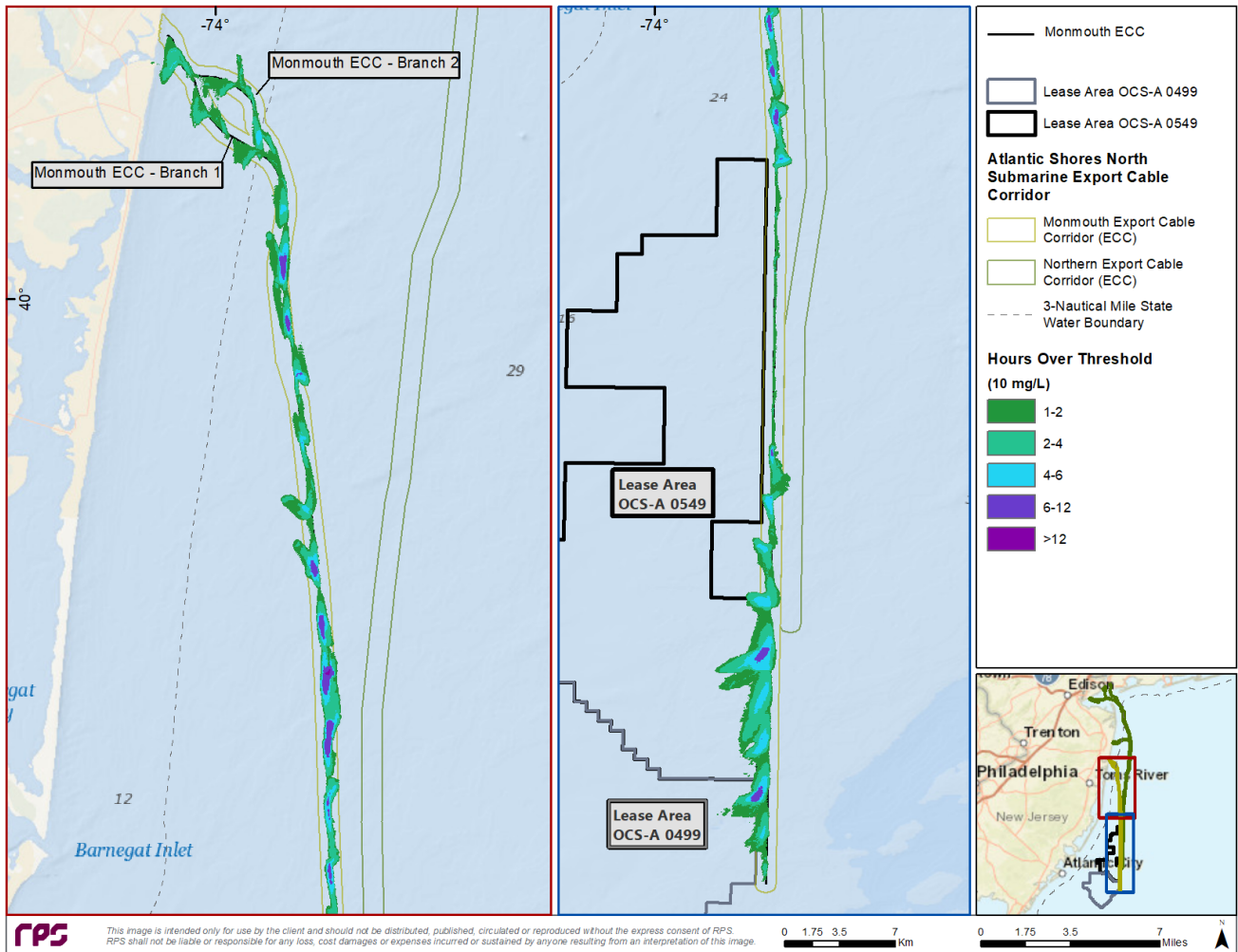


Figure 3-51: Map of Duration of TSS  $\geq 10$  mg/L Associated with Cable Burial along the Monmouth ECC for Branch 1 and Branch 2.

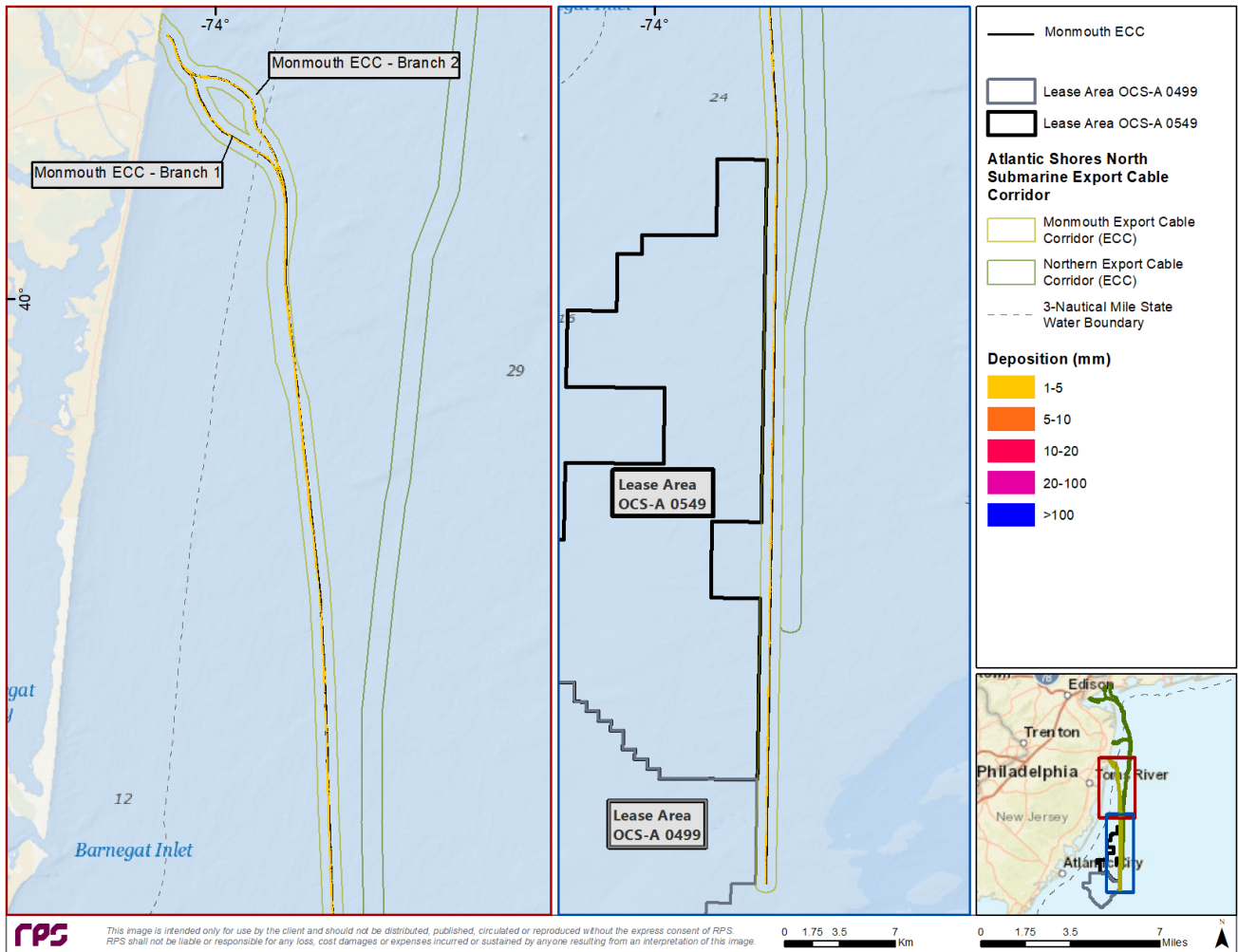


Figure 3-52: Map of Deposition Thickness Associated with Cable Burial along the Monmouth ECC for Branch 1 and Branch 2.

### 3.3.6 Landfall Approaches: HDD Pit Construction

#### ***Northern ECC Landfall Approach – Representative HDD Pit Scenario***

The representative Northern ECC Landfall Approach simulation of HDD pit excavation was modeled assuming side cast of sediments at the water surface. These results are representative of backfill operations as there will be sufficient time between activities thus allowing TSS concentrations to return to ambient prior to backfilling. The highest concentrations of suspended sediment tended were predicted to remain around the HDD pit, with concentrations decreasing radially from the source (Figure 3-53). Rather than forming concentric circles of decreasing concentrations around the HDD pit, the strong oscillating currents near the delta formed a plume that was advected northeast and southwest, parallel to the shoreline (Figure 3-54). The tail of the plume, with maximum concentrations ranging from 10-25 mg/L, extended approximately 1.85 km from the HDD Pit (Table 3-8). Introduction at the surface increases the time it takes for sediment to deposit on the seabed, thus subjecting it to more tidal oscillations and longer durations exceeding TSS concentration thresholds.

Most locations within the plume experienced exposures  $\geq 10$  mg/L for less than 6 hours, with a maximum duration of exposure  $\geq 10$  mg/L centered at the HDD pit lasting just over 10 hours (Figure 3-55). This was due to the duration of the release and continual introduction of sediments at the water surface for the entire excavation operation. Due to complex hydrodynamics and strong currents surrounding the HDD pit, only a small area (0.01 km<sup>2</sup>) overlaying the source was predicted to have deposits exceeding 1 mm (Figure 3-56). Due to the high fraction of coarse material, and the relatively large volume released at the same location, depositional patterns were centered around the HDD pit, with maximum depositional thicknesses predicted to be  $>100$  mm. The depositional areas exceeding all thresholds above 1 mm were predicted to be less than 0.01 km<sup>2</sup>.

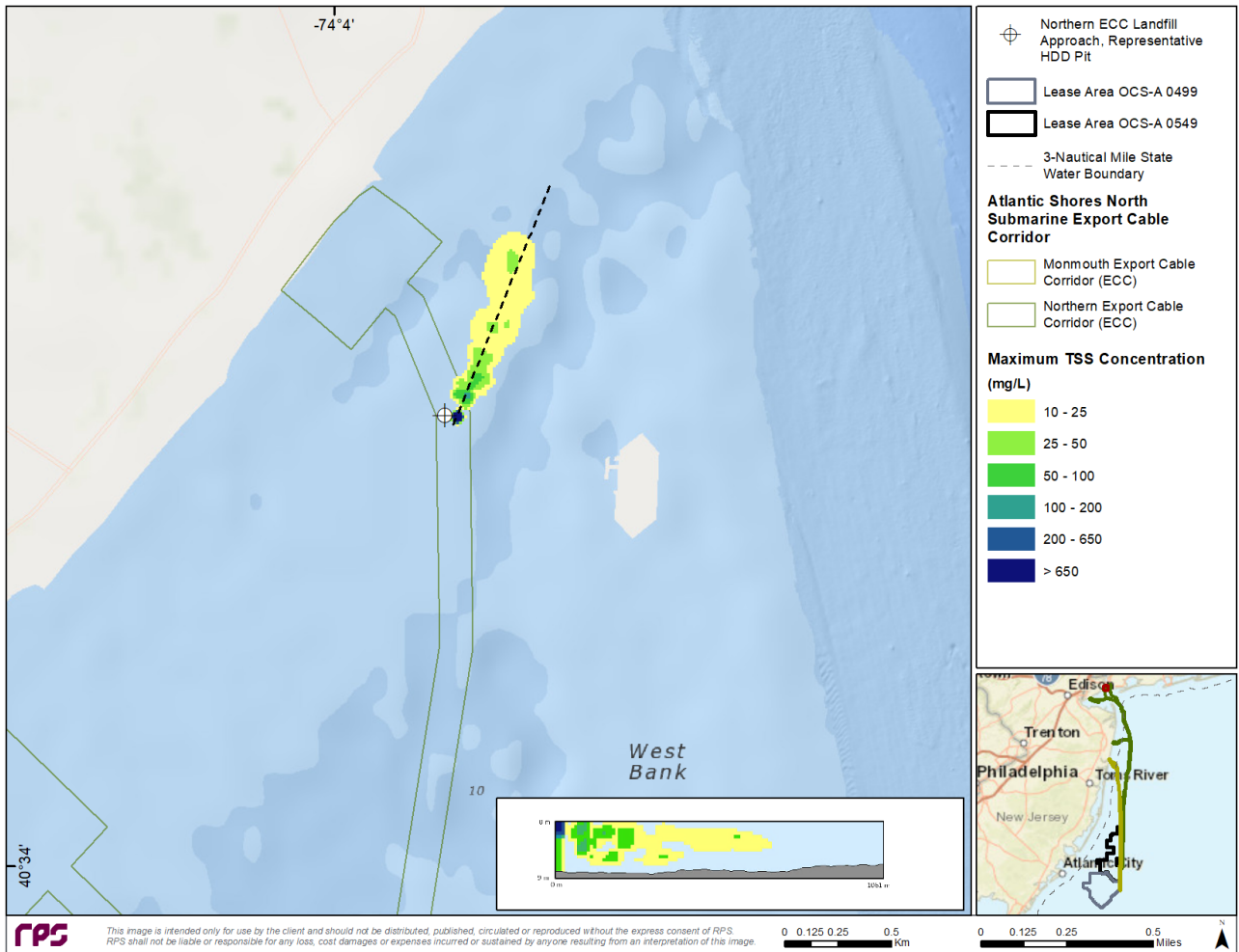


Figure 3-53: Snapshot of instantaneous TSS concentrations for a time step during the Representative HDD Pit - Northern ECC Landfall Approach.

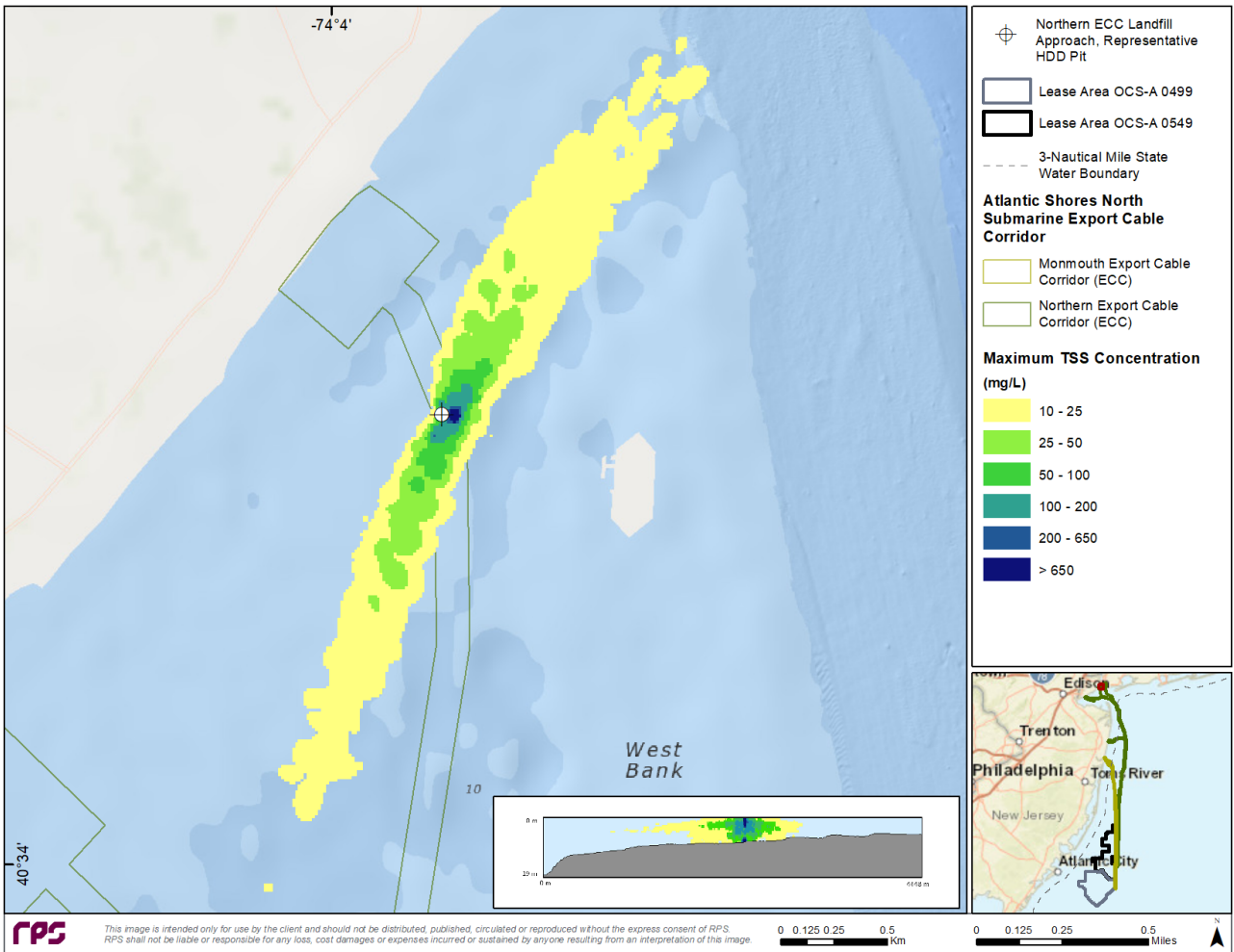


Figure 3-54: Map of time-integrated maximum concentrations associated with the Representative HDD Pit - Northern ECC Landfall Approach.

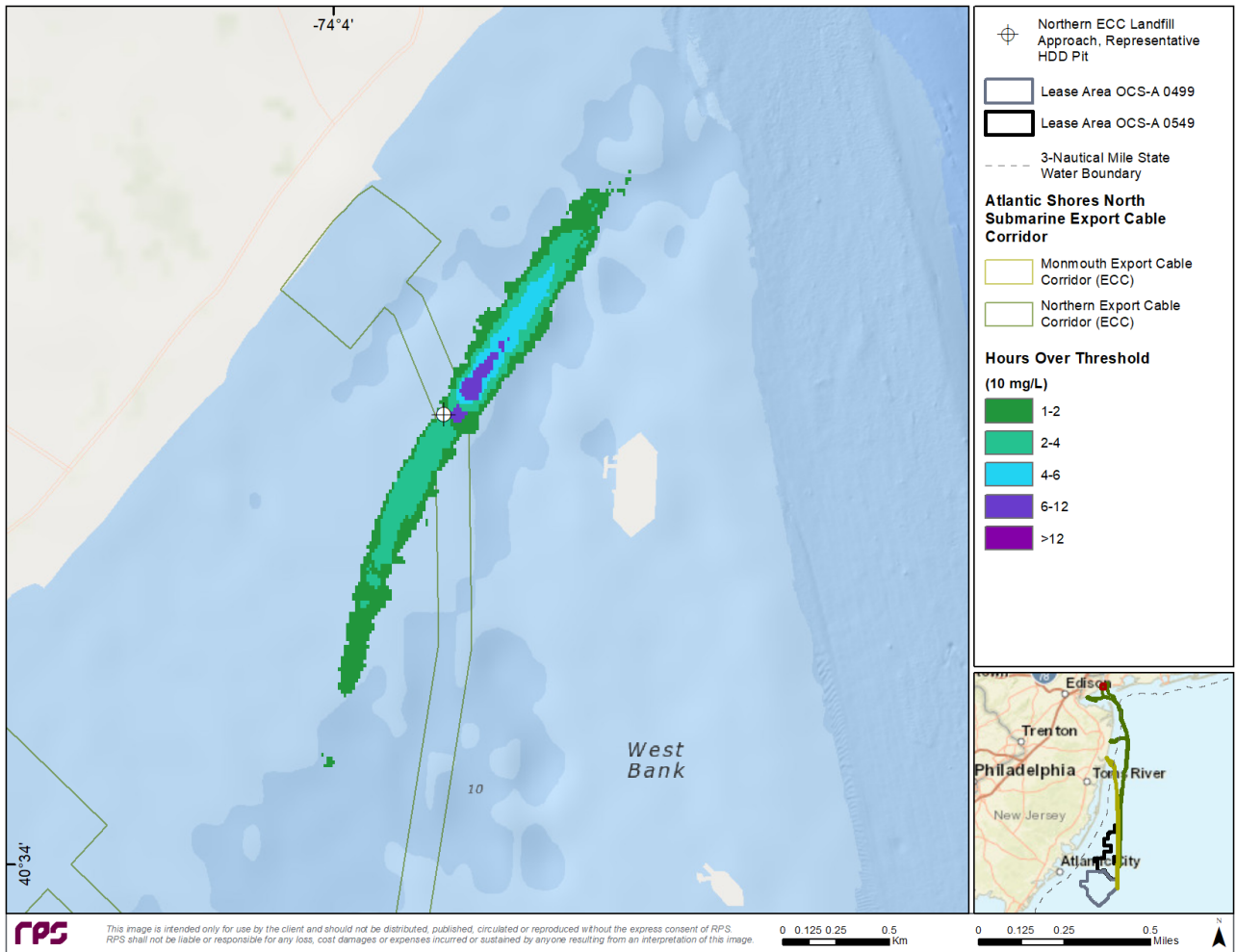


Figure 3-55: Map of duration of TSS ≥ 10 mg/L associated with the Representative HDD Pit - Northern ECC Landfall Approach.

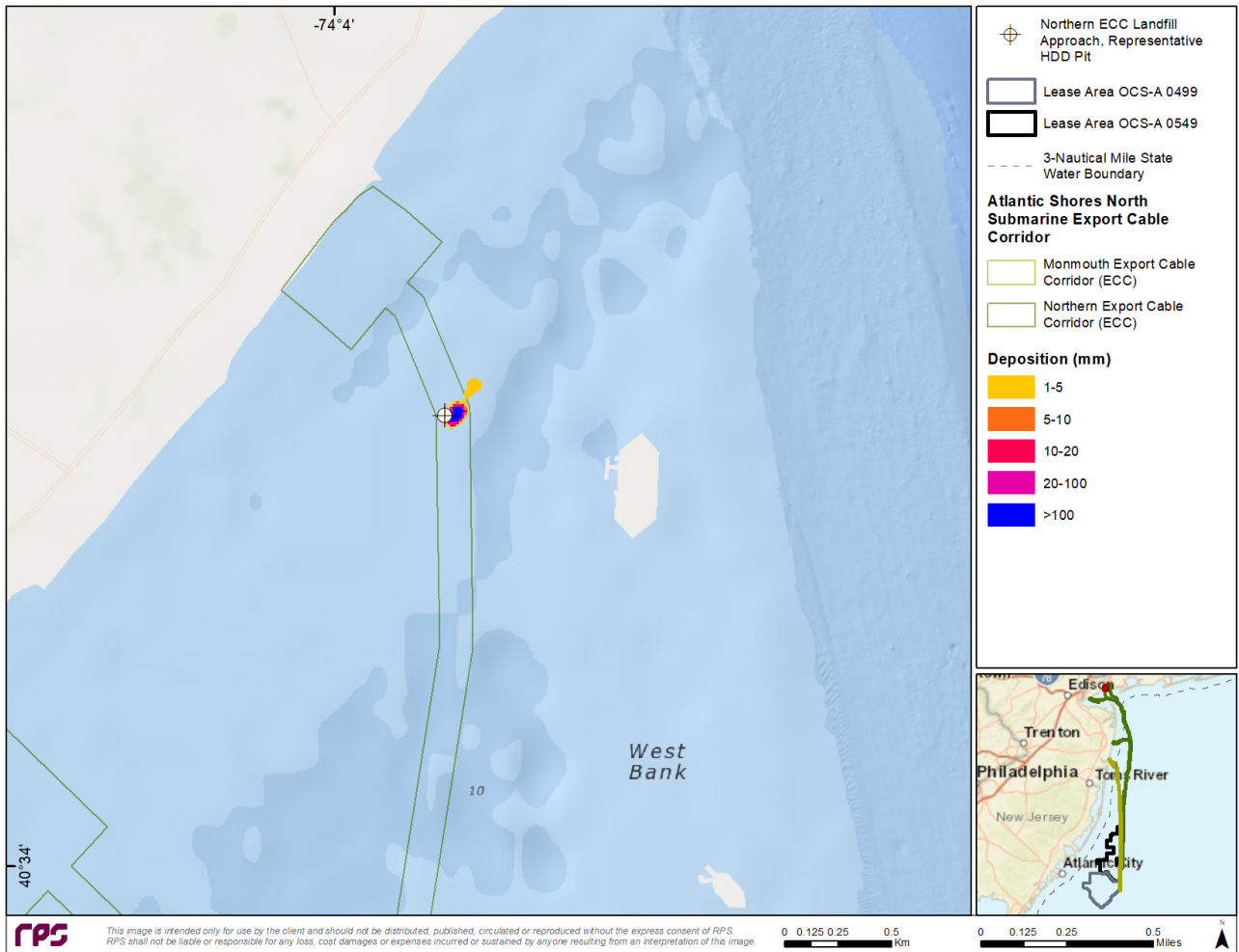


Figure 3-56: Map of deposition thickness associated with the Representative HDD Pit - Northern ECC Landfall Approach.

**Monmouth ECC Landfall Approach – Representative HDD Pit Scenario**

As with the Northern ECC Landfall Approach simulation of HDD pit excavation, the Monmouth ECC representative HDD Pit simulation was modeled assuming the side cast of sediments at the water surface. These results are representative of backfill operations as there will be sufficient time between activities thus allowing TSS concentrations to return to ambient prior to backfilling. The highest water column concentrations were centered around the HDD pit, with concentrations decreasing radially from the point source (Figure 3-57). The footprint of the plume was oblong and surrounded the HDD pit, with biases in concentrations north and south due to the oscillating currents. The tail of the plume, with maximum concentrations ranging from 10-25 mg/L, was predicted to extend 3.30 km south of the HDD pit (Table 3-8). The length of the maximum excursion to the  $\geq 10$  mg/L contour can be attributed to sediment being introduced to the water column at the surface rather than close to the seabed, and the conservative assumption that no cofferdam or mitigation technique would be used during construction (Figure 3-58).

Introduction at the surface increases the time it takes for sediment to deposit on the seabed, thus subjecting it to more tidal oscillations. Most locations within the plume experienced exposures  $\geq 10$  mg/L for less than 6 to 12 hours with a maximum duration of exposure  $\geq 10$  mg/L centered at the HDD pit lasting 12 to 24 hours (Figure 3-58). Some sediment was transported south by the currents and temporarily entered the Manasquan Inlet. While the durations indicate sediment may remain in the inlet for up to 4 hours, this value is cumulative over the entire simulation; it does not indicate that sediment remained continuously suspended in the inlet for this length of time. However, due to stronger currents in the channel, the sediment was predicted to be unable to deposit. Depositional patterns were centered around the HDD pit, with maximum depositional thicknesses ranging between 10-20 mm (Figure 3-59).



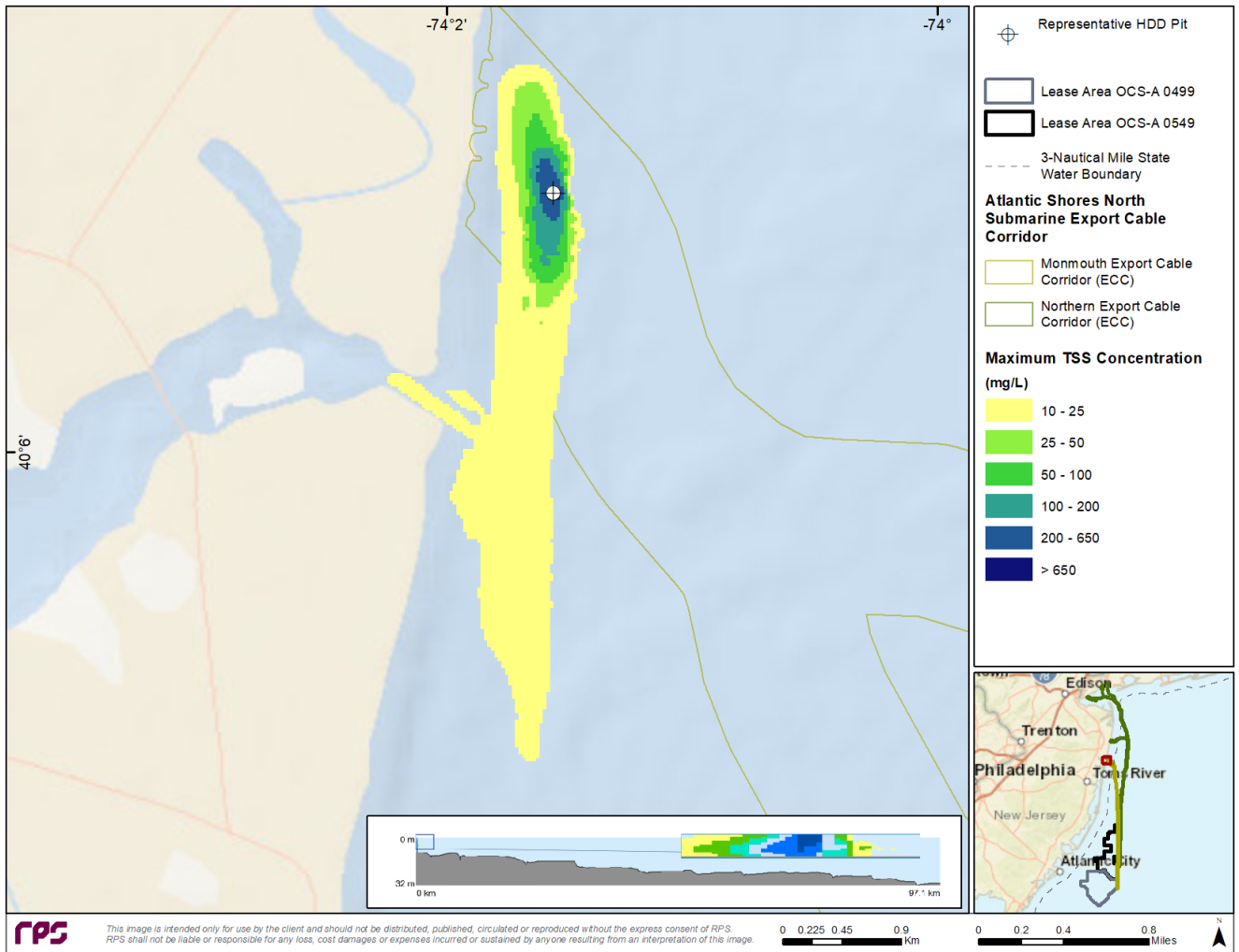


Figure 3-57: Map of Time-Integrated TSS Concentrations Associated with Monmouth ECC Representative HDD Pit Excavation.

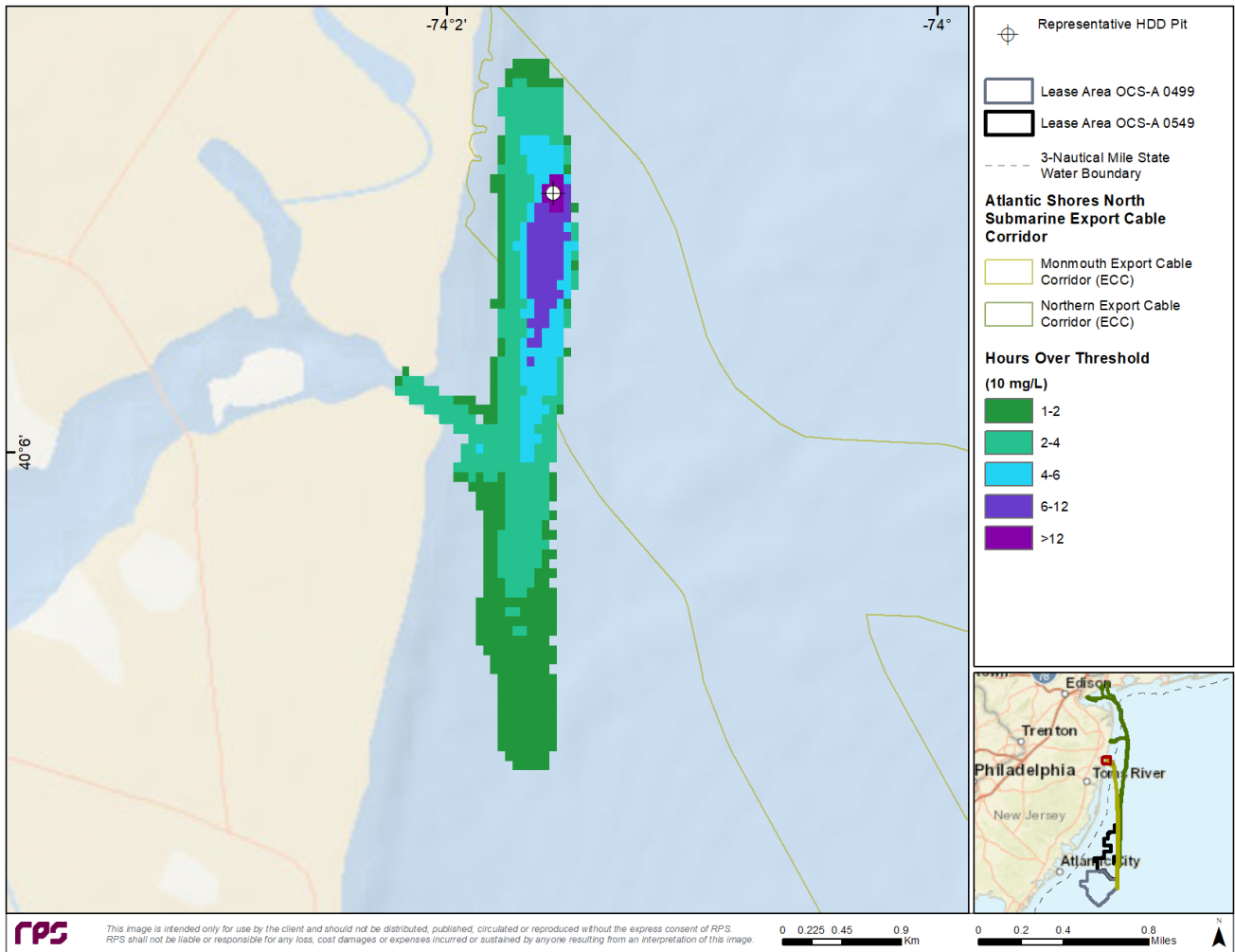


Figure 3-58: Map of Duration of TSS  $\geq 10$  mg/L Associated with Monmouth ECC Representative HDD Pit Excavation.

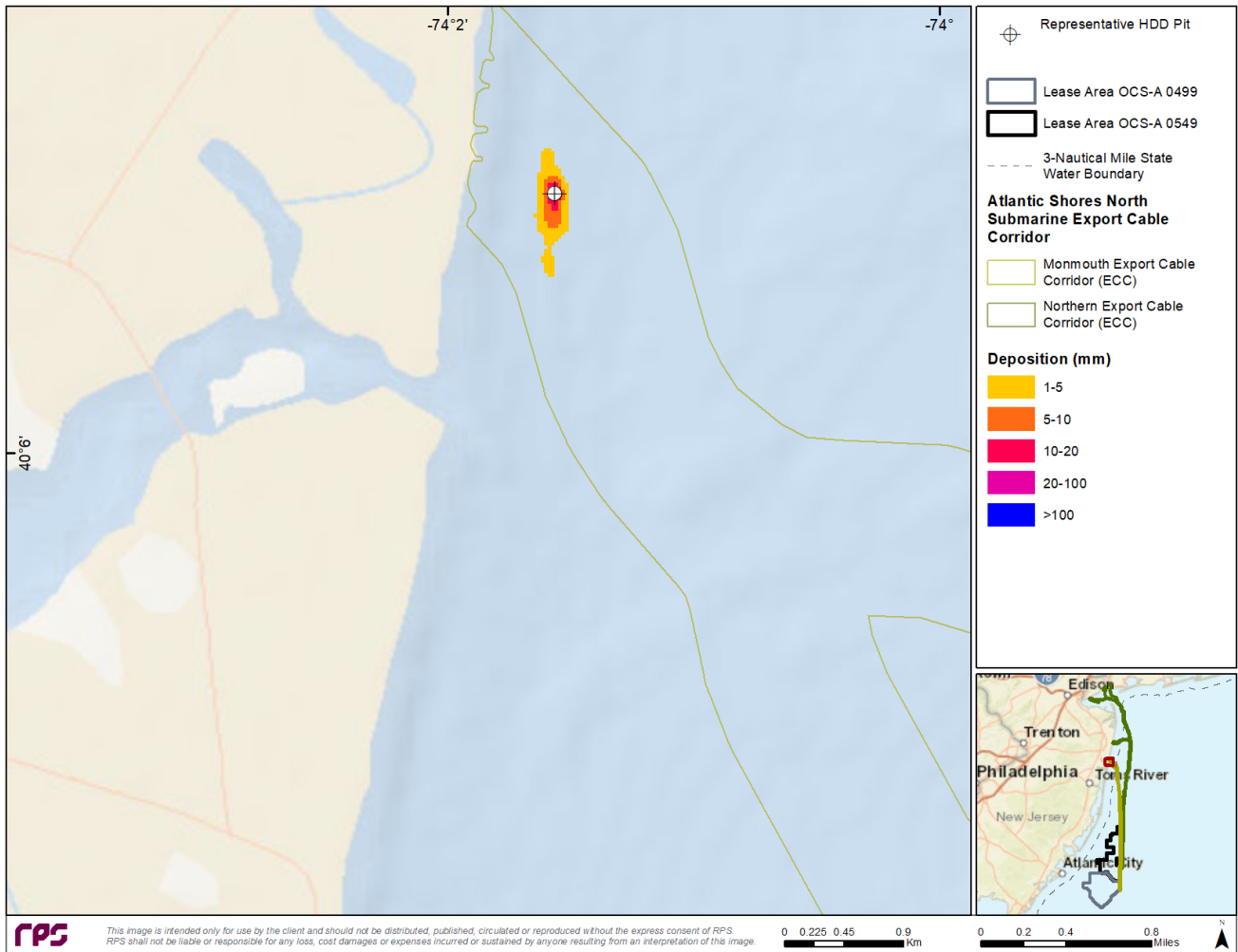


Figure 3-59: Map of Deposition Thickness Associated with Monmouth ECC Representative HDD Pit Excavation.

### 3.3.7 Results Discussion

Consistent with the PDE, this study simulated multiple scenarios to capture a conservative design and range of effects associated with seabed preparation in the Lease Area and the ECCs, the installation of IACs in the Lease Area, offshore export cables in the two ECCs, and landfall approaches. All seabed preparation simulations were modeled using TSHD and conservative equipment parameters (i.e., 100% of mass released at or near the water surface). For sandwave clearance simulations and due to the periodic disposal of sediment, the resulting footprint exhibited higher concentrations especially when currents were parallel with the route, because this resulted in compounding plumes.

The discrete locations of deposition along the route were a product of the periodic disposal of sediments during dump and overflow and can be attributed to the relatively large volume of sediment released at or near the water surface, as compared to the continual release of sediment near the seabed for the cable installation simulations. Above-ambient TSS concentrations stemming from sandwave clearance activities extended farther from the route centerline compared with the cable installation or HDD simulations due to the introduction of sediments at the water surface and the orientation of the route to the currents. When comparing the sandwave clearance results to the seabed foundation preparation simulations, the time for water column concentrations to dissipate to less than 10 mg/L were of similar magnitude for the Large OSS foundation simulations. The representative IAC sandwave clearance simulation was predicted to take the longest time to dissipate and the representative Northern ECC sandwave clearance simulation was predicted to have the largest maximum extent to the 10 mg/L contour compared to all other construction activities. For all sandwave scenarios, above-ambient TSS concentrations substantially dissipated within 4 to 6 hours and fully dissipated in less than 14.3 hours.

Alternatively, the Large OSS seabed foundation preparation simulations were predicted to have the largest maximum extent of deposition  $\geq 1$  mm and  $\geq 10$  mm compared with all other scenarios. All seabed preparation activities were estimated to have depositional thicknesses exceeding 100 mm, while none of the cable installation or HDD pit scenarios were predicted to have areas greater than 0.01 km<sup>2</sup> associated with deposition  $> 100$  mm. The extent and persistence of the plumes and the extent and thickness of deposition were largely influenced by sediment grain size distribution, the volume of sediment suspended, and the location of the sediment's introduction within the water column; however, other factors of influence include the route orientation relative to currents, timing of the currents, and installation parameters.

Simulations of several possible IAC or offshore export cable installation methods using either jet trenching installation parameters (for IAC and export cable installation) or mechanical trenching installation parameters (for IAC installation only) predicted TSS  $\geq 100$  mg/L and deposition  $\geq 10$  mm stayed relatively close to the route centerline and remained within the bottom few meters of the water column. TSS concentrations  $\geq 10$  mg/L extended a maximum distance of approximately 2.71 km, 2.60 km, and 2.42 km for the Representative IAC (Mechanical Trencher scenario), Monmouth ECC, and Northern ECC cable installations, respectively. For the landfall approach scenarios, it was assumed that no cofferdam was deployed during construction activities, an excavator was used, and sediment was introduced at the surface to simulate side casting directly into the water. This resulted in a maximum distance for the predicted above-ambient TSS concentrations  $\geq 10$  mg/L of approximately 3.30 km and 1.85 km for the Monmouth and Northern representative HDD pits, respectively.

Model scenarios indicate that higher TSS concentrations (i.e.,  $\geq 100$  mg/L) associated with the installation of the IAC, Monmouth ECC, and Northern ECC model scenarios were constrained to the bottom of the water column and were short-lived. For the IAC model scenarios, above-ambient TSS concentrations substantially dissipated within 4 to 6 hours and fully dissipated in 8.7 hours. For the Northern ECC and Monmouth ECC model scenarios, above-ambient TSS concentrations substantially dissipated within 2 to 6 hours but require approximately 17.7 hours to fully dissipate. This increased time compared to the IAC modeled scenarios is likely due to the relatively longer routes (i.e., larger volume of suspended sediment), the routes' orientations in relation to currents, and the more frequent occurrence of fine sediment along these routes.

For the landfall approach scenarios, the tails of the plumes oscillated with the currents, and higher concentrations (e.g.,  $> 650$  mg/L) remained centered around the source. After the excavation subsided, the concentrations dissipated due to the strong hydrodynamic forcing conditions. Above-ambient TSS

concentrations around the HDD pits dissipated within 12.3 hours for the Monmouth HDD pit and 10.3 hours for the Northern ECC HDD pit. The Monmouth HDD pit model's larger areas of TSS concentrations above thresholds and the longer time for the plume to diminish to ambient conditions may be attributed to the release in deeper water, the higher fraction of fine sediments taking longer to settle, and the slightly stronger currents transporting the sediments parallel with the shore. For the HDD modeling, a conservative approach was used by assuming no mitigation techniques would be deployed during construction activities (e.g., cofferdam, silt screen) and sediment would be side cast rather than being stored on a barge. Use of a cofferdam would likely reduce the extent of the plume and minimize transport of the plume by currents, thus resulting in more localized settling of sediment around the release location.

For the Lease Area IAC installation simulations, deposition  $\geq 1$  mm was not predicted to result from mechanical trenching and was predicted to be de minimis (i.e.,  $<0.01$  km<sup>2</sup> with a max extent of 0.05 km) as a result of jet trenching. This is likely due to the orientation of the route with respect to the currents and the high fraction of fine material within that location. Variations in plume extent and duration for IAC installation can be attributed to differences in advance rates, which impacted the timing of the currents, and because the same volume of sediment was released over a longer period. Deposition  $\geq 1$  mm was limited to 0.20 km from the Monmouth ECC centerline and to 0.09 km of the Northern ECC centerline for the cable installation scenarios. For the jet-trenching cable installation scenarios, the maximum deposition associated with the IAC, Northern ECC, and Monmouth ECC was less than 1 mm, between 1-5 mm, and between 10-20 mm, respectively.

For the Monmouth and Northern representative HDD pit excavations, deposition  $\geq 1$  mm was predicted to extend a maximum distance of 0.48 km and 0.15 km, respectively. The representative Monmouth HDD pit excavation scenario was predicted to be the HDD pit with higher areas of deposition for the 1 mm, 5 mm, and 20 mm thresholds due to a higher fraction of fine sediment and the strong currents in that region. However, the representative Northern HDD pit excavation was predicted to have small areas ( $<0.01$  km<sup>2</sup>) exceeding the deposition threshold of 100 mm because the pit area primarily consisted of coarse sediment and therefore settled quickly within the vicinity of the source.

While the plume patterns for the respective representative IAC scenarios, offshore export cable scenarios, and HDD pit construction simulations were generally similar, differences in the extent and persistence of the plumes and the extent and thickness of deposition may be attributed to a variety of factors, including the following: the respective route orientation relative to currents, the timing of the currents, the depth at which the sediment is introduced to the water column, the relevant installation parameters, the volume of suspended sediment, and sediment grain size distribution.

This study summarizes a comprehensive analysis of the potential sediment disturbing activities associated with the construction activities anticipated within the Lease Area and ECCs. Several conservative assumptions were applied to the various scenarios and are outlined throughout this report. Based on the assumptions and model inputs used in this evaluation, results from this assessment provide an upper bound of the potential environmental impacts induced during seabed preparation, cable installation, and HDD pit excavation and backfill.

## 4 REFERENCES

- Anderson, EP, Mackas, DL. 1986. Lethal and sublethal effects of a molybdenum mine tailing on marine zooplankton: mortality, respiration, feeding and swimming behavior in *Calanus marshallae*, *Metridia pacifica* and *Euphausia pacifica*. *Mar Environ Res.* 19(2):131-155.
- Anderson, E., Johnson, B., Isaji, T., & Howlett, E. 2001. SSFATE (Suspended Sediment FATE), a model of sediment movement from dredging operations. In WODCON XVI World Dredging Congress (pp. 2-5).
- Berry, WJ, Rubinstein, NI, Hinchey, EH, Klein-MacPhee, G, Clarke, DG. 2011. Assessment of dredging-induced sedimentation effects on Winter Flounder (*Pseudopleuronectes americanus*) hatching success: results of laboratory investigations. Paper presented at: WEDA, 2011. Proceedings of the Western Dredging Association Technical Conference and Texas A&M Dredging Seminar; Nashville, Tennessee.
- Bratton, D.C. and Womeldorf, C.A., 2011. The wind shear exponent: comparing measured against simulated values and analyzing the phenomena that affect the wind shear. In *Energy Sustainability* (Vol. 54686, pp. 2245-2251).
- Cake, EW, Jr (Gulf Coast Research Laboratory). 1983. Habitat suitability index models: Gulf of Mexico American oyster. U.S. Fish and Wildlife Service. Report nr FWS-OBS 82/10.57. 37 p.
- Copernicus Climate Change Service (C3S), 2020. ERA5 hourly data on single levels from 1979 to present. Copernicus Climate Change Service Climate Data Store (CDS), accessed May, 30, 2022. DOI: 10.24381/cds.adbb2d47.
- Delft3D Google Scholar, 2022. "Delft3D". Available at: <https://scholar.google.nl/scholar?hl=nl&q=delft3d&btnG=&lr=> (Accessed: 10/26/2022).
- Deltares, D., 2022. D-Flow FM user manual. Deltares Delft, The Netherlands, 330.
- Doran, K. J., Long, J. W., Birchler, J. J., Brenner, O. T., Hardy, M. W., Morgan, K. L. M., Stockdon, H. F., & Torres, M. L., 2020. Lidar-derived Beach Morphology (Dune Crest, Dune Toe, and Shoreline) for U.S. Sandy Coastlines [Data set]. U.S. Geological Survey. <https://doi.org/10.5066/F7GF0S0Z>
- Egbert, G. D., Bennett, A. F., & Foreman, M. G. 1994. TOPEX/POSEIDON tides estimated using a global inverse model. *Journal of Geophysical Research: Oceans*, 99(C12), 24821-24852.
- Egbert, G. D., & Erofeeva, S. Y. 2002. Efficient inverse modeling of barotropic ocean tides. *Journal of Atmospheric and Oceanic Technology*, 19(2), 183-204.
- Essink, K. 1999. Ecological effects of dumping of dredged sediments; options for management. *J Coast Conserv.* 5:69–80.
- Fabricius, KE. 2005. Effects of terrestrial runoff on the ecology of corals and coral reefs: review and synthesis. *Mar Pollut Bull.* 50:125-146.
- GEBCO Bathymetric Compilation Group, 2021. The GEBCO\_2021 Grid - a continuous terrain model of the global oceans and land. NERC EDS British Oceanographic Data Centre NOC. doi:10.5285/c6612cbe-50b3-0cff-e053-6c86abc09f8f
- Gilmour, J. 1999. Experimental investigation into the effects of suspended sediment on fertilization, larval survival, and settlement in a scleractinian coral. *Mar Biol.* 135:451-462.
- Hendrick, VJ, Hutchison, ZL, Last, KS. Sediment Burial Intolerance of Marine Macroinvertebrates. *PLoS ONE.* 2016; 11(2): e0149114.
- Hersbach, H., Bell, B., Berrisford, P., Hirahara, S., Horányi, A., Muñoz-Sabater, J., Nicolas, J., Peubey, C., Radu, R., Schepers, D. and Simmons, A., 2020. The ERA5 global reanalysis. *Quarterly Journal of the Royal Meteorological Society*, 146(730), pp.1999-2049.

- Johnson, B. H., Andersen, E., Isaji, T., Teeter, A. M., & Clarke, D. G. 2000. Description of the SSFATE numerical modeling system (No. ERDC-TN-DOER-E10). Army Engineer Waterways Experiment Station Vicksburg MS Engineer Research And Development Center.
- Kernkamp, H.W., Van Dam, A., Stelling, G.S., de Goede, E.D. (2011). Efficient scheme for the shallow water equations on unstructured grids with application to the Continental Shelf. *Ocean Dynamics*, 61(8), 1175–1188. <https://doi.org/10.1007/s10236-011-0423-6>
- Lesser, G.R., Roelvink, J. V, van Kester, J.T.M., & Stelling, G. (2004). Development and validation of a three-dimensional morphological model. *Coastal engineering*, 51(8-9), 883–915. <https://doi.org/10.1016/j.coastaleng.2004.07.014>
- Lin, J., Wang, H. V., Oh, J. H., Park, K., Kim, S. C., Shen, J., & Kuo, A. Y. 2003. A new approach to model sediment resuspension in tidal estuaries. *Journal of coastal research*, 76-88.
- Murphy, RC. 1985. Factors affecting the distribution of the introduced bivalve, *Mercenaria*, in a California lagoon- the importance of bioturbation. *J Mar Res.* 43:673-692.
- National Data Buoy Center (NDBC), 2022. Available at [https://www.ndbc.noaa.gov/station\\_history.php?station=44065](https://www.ndbc.noaa.gov/station_history.php?station=44065) (Accessed: 2022).
- New York State Department of Environmental Conservation, 2016. New York State GIS Clearinghouse. Available at <https://gis.ny.gov/gisdata/inventories/member.cfm?organizationID=529> (Accessed: 2022).
- National Oceanic and Atmospheric Administration (NOAA). Bathymetric Data Viewer. Accessed 2020a. Retrieved from <https://maps.ngdc.noaa.gov/viewers/bathymetry/>.
- NOAA. Accessed 2020b. Harmonic Constituents for Multiple Locations [ASCII Data]. Retrieved from <https://tidesandcurrents.noaa.gov/>.
- NOAA. NDBC. Accessed 2020c. Meteorological Data for Multiple Locations. Retrieved from <https://www.ndbc.noaa.gov/>.
- Rayment, WJ. 2002. Semi-permanent tube-building amphipods and polychaetes in sublittoral mud or muddy sand. Plymouth: Marine Biological Association of the United Kingdom. Marine Life Information Network: Biology and Sensitivity Key Information Sub-programme Available from: <http://www.marlin.ac.uk>.
- Read, PA, Anderson, KJ, Matthews, JE, Watson, PG, Halliday, MC, Shiells, GM. 1982. Water quality in the Firth of Forth. *Mar Pollut Bull.* 13:421-425.
- Read, PA, Anderson, KJ, Matthews, JE, Watson, PG, Halliday, MC, Shiells, GM. 1983. Effects of pollution on the benthos of Firth of Forth. *Mar Pollut Bull.* 14:12-16.
- Seifi, F., Deng, X., Baltazar Andersen, O., 2019. Assessment of the accuracy of recent empirical and assimilated tidal models for the Great Barrier Reef, Australia, using satellite and coastal data. *Remote Sensing* 11, 1211.
- Soulsby, R.L. 1998. *Dynamics of Marine Sands*. Thomas Telford, England.
- Swanson, C., D. Mendelsohn, D. Crowley, and Y. Kim, 2012. Monitoring and modeling the thermal plume from the Indian Point Energy Center in the Hudson River. Proceedings of the Electric Power Research Institute Third Thermal Ecology and Regulation Workshop, Maple Grove, MN, 11-12 October 2011.
- Swanson, J. C., Isaji, T., Ward, M., Johnson, B. H., Teeter, A., & Clarke, D. G. 2000. Demonstration of the SSFATE numerical modeling system. DOER Technical Notes Collection (TN DOER-E12). US Army Engineer Research and Development Center, Vicksburg, MS. <http://www.wes.army.mil/el/dots/doer/pdf/doere12.pdf>.
- Swanson, J. C., & Isaji, T. 2006. Modeling dredge-induced suspended sediment transport and deposition in the Taunton River and Mt. Hope Bay, Massachusetts. In WEDA XXVII/38th TAMU Dredging Seminar, June (pp. 25-28).

- Swanson, J. C., Isaji, T., Clarke, D., & Dickerson, C. 2004. Simulations of dredging and dredged material disposal operations in Chesapeake Bay, Maryland and Saint Andrew Bay, Florida. In WEDA XXIV/36th TAMU Dredging Seminar (pp. 7-9).
- Swanson, J. C., Isaji, T., & Galagan, C. 2007. Modeling the ultimate transport and fate of dredge-induced suspended sediment transport and deposition. Proceedings of the WODCON XVIII, 27.
- Teeter, A. M. 1998. Cohesive sediment modeling using multiple grain classes, Part I: settling and deposition. Proceedings of INTERCOH.
- Turner, E.J. Miller, DC. 1991. Behavior and growth of *Mercenaria* during simulated storm events. *Mar Biol.* 111:55-64.
- United States Geological Survey (USGS). Water Data for Multiple Locations. Accessed 2020. Retrieved from <https://waterdata.usgs.gov/nwis>.
- Van Rijn, L. C. 1989. Handbook sediment transport by currents and waves. Delft Hydraulics Laboratory.
- Wessel, P., and Smith, W.H.F., 1996. A global, self-consistent, hierarchical, high-resolution shoreline database, *J. Geophys. Res.*, 101(B4), 8741–8743, doi:10.1029/96JB00104. (Accessed: 2022).
- Wilber, DH, Clarke, DG. 2001. Biological effects of suspended sediments: a review of suspended sediment impacts on fish and shellfish with relation to dredging activities in estuaries. *N Am J Fish Manag.* 21(4): 855-875.